



# **Effects of H<sub>2</sub>O<sub>2</sub> signalling originated in chloroplasts and peroxisomes**

Kumulative Dissertation

zur Erlangung des Doktorgrades  
der Mathematisch-Naturwissenschaftlichen Fakultät  
der Heinrich-Heine-Universität Düsseldorf

vorgelegt von

**NilsJaspert**  
aus Dortmund

Düsseldorf, April, 2014

Aus dem Institut für Molekulare Physiologie und Biotechnologie der Pflanzen  
der Heinrich-Heine Universität Düsseldorf

Gedruckt mit der Genehmigung der Mathematisch-Naturwissenschaftlichen Fakultät der  
Heinrich-Heine-Universität Düsseldorf

Referent: PD Dr. Veronica G. Maurino

Korreferent: Prof. Dr. Jürgen Zeier

Tag der mündlichen Prüfung:

26.06.2014

## **Eidesstattliche Versicherung und Selbstständigkeitserklärung**

Ich versichere an Eides Statt, dass die Dissertation von mir selbständig und ohne unzulässige fremde Hilfe unter Beachtung der „Grundsätze zur Sicherung guter wissenschaftlicher Praxis an der Heinrich-Heine-Universität Düsseldorf“ erstellt worden ist. Diese Dissertation habe ich in dieser oder ähnlicher Form noch bei keiner anderen Fakultät vorgelegt. Ich habe bisher noch keine erfolglosen Promotionsversuche unternommen.

Düsseldorf, 14.04.2014

---

Nils Jaspert



## Summary

Hydrogen peroxide ( $H_2O_2$ ) operates as a signalling molecule in eukaryotes, but the specificity of its signalling capacities remains largely unrevealed. In the present thesis, we analysed whether a moderate production of  $H_2O_2$  in different organelles of plant cells has divergent effects on the transcriptome.

*A. thaliana* overexpressing glycolate oxidase in the chloroplasts (GO-plants) and plants deficient in peroxisomal catalase (*cat2* plants) were grown under non-photorespiratory conditions and then transferred to photorespiratory conditions to induce  $H_2O_2$  production in chloroplasts and peroxisomes, respectively. By using existing quantitative real-time PCR (qRT-PCR) platforms we first analysed the response of 187 ROS responsive genes and 1880 transcription factors (TF) in GO-plants. Our data revealed coordinated expression changes of genes of specific functional networks 0.5 h after induction of  $H_2O_2$  production in chloroplasts, including the induction of indole glucosinolate and camalexin biosynthesis genes. The analysis of TF shows an upregulation of expression of genes specifically affecting development.

By using microarray analysis we showed that  $H_2O_2$  originated in specific organelles induces two kinds of responses: one that integrates signals independently from the subcellular site of production and other signals, which are dependent of the  $H_2O_2$  production site. While  $H_2O_2$  produced in peroxisomes induces protein repair responses,  $H_2O_2$  produced in chloroplasts induces early signalling responses through the control of gene transcription and secondary signalling messengers. The comparison between *cat2* and GO-plants show that genes involved in wounding and pathogen attack response, like camalexin, indole glucosinolates and stigmaterol biosynthetic genes are specifically induced by  $H_2O_2$  produced in chloroplasts. Indeed, chloroplastic production of  $H_2O_2$  induces the accumulation of 4MO-I3M and stigmaterol.

We further analysed the substrate specificity of peroxisomal  $H_2O_2$ -producing (L)-2 hydroxyacid oxidases. We determined the enzymatic kinetics of GO1, GO2 and GO3. Our data revealed that GO1 and GO2 use glycolate, and GO3 can use glycolate and L-lactate as substrates. To assess the *in vivo* substrate of GO3, loss-of-function mutants (*go3*) were isolated and GO3 overexpressing lines were generated. Root development on  $\frac{1}{2}$  MS-plates containing glycolate was impaired in all genotypes analysed. In contrast, root development on medium containing L-lactate was impaired in *go3* lines with respect to the wild-type, while GO3 overexpressing lines showed longer roots than wild-type. Next a complementation assay

## Summary

---

in yeast deficient in CYB2, which metabolize L-lactate, was conducted. The deficient yeast is not able to grow on L-lactate as sole carbon source. Overexpression of GO3 from *A. thaliana* complements this phenotype, strongly suggesting that L-lactate is the *in vivo* substrate of GO3.

## Zusammenfassung

H<sub>2</sub>O<sub>2</sub> ist ein Signalmolekül in Eukaryoten, jedoch ist die spezifische Wirksamkeit der Signalwirkung bisher weitestgehend unbekannt. In der vorliegenden Arbeit haben wir analysiert, ob eine moderate Produktion von H<sub>2</sub>O<sub>2</sub> in verschiedenen pflanzlichen Zellorganellen divergente Effekte auf das Transkriptom ausübt.

*A. thaliana* Pflanzen, welche die Glycolat Oxidase1 in den Chloroplasten überexprimieren (GO-Pflanzen) und Pflanzen, die einen Funktionsverlust der peroxisomalen catalase2 (*cat2* Pflanzen) aufweisen, wuchsen unter nicht-photorespiratorischen Bedingungen an und wurden dann in photorespiratorische Bedingungen transferiert, um die H<sub>2</sub>O<sub>2</sub> Produktion in den Chloroplasten und den Peroxisomen zu induzieren. Durch die Verwendung von existierenden quantitativen real-time PCR (qRT-PCR) Plattformen haben wir zunächst die Antwort von 187 ROS-antwortenden Genen und 1880 Transkriptionsfaktoren (TF) in GO-Pflanzen untersucht. Die Daten legen eine koordinierte Expressionsänderung von Genen eines spezifischen funktionellen Netzwerks, innerhalb von 0,5 Stunden nach Induktion der H<sub>2</sub>O<sub>2</sub> Produktion in den Chloroplasten und Peroxisomen inklusive der Induktion von Indol Glukosinolat und Camalexin Biosynthese Gene, nahe. Die Analyse der TF zeigte eine Hochregulierung der Expression von speziellen entwicklungsbeeinflussenden Genen.

Durch die Verwendung von Microarray Analysen, konnten wir zeigen, dass in spezifischen Organellen produziertes H<sub>2</sub>O<sub>2</sub>, zwei verschiedene Arten von Antworten induziert: Antworten, die unabhängig vom subzellularen Ort der Produktion agieren und Antworten, welche abhängig vom Ort der Produktion von H<sub>2</sub>O<sub>2</sub> agieren. Während in Peroxisomen produziertes H<sub>2</sub>O<sub>2</sub> Antworten der Protein Reparatur induziert, induziert in den Chloroplasten produziertes H<sub>2</sub>O<sub>2</sub> frühe Signalantworten durch die Kontrolle der Gen Transkription und sekundäre Signal Moleküle. Der Vergleich zwischen *cat2* und GO-Pflanzen zeigt, dass H<sub>2</sub>O<sub>2</sub>, welches in den Chloroplasten produziert wurde, speziell Gene, welche in der Antwort auf Verwundung und Pathogen Befall involviert sind, wie Camalexin, Indol Glukosinolat und Stigmasterol Biosynthese Gene, induziert. So konnte auch gezeigt werden, dass chloroplastidär produziertes H<sub>2</sub>O<sub>2</sub> die Akkumulation von 4MO-I3M (Glukosinolat) und Stigmasterol induziert.

Des Weiteren haben wir die Substratspezifität der peroxisomalen H<sub>2</sub>O<sub>2</sub> produzierenden (L)-2 Hydroxyacid Oxidasen analysiert. Es wurden die Enzymkinetiken von GO1, GO2 und GO3 bestimmt. Die Daten zeigen, dass GO1 und GO2 Glycolat und GO3 Glycolat und L-Laktat als Substrate verwenden können. Um das *in vivo* Substrat von GO3 bestimmen zu können,

wurden Funktionsverlustmutanten der GO3 (*go3*) isoliert und GO3 Überexpressionslinien generiert. Die Wurzelentwicklung auf MS-Medium, welches Glycolat enthält, zeigte in allen analysierten Genotypen eine negative Beeinflussung. Im Gegensatz dazu, zeigten nur die *go3* Linien, auf MS-Medium, welches mit L-Laktat versetzt war, im Vergleich zum Wild Typ kürzere Wurzeln, während die Überexpressionslinien der GO3 im Vergleich zum Wild Typ längere Wurzeln aufwiesen. Als nächstes wurde ein Komplementationsassay in Hefen mit einem Defekt in *CYB2*, ein L-Laktat metabolisierendes Protein, durchgeführt. Diese Hefen sind nicht in der Lage auf Medium mit L-Laktat als einziger Kohlenstoffquelle zu wachsen. Die Überexpression von GO3 aus *A. thaliana* komplementiert diesen Phänotyp, was darauf hinweist, dass L-Laktat das *in vivo* Substrat von GO3 darstellt.



## Table of contents

Summary .....	V
Zusammenfassung .....	VII
List of abbreviations .....	X
1. Introduction .....	1
1.1 Reactive Oxygen Species in plants .....	1
1.1.1 ROS production at the plasma membrane .....	2
1.1.2 ROS production in mitochondria .....	3
1.1.3 ROS production in chloroplasts .....	4
1.1.4 ROS Production in peroxisomes .....	5
1.2 Photorespiration .....	6
1.3 Glycolate oxidase in plants .....	8
1.3.1 Glycolate oxidase family in <i>A. thaliana</i> .....	8
1.4 Analysing ROS effects <i>in planta</i> .....	9
1.4.1 GO-plants: Overexpression of GO 1 in chloroplast of <i>A. thaliana</i> .....	10
1.4.2 <i>cat2-2</i> plants: An <i>A. thaliana</i> mutant deficient in catalase 2 .....	11
1.5 Goals of the present study .....	11
2. Discussion and Outlook .....	13
3. Theses .....	15
4. References .....	17
5. Manuscripts .....	25
5.1 Expression of ROS-responsive genes and transcription factors after metabolic formation of H <sub>2</sub> O <sub>2</sub> in chloroplasts .....	26
5.2 Spatial H <sub>2</sub> O <sub>2</sub> Signalling Specificity: H <sub>2</sub> O <sub>2</sub> from Chloroplasts and Peroxisomes Modulates the Plant Transcriptome Differentially .....	55
5.3 Substrate specificities of peroxisomal H <sub>2</sub> O <sub>2</sub> -producing (L)-2 hydroxyacid oxidases. ....	149

**List of abbreviations**

$\mu\text{l}$	microliter
$\mu\text{M}$	Micromole
$^1\text{O}_2$	Singulet oxygen
2-PG	2-phosphoglycolate
3-PGA	3-Phosphoglycerate
ASP	ascorbate peroxidases
Ca	Calcium
Cat	Catalase
CDPK	Calcium-dependent protein kinases
DiT1/DiT2	Dicarboxylate translocators 1/ 2
DNA	Desoxyribonucleinacid
Fd-GOGAD	Synthetase/ferredoxin-dependent glutamate-oxoglutarate aminotransferase
GDC	Glycine decarboxylase complex
GGAT	Glutamate/-glyoxylate aminotransferase
GlcDH	Glycolate dehydrogenase
GLYK	Glycerate kinase
GO	Glycolate oxidase
$\text{H}_2\text{O}_2$	Hydrogen Peroxide
HPR	Hydroxypyruate reductase
Hsfs	heat shock factors
IHAOX	(L)-2-hydroxyacid oxidases
MAPK	mitogen-activated protein kinase
MDHA	Monodehydroascorbate
Ms	millisecond
MV	Methylviologen

## List of abbreviations

---

NADPH	Nicotinamidadeninukleotidphosphate
Nm	Nanometre
NOX	NADPH-oxidases
O <sub>2</sub> <sup>-</sup>	superoxide anion radical
OH <sup>-</sup>	hydroxyl radical
PS	Photosystem
Rboh	Respiratory-burst oxidase homolog
ROS	Reactive oxygen species
RubisCO	Ribulose-1,5-bisphosphat carboxylase/oxygenase
SHMT	Serin-hydroxymethyl-transferase
SOD	superoxide dismutases

## 1. Introduction

### 1.1 Reactive Oxygen Species in plants

The evolution of aerobic metabolic processes in plants (e.g. respiration and photosynthesis) unavoidably led to the production of reactive oxygen species (ROS), such as singlet oxygen ( $^1\text{O}_2$ ), the superoxide anion radical ( $\text{O}_2^-$ ), the hydroxyl radical ( $\text{OH}^\cdot$ ), and hydrogen peroxide ( $\text{H}_2\text{O}_2$ ) in different cellular compartments. ROS possess a strong oxidizing potential that leads to damage of a variety of biological molecules and are therefore unwelcome byproducts of normal metabolic processes in aerobic organisms (Petrov and Van Breusegem, 2012). They can cause oxidative damage to proteins, DNA, and lipids and can lead to cell death (Apel and Hirt, 2004; Queval *et al.*, 2007).

In the last decade it became clear that ROS can also act as signalling molecules involved in a plethora of functions. Especially,  $\text{H}_2\text{O}_2$  is involved in both, the communication with external biotic and abiotic stimuli and the control of developmentally regulated processes, like cell elongation (Petrov and Van Breusegem, 2012; Foreman *et al.*, 2003). Among ROS compounds,  $\text{H}_2\text{O}_2$  received the most attention of scientist. In comparison to other ROS it has a relative long half-life (1 ms) and can traverse cellular membranes and migrate to different compartments (Bienert *et al.*, 2006).

Until now it is not totally clear, how ROS act in signal cascades (Petrov and Van Breusegem, 2012). It is possible, that redox-sensitive transcription factors that orchestrate downstream cascades directly perceive an increase in  $\text{H}_2\text{O}_2$  concentration. Candidates for this could be class A heat shock factors (Hsfs), which change their conformation in the presence of ROS. Due to this transcription can be activated (Petrov and Van Breusegem, 2012). It was shown that Hsfs are responsive for oxidative stress signalling both in animals and plants (Miller and Mittler, 2006).

Another possibility for signalling is that ROS oxidize peptides, which act as second messengers (Møller and Sweetlove, 2010). In this case specific signals from different organelles, e.g. chloroplasts and peroxisomes, are possible. These signals could activate specific nuclear encoded genes.

It is furthermore possible that mitogen-activated protein kinases (MAPKs) play a role in ROS signalling. MAPKs in plants form a large network implicated in a vast array of functions (Zhang *et al.*, 2006; Xing *et al.*, 2008). They can either be activated by  $\text{H}_2\text{O}_2$  accumulation, or trigger an  $\text{H}_2\text{O}_2$ -induced oxidative burst themselves (Petrov and Van Breusegem, 2012). The

ANP1 - a MAPK - represents one example for this process. ANP1 is activated by ROS and in turn initiates a phosphorylation cascade involving other MAPK (Kovtun *et al.*, 2000). MAPK cascades upstream and downstream of H<sub>2</sub>O<sub>2</sub> are known, which show the high complexity of H<sub>2</sub>O<sub>2</sub> signalling (Petrov and Van Breusegem, 2012).

Due to the dual function of ROS, plants use specific enzymes and other mechanisms to hold a balance between ROS production and scavenging, such as catalases, superoxide dismutases (SOD), ascorbate peroxidases (ASP) and glutathione (Bhattacharjee, 2005).

### 1.1.1 ROS production at the plasma membrane

Plasma membrane NADPH-oxidases (NOX) are important sources of ROS (Sagi and Fluhr, 2001). In plants NOX homologs have been named respiratory burst oxidase homologs (Rboh) and are involved in ROS production in response to pathogen attack. After infection, Rboh leads to an oxidative burst, which should prevent a further spread of the pathogen (Sagi and Fluhr, 2001; Torres *et al.*, 2002; Lamb and Dixon, 1997). During the oxidative burst, NOX transfers electrons from NADPH to O<sub>2</sub> leading to the formation of O<sub>2</sub><sup>-</sup>, which is further dismutated to H<sub>2</sub>O<sub>2</sub> through the activity of SODs (Lamb and Dixon, 1997).

Sagi and Fluhr (2006) postulated that NOX are activated through Ca<sup>2+</sup> as a part of elicitor-induced defence responses. For example in tobacco cells, elicitors induce dynamic cytosolic Ca<sup>2+</sup> spiking from a resting level of 50 - 100 nM to 1 - 5 μM in 2 – 5 min (Lecourieux *et al.*, 2002) which precede the activation of NOX (Nürnbergger and Scheel, 2001). Another hypothesis indicates, that calcium-dependent protein kinases (CDPK) from *Solanum tuberosum* phosphorylates two calcium-binding domains (EF-hand) at the N-terminal domain of NOX, which leads to its activation (Kobayashi *et al.*, 2007) (Fig. 1). Ogasawara *et al.* (2008) reported that the regulation of ROS production in *A. thaliana* is mediated by the Ca<sup>2+</sup> depended activation of the NOX subunit AtRbohD. Beside the function in defence response after pathogen attack, ROS produced from NOX has some other functions e.g. in development, hormone biosynthesis and cellular signal transduction of plants (Foreman *et al.*, 2003; Kwak *et al.*, 2003).

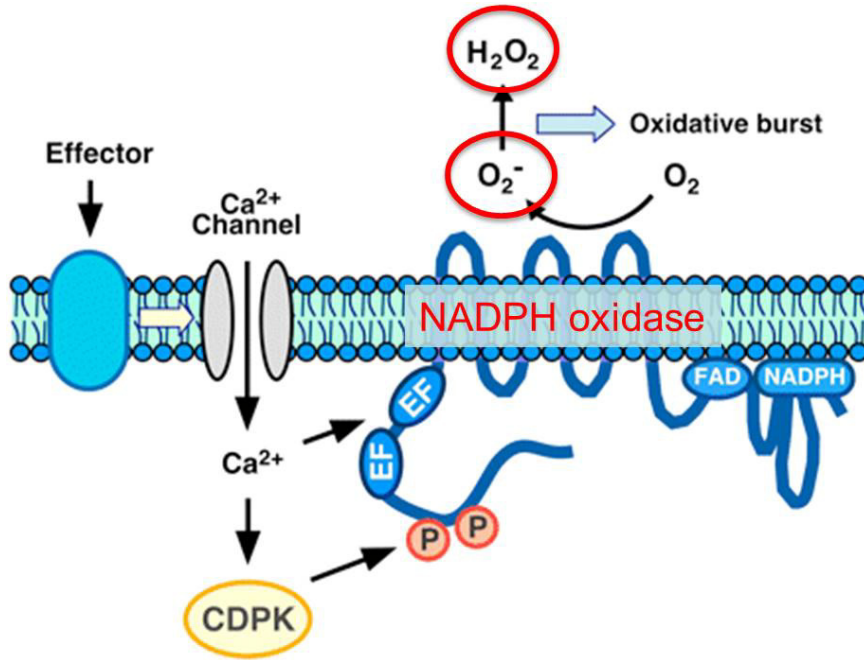


**Figure 1: Model for NOX regulation and ROS production in plants.** CDPK: calcium-dependent protein kinase (modified from Kobayashi *et al.*, 2007)

### 1.1.2 ROS production in mitochondria

While mitochondria are the major site of ROS production in mammalian cells (Tripathy and Oelmüller, 2012), mitochondrial ROS production in plants is marginal.

In case of an overreduction of the mitochondrial respiration chain complex I and III can transfer electrons to O<sub>2</sub>, which leads to the generation of O<sub>2</sub><sup>-</sup>. Both complexes release this radical to the mitochondrial matrix, but complex III may also release it to the intermembrane space (Vanlerberghe, 2013). In the intermembrane space, as well as in the matrix, O<sub>2</sub><sup>-</sup> is converted to H<sub>2</sub>O<sub>2</sub> by SOD (Fig. 2). In further steps, mitochondrial peroxidases catalyse the reduction of H<sub>2</sub>O<sub>2</sub> to H<sub>2</sub>O through the reduction of ascorbate. This process is known as the ascorbate-glutathion-cycle (Lázaro *et al.*, 2013).

Furthermore, an alternative oxidase is localised in mitochondria of plants, which avoids an overreduction of the respiratory chain. This alternative oxidase is induced by H<sub>2</sub>O<sub>2</sub> (Wagner, 1995). In case of an overreduction the respiration chain components can reduce ubiquinone beside the reduction of O<sub>2</sub>. The alternative oxidase uses the reduced ubiquinone to catalyse the reduction of O<sub>2</sub> to H<sub>2</sub>O (Vanlerberghe, 2013) so that the oxidized ubiquinone is available again for reduction and the generation of ROS decreased.

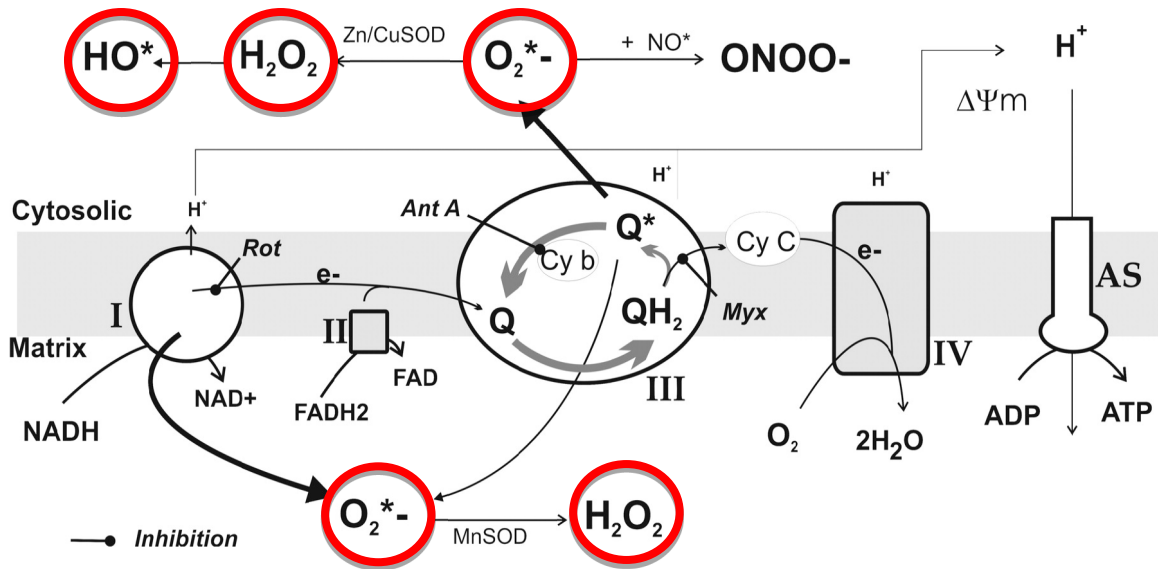


Figure 2: ROS production in the mitochondrion. Cy C: cytochrom c; Q: ubiquinone

### 1.1.3 ROS production in chloroplasts

In plants, ROS are mainly produced in chloroplasts. During photosynthesis  $^1\text{O}_2$  can be generated at photosystem (PS) II (Fig. 3). The reaction centre of PS II consists of a heterodimer of D1 and D2 proteins and cytochrome  $b_{559}$ . Furthermore, the prosthetic groups chlorophyll P680, pheophytin and the quinone electron acceptors  $Q_A$  and  $Q_B$  bind to the heterodimer of PS II. An excitation of this reaction centre leads to a charge separation between P680 and pheophytin as well as to a reduction of  $Q_A$  and  $Q_B$  (Barber, 1998). During excess light irradiation, the plastoquinone pool  $Q_A$  and  $Q_B$  is overreduced and as a consequence the charge separation cannot be completed. Under these conditions, formation of the triplet state of P680 takes place, which lead to the generation of  $^1\text{O}_2$  (Fig. 3) (Hideg *et al.*, 1998; Apel and Hirt, 2004).

The PS I is another site for the ROS production. During excess light irradiation ferredoxin is overreduced and can transfer an electron to  $\text{O}_2$ , which leads to the generation of  $\text{O}_2^-$ . This reaction is called Mehler-reaction (Mehler, 1951). In further reactions the SOD catalyses the disproportionation of  $\text{O}_2^-$  to  $\text{H}_2\text{O}_2$ , which is detoxified by ASP producing monodehydroascorbate (MDHA). In the next step MDHA can be converted spontaneously to ascorbate by reduced ferredoxin (Fig. 3) (Apel and Hirt, 2004). Alternatively, a NADPH dependent monodehydroascorbate-dehydrogenase can reduce two molecules of monodehydroascorbate to ascorbate (Apel and Hirt, 2004).

## 1. Introduction

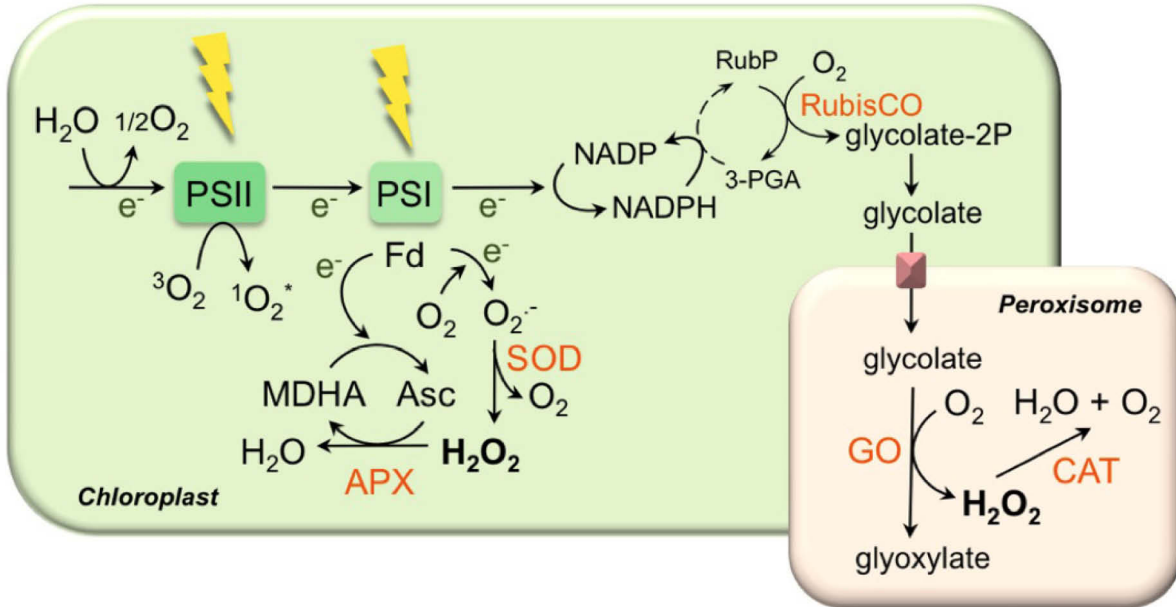


**Figure 3: ROS production in chloroplast and peroxisomes.** In peroxisomes only the  $H_2O_2$  producing reaction of glycolate oxidase is shown. APX: ascorbate peroxidase; SOD: superoxidismutase; GO: glycolate oxidase; cat: catalase, MDHA: monodehydroascorbate; Asc: ascorbate

### 1.1.4 ROS Production in peroxisomes

In most eukaryotic organisms, including plants, peroxisomes are probably the major sites for intracellular  $H_2O_2$  production. They have an important role to maintain the redox balance in cells. Due to that peroxisomes have effective mechanisms to detoxify  $H_2O_2$ . In peroxisomes some scavenging enzymes like ASP and catalase are located. The most important enzyme for the detoxification of  $H_2O_2$  in peroxisomes is catalase. ASP has a high affinity towards  $H_2O_2$  and is able to detoxify low concentrations of  $H_2O_2$ . Catalase has a lower affinity towards  $H_2O_2$  and is able to detoxify high concentrations of  $H_2O_2$  (Costa *et al.*, 2010). Catalase catalyses the following reaction:  $2 H_2O_2 \rightarrow 2 H_2O + O_2$ . In *A. thaliana* a loss-of-function mutant of this gene leads to enhanced oxidative stress especially under high light (Queval *et al.*, 2007). In plants  $\beta$ -oxidation and the photorespiratory pathway produce high amounts of  $H_2O_2$  (del Rio *et al.*, 2006).

During  $\beta$ -oxidation fatty acids are converted to acetyl-CoA, which can be later converted to hexoses in plants. This process is essential in the mobilization of seed oil reserves, which were laid down during seed development predominantly as triacylglycerol (Hu *et al.*, 2012). In this process Acyl-CoA is converted to 2-*trans*- enoyl CoA. During this reaction acyl-CoA-oxidase, transfers two electrons to  $O_2$  generating  $H_2O_2$ , which is further detoxified through catalase (Hu *et al.*, 2012).



## 1. Introduction

---

Next to  $\beta$ -oxidation some reactions of the photorespiratory pathway are also localised in the peroxisomes (Maurino and Peterhansel, 2010). High amounts of  $H_2O_2$  are produced during the conversion of glycolate to glyoxylate through glycolate oxidase (GO) (Fig. 3). The photorespiratory pathway is described below.

### 1.2 Photorespiration

Photorespiration is the major source of ROS in peroxisomes during illumination (Fig. 4). Photorespiration is initiated by the oxygenase activity of the ribulose-1,5-bisphosphat carboxylase/oxygenase (RubisCO). In this reaction one molecule 3-phosphoglycerat (3-PGA) and one molecule 2-phosphoglycolate (2-PG) are formed (Tolbert, 1997; Maurino and Peterhansel, 2010). 2-PG can lead to a collapse of photosynthesis as it inhibits photosynthetic enzymes such as phosphofructo-kinase (Anderson, 1971; Kelly and Latzko, 1976) and must therefore be detoxified through the photorespiratory pathway (Fig. 4).

In a stoichiometric way, two molecules of 2-PG are going into the photorespiratory pathway (Tolbert, 1997) and are converted to one molecule 3-PGA and one molecule  $CO_2$ . The photorespiratory pathway takes place in four different compartments: the chloroplast, the peroxisome, the mitochondrion and the cytosol (Fig. 4)(Maurino and Peterhansel, 2010).

In the chloroplast 2-PG is dephosphorylated through 2-phosphoglycolate-phosphatase (PGLP). The produced glycolate is transported for further metabolization to the peroxisome through the plastidal glycolate/-glycerate translocator (Pick *et al.*, 2013). In the peroxisome GO oxidizes glycolate to glyoxylate and  $H_2O_2$  is produced, which is detoxified by a peroxisomal catalase (Queval *et al.*, 2007). The glutamate/-glyoxylate aminotransferase (GGAT) transaminates glyoxylate to glycine using glutamate as amino donor (Liepman and Olsen, 2001; Igarashi *et al.*, 2003). Afterwards glycine is transported to the mitochondrion through an unknown transporter, where it is decarboxylated and deaminated by the glycine decarboxylase complex (GDC) yielding  $CO_2$ ,  $NH_4^+$ , NADH and 5,10-methylene tetrahydrofolate (Engel *et al.*, 2007). The latter is used by serine-hydroxymethyl-transferase (SHMT) (Somerville and Ogren, 1981) to synthesize serine by transferring the activated  $C_1$  unit onto another molecule of glycine (Maurino and Peterhansel, 2010). Due to the reaction of GDC one quarter of carbon is lost through  $CO_2$ .

Furthermore an equimolar amount of  $NH_4^+$  is released, which need to be reassimilated. The relevance of this process is essential for the metabolism of plants (Jamai *et al.*, 2009).

## 1. Introduction

---

The reassimilation of  $\text{NH}_4^+$  is catalysed by glutamine synthetase/ferredoxin-dependent glutamate-oxoglutarate aminotransferase (Fd-GOGAD) cycle (Keys, 2006). For this cycle a continuous exchange of glutamate and oxoglutarate against malate through the dicarboxylate translocators 1 and 2 (DiT1 and DiT2) is necessary (Weber *et al.*, 1995).

The serine produced from SHMT is transported back to the peroxisomes, where hydroxypyruvate is produced through Serine-Glyoxylate aminotransferase (Liepman and Olsen, 2001). In a further reaction, hydroxypyruvate is reduced to glycerate through hydroxypyruvate reductase (HPR) 1 (Timm *et al.*, 2008). Alternative to the reduction of hydroxypyruvate through HPR 1 in the peroxisomes, Timm *et al.* (2008) could show a reduction of hydroxypyruvate through the HPR 2 in cytosol (Fig. 4). The final steps in photorespiration are the transport of glycerate to chloroplast through the plastidal glycolate/-glycerate translocator (Pick *et al.*, 2013) and the phosphorylation of glycerate to 3-PGA through glycerate kinase (GLYK) (Boldt *et al.*, 2005). 3-PGA can be metabolized in the Calvin-Benson cycle.

## 1. Introduction

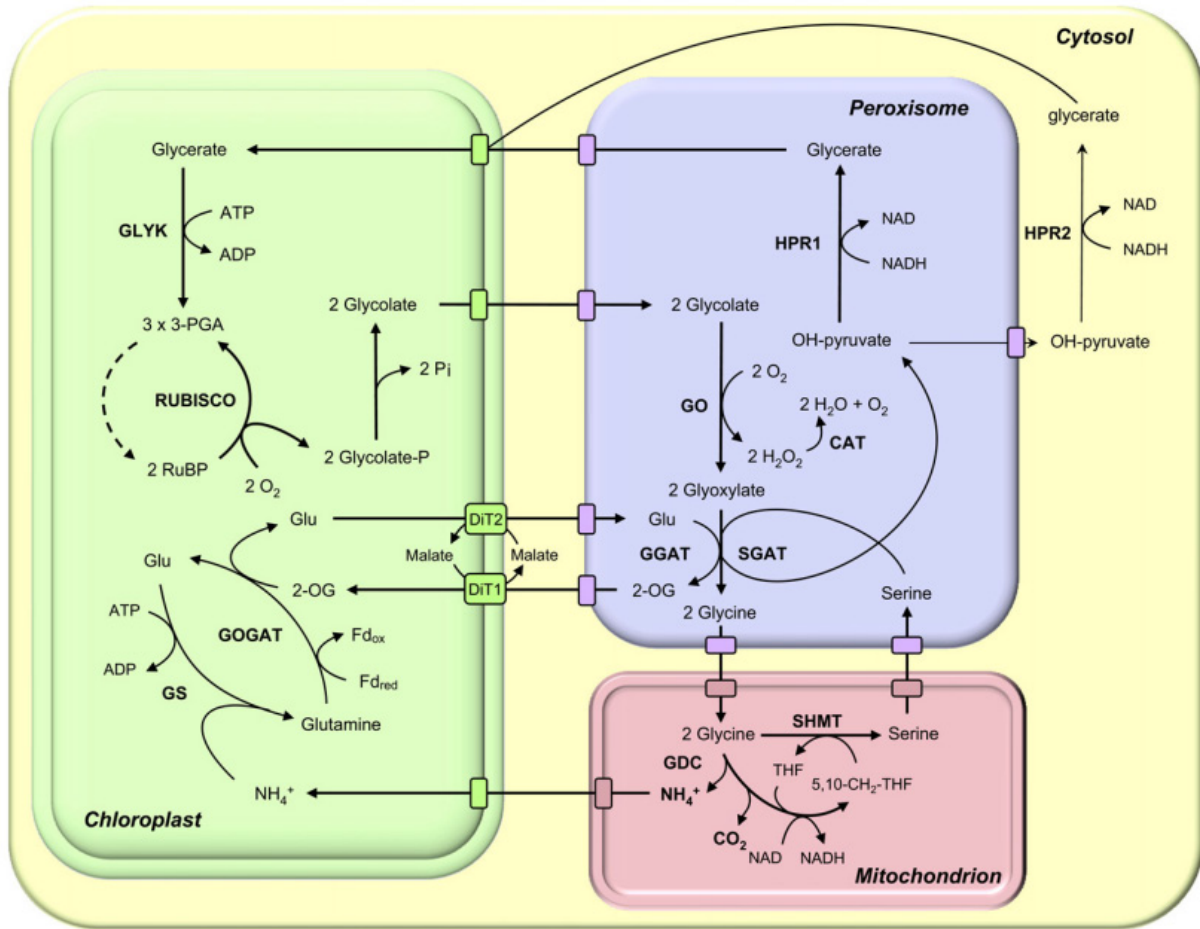


**Figure 4: Scheme of the photorespiratory cycle of a C3 plant.** The enzymes are highlighted in bold. RUBISCO: Ribulose-1,5 biphosphate carboxylase/oxygenase; PGLP: phosphoglycolate-phosphatase; GO: glycolate oxidase; cat: catalase; GGAT: glutamate-glyoxylate aminotransferase; GOGAT: glutamate-oxoglutamate-aminotransferase; GS: glutamine-synthetase; GDC: glycine decarboxylase complex; SHMT: serine-hydroxymethyl-transferase; SGAT: serine-glyoxylate-aminotransferase; HPR: hydroxypyruvate reductase; (modified from Maurino and Peterhansel, 2010).

### 1.3 Glycolate oxidase in plants

In the first steps of the photorespiratory pathway glycolate, a toxic 2-hydroxy acid is produced. In different organisms glycolate is detoxified via two different enzymes. In cyanobacteria and chlorophyta, glycolate oxidation is catalysed by glycolate dehydrogenase (GlcDH) (Nelson and Tolbert, 1970; Beezley *et al.*, 1976; Eisenhut *et al.*, 2008). In contrast to that land plants and charophyceae use a glycolate oxidase to convert glycolate to glyoxylate with the parallel production of H<sub>2</sub>O<sub>2</sub> (Stabenau and Winkler, 2005; Esser *et al.*, 2014).

#### 1.3.1 Glycolate oxidase family in *A. thaliana*

In *A. thaliana* glycolate oxidase belongs to the L-2HAOX gene family. This family is composed of 5 proteins divided in two groups: the short-chain (L)-2-hydroxyacid-oxidases (GO) and the long-chain (L)-2-hydroxyacid oxidases (IHAOX) (Esser *et al.*, 2014). AtGO1

## 1. Introduction

---

(GO1, At3g4420), AtGO2 (GO2, At3g14415) and AtGO3 (GO3, At4g18360) belong to the GO subfamily. GO1 and GO2 are both involved in photorespiration (Foyer *et al.*, 2009; see 1.2). They have a main preference for glycolate as substrate as oxidase (Tab. 1)(Kuhn, 2012). It is postulated, that GO1 and GO2 activate RubisCO activase (Xu *et al.*, 2009). GO3 is mainly expressed in roots and senescing leaves and has a similar preference for glycolate and L-lactate as substrates (Tab. 1) (Engqvist, 2010; Kuhn, 2012). GO3 would be involved in non-photorespiratory processes.

**Table 1: kinetic constants of *A. thaliana* GO1, GO2 and GO3.** The electron acceptor used was O<sub>2</sub> (oxidase activity). The substrate concentrations varied from 0 mM to 37.9 mM and 1 µg to 5 µg, purified enzyme were used. Km and Vmax values were determined using the nonlinear regression fit to the Michaelis Menten equation  $f(x) = \frac{ax}{b+x}$  (Sigma Plot software). Shown are mean values ± Standard Error of three independent experiments (modified from Kuhn, 2012).

	K <sub>m</sub> (µM)	k <sub>cat</sub> (min <sup>-1</sup> )	k <sub>cat</sub> /K <sub>m</sub> (min <sup>-1</sup> mM <sup>-1</sup> )
<b>GO1</b>			
L-lactate	2753 ± 165	114 ± 2	41
Glycolate	278 ± 13	254 ± 2	911
<b>GO2</b>			
L-lactate	4905 ± 241	116 ± 2	24
Glycolate	327 ± 21	224 ± 4	744
<b>GO3</b>			
L-lactate	420 ± 4	80 ± 2	190
Glycolate	144 ± 10	104 ± 1	725

AtHAOX1 (At3g14130) and AtHAOX2 (At3g14150) belong to the IHAOX subfamily (Esser *et al.*, 2014). They are mainly expressed in dry seeds (Winter *et al.*, 2007). It was shown that IHAOX1 preferentially oxidizes long-chain 2-hydroxyacids, although IHAOX2 preferentially oxidises medium-chain 2-hydroxyacids (Esser *et al.*, 2014). It is thus likely that IHAOX in plants are involved in the conversion or degradation of 2-hydroxyacids produced during fatty acid or amino acid metabolism (Esser *et al.*, 2014).

### 1.4 Analysing ROS effects *in planta*

To analyse the effects of ROS on different plant processes, invasive and non-invasive methods are available. Invasive methods use the application of ROS reducing agents. For

## 1. Introduction

---

example the application of methylviologen (MV) leads to the production of  $O_2^-$  in chloroplasts. During illumination MV transfers electrons to  $O_2$  and the PS I transfers electrons to MV, which lead to a continuous production of  $O_2^-$  (Maurino and Flügge, 2008). Another example for an invasive system is the exogenous application of  $H_2O_2$ . The application of  $H_2O_2$  to *A. thaliana* plants and cultured cells has allowed to obtain the first analyses of transcriptional gene networks (Maurino and Flügge, 2008).

Next to the invasive systems, non-invasive systems, such as loss-of-function mutants or overexpressing plants, are used. Loss-of-function plants of copper-zinc superoxide dismutase represent a good method to analyse the importance of the water-water-cycle during photosynthesis (Rizhsky *et al.*, 2003).

Cytosolic *apx1* loss-of-function mutants presented an accumulation of  $H_2O_2$ , suppression of growth and lower rates of photosynthesis (Pnueli *et al.*, 2003).

Other non-invasive systems used to enhance  $H_2O_2$  levels in chloroplasts and peroxisomes are transgenic plants overexpressing GO in the chloroplasts (GO-plants) (Fahnenstich *et al.*, 2008) and catalase loss-of-function mutants (*cat2-2* plants) (Queval *et al.*, 2007), respectively.

### 1.4.1 GO-plants: Overexpression of GO 1 in chloroplast of *A. thaliana*

As mentioned before (see 1.2) GO1 (At3g14420) is a photorespiratory enzyme localized to peroxisomes, which catalyses the conversion of glycolate to glyoxylate. During this reaction, electrons are transferred to  $O_2$ , which leads to the production of  $H_2O_2$ . In peroxisomes catalase 2 (At4g35090) detoxifies these  $H_2O_2$  to  $H_2O$  and  $O_2$ .

Fahnenstich *et al.* (2008) produced *A. thaliana* plants that overexpress GO 1 in chloroplasts (GO-plants) leading to the conversion of glycolate to glyoxylate directly in the chloroplasts. Under photorespiratory conditions the chloroplasts of GO-plants produced higher amounts of  $H_2O_2$  than the wild-type (Fahnenstich *et al.*, 2008; Balazadeh *et al.*, 2012). By growing the GO-plants under high  $CO_2$  concentrations or low light the GO-plants behave like wild-type. The photorespiratory phenotype can be induced by transferring high  $CO_2$  growing plants to ambient  $CO_2$  concentrations or high light. During these conditions photorespiration takes place and 2-PG is produced (see 1.2) (Fahnenstich *et al.*, 2008). The GO-plants had a 20 % - 50 % higher activity of GO compared to wild-type. Due to the higher amount of  $H_2O_2$  in chloroplasts, antioxidant enzyme activities are also enhanced but these increments are not high enough to efficiently scavenge the excess  $H_2O_2$  produced (Fahnenstich *et al.*, 2008).

Due to the enhanced level of  $H_2O_2$  produced, the GO-plants are smaller than the wild-type and show oxidative lesions in the leaves. Because the GO-plants allowed the induction of

H<sub>2</sub>O<sub>2</sub> production in chloroplasts by changing CO<sub>2</sub> levels and light conditions, they represent an effective non-invasive model to analyse the effects of H<sub>2</sub>O<sub>2</sub> produced in chloroplasts.

### 1.4.2 *cat2-2* plants: An *A. thaliana* mutant deficient in catalase 2

The first discovered and characterized antioxidant enzyme was catalase. This enzyme is ubiquitously expressed among animals and plants (Kirkman and Gaetani, 2007). It catalyses the conversion of H<sub>2</sub>O<sub>2</sub> to water and oxygen:  $2 \text{H}_2\text{O}_2 \rightarrow 2 \text{H}_2\text{O} + \text{O}_2$  (Fig. 4). *A. thaliana* possesses three genes encoding catalase (Frugoli *et al.*, 1996). Catalase is exclusively located in peroxisomes. Catalase 1 (At1g20630) is mainly expressed in pollen and seeds, catalase 2 (At4g35090) is mainly expressed in photosynthetic tissues as well as, in roots and seeds. Catalase 3 (At1g20620) is associated with vascular tissues and also in leaves (Mhamdi *et al.*, 2010).

In *A. thaliana* a loss-of-function of the catalase 2 leads to enhanced levels of H<sub>2</sub>O<sub>2</sub> (Vandenabeele *et al.*, 2004; Queval *et al.*, 2007). Compared to other scavenging enzymes, such as APX, catalase has a low affinity to H<sub>2</sub>O<sub>2</sub>, but a high turnover rate. Deficiencies in this enzyme cannot be complemented by other scavenging enzymes (Mhamdi *et al.*, 2010).

Because the catalase 2 is also a part of the photorespiratory pathway a loss-of-function of this enzyme leads to a photorespiratory phenotype. Plants lacking catalase 2 (*cat2*) present oxidative lesions and are smaller than the wild-type (Queval *et al.*, 2007). The *cat2* plants do not show any phenotype if they grow under high CO<sub>2</sub> concentrations or low light (Queval *et al.*, 2007). Under these conditions the photorespiratory pathway is decreased and less H<sub>2</sub>O<sub>2</sub> is produced. In present work, catalase-deficient plants having 10-15 % of total wild-type catalase activity (*cat2-2*-plants; N576998; Queval *et al.*, 2007) are used.

The *cat2-2* plants are a good tool to analyse the effects of H<sub>2</sub>O<sub>2</sub> that is produced in a higher amount in peroxisomes. The production of higher amounts of H<sub>2</sub>O<sub>2</sub> is easily induced by changing CO<sub>2</sub> or light conditions.

### 1.5 Goals of the present study

The specific goals of this work are:

- To analyse the effects of H<sub>2</sub>O<sub>2</sub> as a signalling molecule in plants. It should be analysed if the site of H<sub>2</sub>O<sub>2</sub> production differentially regulates the *A. thaliana* transcriptome. In this context the GO- (see 1.4.1.) and *cat2-2* plants (see 1.4.2) are used to analyse the

## 1. Introduction

---

effects of H<sub>2</sub>O<sub>2</sub> production in chloroplasts and in peroxisomes, respectively. It is of special interest to find out which genes and metabolic pathways are regulated by H<sub>2</sub>O<sub>2</sub> produced in these organelles.

- To find out which role GO3 plays in plant metabolism. This enzyme is mainly found in roots and senescing leaves. A kinetic analysis showed that both L-lactate and glycolate could be good substrates of this enzyme. Due to this it should be find out, if GO3 is able to use L-lactate or glycolate as substrate *in planta*.

### 2. Discussion and Outlook

Plants are sessile organisms, which are exposed to many biotic and abiotic stresses. To regulate the responses to these stresses, they need a wide spectrum of chemical signals and cascades. One example for chemical signals in plants are ROS, especially H<sub>2</sub>O<sub>2</sub>. H<sub>2</sub>O<sub>2</sub> is a hub which can be influenced by upstream processes like the induction of Ca<sup>2+</sup> and influence downstream processes like the catalase activity (Costa *et al.*, 2010). There are other data which show that H<sub>2</sub>O<sub>2</sub> also regulates Ca<sup>2+</sup> ion fluxes (Petrov and Van Breusegem, 2012). All this data show that H<sub>2</sub>O<sub>2</sub> forms a complicated network with other signalling molecules. This network is still mostly uncharacterized. It is also not totally understand if the site of H<sub>2</sub>O<sub>2</sub> production is essential for the way of signalling.

In the present thesis the effects of H<sub>2</sub>O<sub>2</sub> produced in chloroplasts or peroxisomes to the plant transcriptome were analysed. Therefore *A. thaliana* glycolate oxidase overexpressed in chloroplasts and plants deficient in peroxisomal *cat2* were used. After transfer of GO and *cat2* lines from non-photorespiratory to photorespiratory conditions, production of H<sub>2</sub>O<sub>2</sub> was induced in chloroplasts and peroxisomes, respectively. The results of the thesis show that there are changes in transcriptome after induction of H<sub>2</sub>O<sub>2</sub> production. It was also seen, that there are differences in gene expression changes dependent to the site of H<sub>2</sub>O<sub>2</sub> production.

Genes specifically induced by peroxisomal H<sub>2</sub>O<sub>2</sub> are mainly distributed in two functional categories: 39 % encode proteins with functions in defence and/or detoxification, while 36 % encode proteins with functions in protein folding and repair, including many heat shock proteins.

In contrast to these genes encoding proteins with a putative/known function specifically induced by chloroplastic produced H<sub>2</sub>O<sub>2</sub> are distributed in a few categories, such as transcription factors, signalling functions, proteins in defence and detoxification and proteins with functions in intermediary metabolism. For example the transcription factor WRKY33 which is a part of the biosynthesis of camalexin shows a 22.3 fold higher expression in GO-plants than in wild-type within the first 30 minutes after induction of H<sub>2</sub>O<sub>2</sub>. Interestingly no significant differences in concentration of camalexin were measured in GO-plants. In contrast to that the glucosinolate 4MO-I3M and stigmasterol, which are also important in pathogen response (Pfalz *et al.*, 2009; Griebel and Zeier, 2010) show a higher concentration in GO plants compared to wild-type. The data, as presented above, suggest that some responses to pathogens and wounding might start in the chloroplasts. It would be interesting to analyse the



## 2. Discussion and Outlook

---

connection of  $H_2O_2$  and salicylic acid, another important signal molecule in pathogen response. Is there a difference of salicylic acid concentration when  $H_2O_2$  is produced in chloroplasts or peroxisomes?

In the present thesis the possible substrate for the GO3 was also analysed. The data suggest that L-lactate is the substrate for GO3 *in vivo*. But it is not possible to exclude a parallel use of glycolate as substrate. The GO3 is mainly expressed in roots and senescing leaves. At the moment it is not clear how the exact function of GO3 in plants look like. Is it involved in L-lactate metabolism for example after anoxia? What is its role in senescence of plants? The data suggest that, independent of the use of L-lactate or glycolate as substrate,  $H_2O_2$  is produced. Maybe this  $H_2O_2$  acts as a signal in L-lactate metabolism or senescence.

Another important question, which needs to be answered is how  $H_2O_2$  acts as signal. The study at hand shows that  $H_2O_2$  produced in either chloroplasts or in chloroplasts and peroxisomes simultaneously highly induced genes recently identified to be involved in mitochondrial retrograde regulation. Here it is interesting to know how  $H_2O_2$  induces the expression of mitochondrial genes. Is  $H_2O_2$  activating a second messenger? Does it influence the genes in mitochondria due to MAPK cascades? Also activated transcription factors could be responsible for activating of genes in mitochondria. These are questions which need to be answered in future research. The data show the complicated network and function of  $H_2O_2$  in plants.

### 3. Theses

In all photosynthetic organisms ROS, especially  $H_2O_2$ , play an important role. In higher concentrations  $H_2O_2$  is toxic for cells. The plants have developed very successful mechanisms to detoxify it. But  $H_2O_2$  also has an important role as signalling molecule; e.g. in defence against pathogens. In higher amount it is toxic to the pathogen cells. Furthermore it induces the programmed cell death in plants, which prevents a spread of pathogens.

Subsequently the three Manuscripts of this thesis are shortly described.

- 1) GO1 catalyses the reaction of glycolate to glyoxylate in parallel production of  $H_2O_2$ . Plants which overexpress GO1 in chloroplasts (GO-plants) produce  $H_2O_2$  in this organelle under photorespiratory conditions. In this thesis GO-plants were used to analyse if  $H_2O_2$  produced in chloroplasts has an early influence on the transcriptome of *A. thaliana*. To this end, existing quantitative real-time PCR platforms for 187 ROS-responsive genes and 1880 TF were used. The data reveal coordinated expression changes of genes of specific functional networks 0.5 h after induction of  $H_2O_2$  in chloroplasts, including the induction of indole glucosinolates and camalexin biosynthesis genes. The analysis of TF profiling shows an upregulation of genes involved in regulation of proanthocyanidin and anthocyanin biosynthesis and of development. (Manuscript 1: Balazadeh *et al.* 2012).
- 2) In plants  $H_2O_2$  is an important signal molecule. Nevertheless until now the specificity of its signalling is still not known completely. In this thesis it was analysed if the site of  $H_2O_2$  production has differential signalling effects on the transcriptome of *A. thaliana*. To achieve this aim GO-plants and *cat2* plants were grown under non-photorespiratory conditions and were then transferred to photorespiratory conditions to induce the production of  $H_2O_2$  in chloroplasts or peroxisomes, respectively. It was shown, that there are two kinds of responses. Some responses are independent of the  $H_2O_2$  production sites and other responses depend to the site of  $H_2O_2$  production. The data reveal that  $H_2O_2$  produced in peroxisomes mainly induces genes involved in protein repair response, while  $H_2O_2$  produced in chloroplasts mainly induces genes involved in wounding and pathogen response, including indole glucosinolate, camalexin and sterol biosynthesis genes. Measurement of the concentration of these

metabolites indicated a significant higher concentration of stigmaterol and the glucosinolate 4MO-I3M in GO-plants compared to the wild-type plants. (Manuscript 2: Sewelam *et al.* 2014).

- 3) The GO1 and GO2 are involved in the photorespiratory pathway, producing H<sub>2</sub>O<sub>2</sub> during the conversion of glycolate to glyoxylate. GO3 is localized in the peroxisomes of roots and senescing leaves. We analysed the kinetic behaviours of these isozymes and showed that GO1 and GO2 use very effectively glycolate, while GO3 has a relatively high catalytic efficiency for both glycolate and L-lactate as substrates. In contrast to the wild-type T-DNA insertion lines for GO3 show a retarded root growth on ½ MS plates containing L-lactate. Contrary overexpression of GO3 show longer roots on plates containing L-lactate. On plates containing glycolate no difference in root growth was observed in any tested lines. Furthermore GO3 was able to complement a loss-of-function of CYB2, a L-lactate metabolising enzyme in yeast. These results indicate that L-lactate may be the *in vivo* substrate of GO3. (Manuscript 3: Kuhn *et al.* 2014).

## 4. References

- Anderson, L.E.** (1971) Chloroplast and cytoplasmic enzymes. II. Pea leaf triose phosphate isomerases. *Biochim. Biophys. Acta*, **235**, 237–244.
- Apel, K. and Hirt, H.** (2004) REACTIVE OXYGEN SPECIES: metabolism, oxidative stress, and signal transduction. *Annu. Rev. Plant Biol.*, **55**, 373–99.
- Balazadeh, S., Jaspert, N., Arif, M., Mueller-Roeber, B. and Maurino, V.G.** (2012) Expression of ROS-responsive genes and transcription factors after metabolic formation of H<sub>2</sub>O<sub>2</sub> in chloroplasts. *Front. Plant Sci.*, **3**, 234.
- Barber, J.** (1998) Photosystem two. *Biochim. Biophys. Acta*, **1365**, 269–277.
- Bechtold, N., Ellis, J. and Pelletier, G.** (1993) In planta Agrobacterium-mediated gene transfer by infiltration of adult Arabidopsis thaliana plants. *Comptes Rendus L Acad. Des Sci. Ser. Iii-Sciences La Vie-Life Sci.*, **316**, 1194–1199.
- Beezley, B.B., Gruber, P.J. and Frederick, S.E.** (1976) Cytochemical localization of glycolate dehydrogenase in mitochondria of chlamydomonas. *Plant Physiol.*, **58**, 315–319.
- Bhattacharjee, S.** (2005) Reactive oxygen species and oxidative burst: Roles in stress, senescence and signal transduction in plants. *Curr. Sci.*, **89**, 1113–1121.
- Bienert, G.P. and Chaumont, F.** (2013) Aquaporin-facilitated transmembrane diffusion of hydrogen peroxide. *Biochim. Biophys. Acta - Gen. Subj.*
- Bienert, G.P., Schjoerring, J.K. and Jahn, T.P.** (2006) Membrane transport of hydrogen peroxide. *Biochim. Biophys. Acta*, **1758**, 994–1003.
- Boldt, R., Edner, C., Kolukisaoglu, U., Hagemann, M., Weckwerth, W., Wienkoop, S., Morgenthal, K. and Bauwe, H.** (2005) D-GLYCERATE 3-KINASE, the last unknown enzyme in the photorespiratory cycle in Arabidopsis, belongs to a novel kinase family. *Plant Cell*, **17**, 2413–2420.
- Bradford, M.M.** (1976) A rapid and sensitive method for the quantitation of microgram quantities of protein utilizing the principle of protein-dye binding. *Anal. Biochem.*, **72**, 248–254.
- Chaouch, S., Queval, G. and Noctor, G.** (2012) AtRbohF is a crucial modulator of defence-associated metabolism and a key actor in the interplay between intracellular oxidative stress and pathogenesis responses in Arabidopsis. *Plant J.*, **69**, 613–627.
- Choi, W.-G. and Roberts, D.M.** (2007) Arabidopsis NIP2;1, a major intrinsic protein transporter of lactic acid induced by anoxic stress. *J. Biol. Chem.*, **282**, 24209–18.

#### 4. References

---

- Costa, A., Drago, I., Behera, S., Zottini, M., Pizzo, P., Schroeder, J.I., Pozzan, T. and Schiavo, F. Lo** (2010) H<sub>2</sub>O<sub>2</sub> in plant peroxisomes: an in vivo analysis uncovers a Ca(2+)-dependent scavenging system. *Plant J.*, **62**, 760–72.
- Cristescu, M.E., Innes, D.J., Stillman, J.H. and Crease, T.J.** (2008) D- and L-lactate dehydrogenases during invertebrate evolution. *BMC Evol. Biol.*, **8**, 268.
- Dean, R.T., Fu, S., Stocker, R. and Davies, M.J.** (1997) Biochemistry and pathology of radical-mediated protein oxidation. *Biochem. J.*, **324** ( Pt 1), 1–18.
- Debska, K., Krasuska, U., Budnicka, K., Bogatek, R. and Gniazdowska, A.** (2013) Dormancy removal of apple seeds by cold stratification is associated with fluctuation in H<sub>2</sub>O<sub>2</sub>, NO production and protein carbonylation level. *J. Plant Physiol.*, **170**, 480–488.
- Dolferus, R., Wolansky, M., Carroll, R., Miyashita, Y., Ismond, K. and Good, A.** (2008) Functional analysis of lactate dehydrogenase during hypoxic stress in Arabidopsis. *Funct. Plant Biol.*, **35**, 131.
- Eisenhut, M., Ruth, W., Haimovich, M., Bauwe, H., Kaplan, A. and Hagemann, M.** (2008) The photorespiratory glycolate metabolism is essential for cyanobacteria and might have been conveyed endosymbiotically to plants. *Proc. Natl. Acad. Sci. U. S. A.*, **105**, 17199–204.
- Engel, N., Daele, K. van den, Kolukisaoglu, U., Morgenthal, K., Weckwerth, W., Pärnik, T., Keerberg, O. and Bauwe, H.** (2007) Deletion of glycine decarboxylase in Arabidopsis is lethal under nonphotorespiratory conditions. *Plant Physiol.*, **144**, 1328–1335.
- Engqvist, M.** (2010) *Characterization of three 2-hydroxy-acid dehydrogenases in the context of a biotechnological approach to short-circuit photorespiration.* Universität zu Köln.
- Esser, C., Kuhn, A., Groth, G., Lercher, M.J. and Maurino, V.G.** (2014) Plant and animal glycolate oxidases have a common eukaryotic ancestor and convergently duplicated to evolve long-chain 2-hydroxy acid oxidases. *Mol. Biol. Evol.*, 1–13.
- Fahnenstich, H., Saigo, M., Niessen, M., Zanor, M.I., Andreo, C.S., Fernie, A.R., Drincovich, M.F., Flügge, U.-I. and Maurino, V.G.** (2007) Alteration of organic acid metabolism in Arabidopsis overexpressing the maize C<sub>4</sub> NADP-malic enzyme causes accelerated senescence during extended darkness. *Plant Physiol.*, **145**, 640–52.
- Fahnenstich, H., Scarpeci, T.E., Valle, E.M., Flügge, U.-I. and Maurino, V.G.** (2008) Generation of hydrogen peroxide in chloroplasts of Arabidopsis overexpressing glycolate oxidase as an inducible system to study oxidative stress. *Plant Physiol.*, **148**, 719–29.
- Feierabend, J. and Beevers, H.** (1972) Developmental studies on microbodies in wheat leaves : I. Conditions influencing enzyme development. *Plant Physiol.*, **49**, 28–32.
- Foreman, J., Demidchik, V., Bothwell, J.H.F., et al.** (2003) Reactive oxygen species produced by NADPH oxidase regulate plant cell growth. *Nature*, **422**, 442–6.

#### 4. References

---

- Foyer, C.H., Bloom, A.J., Queval, G. and Noctor, G.** (2009) Photorespiratory metabolism: genes, mutants, energetics, and redox signaling. *Annu. Rev. Plant Biol.*, **60**, 455–84.
- Fridovich, I.** (1997) Superoxide anion radical, superoxide dismutases, and related matters. *J. Biol. Chem.*, **272**, 18515–18517.
- Frugoli, J.A., Zhong, H.H., Nuccio, M.L., McCourt, P., McPeck, M.A., Thomas, T.L. and McClung, C.R.** (1996) Catalase is encoded by a multigene family in *Arabidopsis thaliana* (L.) Heynh. *Plant Physiol.*, **112**, 327–336.
- Gietz, D., St Jean, A., Woods, R.A. and Schiestl, R.H.** (1992) Improved method for high efficiency transformation of intact yeast cells. *Nucl Acid Res*, **20**, 1425.
- Griebel, T. and Zeier, J.** (2010) A role for beta-sitosterol to stigmasterol conversion in plant-pathogen interactions. *Plant J.*, **63**, 254–68.
- Guiard, B.** (1985) Structure, expression and regulation of a nuclear gene encoding a mitochondrial protein: the yeast L(+)-lactate cytochrome c oxidoreductase (cytochrome b2). *EMBO J.*, **4**, 3265–72.
- Hartl, F.U., Ostermann, J., Guiard, B. and Neupert, W.** (1987) Successive translocation into and out of the mitochondrial matrix: targeting of proteins to the intermembrane space by a bipartite signal peptide. *Cell*, **51**, 1027–1037.
- Hideg, É., Kálai, T., Hideg, K. and Vass, I.** (1998) Photoinhibition of Photosynthesis in Vivo Results in Singlet Oxygen Production Detection via Nitroxide-Induced Fluorescence Quenching in Broad Bean Leaves†. *Biochemistry*, **37**, 11405–11411.
- Hooijmaijers, C., Rhee, J.Y., Kwak, K.J., Chung, G.C., Horie, T., Katsuhara, M. and Kang, H.** (2012) Hydrogen peroxide permeability of plasma membrane aquaporins of *Arabidopsis thaliana*. *J. Plant Res.*, **125**, 147–153.
- Hu, J., Baker, A., Bartel, B., Linka, N., Mullen, R.T., Reumann, S. and Zolman, B.K.** (2012) Plant peroxisomes: biogenesis and function. *Plant Cell*, **24**, 2279–303.
- Igarashi, D., Miwa, T., Seki, M., Kobayashi, M., Kato, T., Tabata, S., Shinozaki, K. and Ohsumi, C.** (2003) Identification of photorespiratory glutamate:glyoxylate aminotransferase (GGAT) gene in *Arabidopsis*. *Plant J.*, **33**, 975–987.
- Jain, V., Kaiser, W. and Huber, S.C.** (2008) Cytokinin inhibits the proteasome-mediated degradation of carbonylated proteins in *Arabidopsis* leaves. *Plant Cell Physiol.*, **49**, 843–852.
- Jamai, A., Salomé, P.A., Schilling, S.H., Weber, A.P.M. and McClung, C.R.** (2009) *Arabidopsis* photorespiratory serine hydroxymethyltransferase activity requires the mitochondrial accumulation of ferredoxin-dependent glutamate synthase. *Plant Cell*, **21**, 595–606.

#### 4. References

---

- Jang, J.Y., Rhee, J.Y., Chung, G.C. and Kang, H.** (2012) Aquaporin as a membrane transporter of hydrogen peroxide in plant response to stresses. *Plant Signal. Behav.*, **7**, 1180–1181.
- Kamada, T., Nito, K., Hayashi, H., Mano, S., Hayashi, M. and Nishimura, M.** (2003) Functional Differentiation of Peroxisomes Revealed by Expression Profiles of Peroxisomal Genes in *Arabidopsis thaliana*. *Plant Cell Physiol.*, **44**, 1275–1289.
- Kelly, G.J. and Lutzko, E.** (1976) Inhibition of spinach-leaf phosphofructokinase by 2-phosphoglycollate. *FEBS Lett.*, **68**, 55–58.
- Keys, A.J.** (2006) The re-assimilation of ammonia produced by photorespiration and the nitrogen economy of C3 higher plants. *Photosynth. Res.*, **87**, 165–175.
- Kirkman, H.N. and Gaetani, G.F.** (2007) Mammalian catalase: a venerable enzyme with new mysteries. *Trends Biochem. Sci.*, **32**, 44–50.
- Kobayashi, M., Ohura, I., Kawakita, K., Yokota, N., Fujiwara, M., Shimamoto, K., Doke, N. and Yoshioka, H.** (2007) Calcium-dependent protein kinases regulate the production of reactive oxygen species by potato NADPH oxidase. *Plant Cell*, **19**, 1065–80.
- Kovtun, Y., Chiu, W.L., Tena, G. and Sheen, J.** (2000) Functional analysis of oxidative stress-activated mitogen-activated protein kinase cascade in plants. *Proc. Natl. Acad. Sci. U. S. A.*, **97**, 2940–2945.
- Kuhn, A.** (2012) *Functional characterization of 2-hydroxy acid oxidases / dehydrogenases in Arabidopsis thaliana*. Universität zu Köln.
- Kwak, J.M., Mori, I.C., Pei, Z.-M., et al.** (2003) NADPH oxidase AtrbohD and AtrbohF genes function in ROS-dependent ABA signaling in *Arabidopsis*. *EMBO J.*, **22**, 2623–33.
- Laemmli, U.K.** (1970) Cleavage of structural proteins during the assembly of the head of bacteriophage T4. *Nature*, **227**, 680–685.
- Lamb, C. and Dixon, R. a.** (1997) the Oxidative Burst in Plant Disease Resistance. *Annu. Rev. Plant Physiol. Plant Mol. Biol.*, **48**, 251–275.
- Lázaro, J.J., Jiménez, A., Camejo, D., Iglesias-Baena, I., Martí, M.D.C., Lázaro-Payo, A., Barranco-Medina, S. and Sevilla, F.** (2013) Dissecting the integrative antioxidant and redox systems in plant mitochondria. Effect of stress and S-nitrosylation. *Front. Plant Sci.*, **4**, 460.
- Lecourieux, D., Mazars, C., Pauly, N., Ranjeva, R. and Pugin, A.** (2002) Analysis and Effects of Cytosolic Free Calcium Increases in Response to Elicitors in *Nicotiana plumbaginifolia* Cells. *Plant Cell Online*, **14**, 2627–2641.

#### 4. References

---

- Liepman, A.H. and Olsen, L.J.** (2001) Peroxisomal alanine : glyoxylate aminotransferase (AGT1) is a photorespiratory enzyme with multiple substrates in *Arabidopsis thaliana*. *Plant J.*, **25**, 487–498.
- Linka, N., Theodoulou, F.L., Haslam, R.P., Linka, M., Napier, J.A., Neuhaus, H.E. and Weber, A.P.M.** (2008) Peroxisomal ATP import is essential for seedling development in *Arabidopsis thaliana*. *Plant Cell*, **20**, 3241–3257.
- Maurino, V.G. and Flügge, U.-I.** (2008) Experimental systems to assess the effects of reactive oxygen species in plant tissues. *Plant Signal. Behav.*, **3**, 923–928.
- Maurino, V.G. and Peterhansel, C.** (2010) Photorespiration: current status and approaches for metabolic engineering. *Curr. Opin. Plant Biol.*, **13**, 249–56.
- MEHLER, A.H.** (1951) Studies on reactions of illuminated chloroplasts. II. Stimulation and inhibition of the reaction with molecular oxygen. *Arch. Biochem. Biophys.*, **34**, 339–351.
- Mhamdi, A., Noctor, G. and Baker, A.** (2012) Plant catalases: Peroxisomal redox guardians. *Arch. Biochem. Biophys.*, **525**, 181–194.
- Mhamdi, A., Queval, G., Chaouch, S., Vanderauwera, S., Breusegem, F. Van and Noctor, G.** (2010) Catalase function in plants: a focus on *Arabidopsis* mutants as stress-mimic models. *J. Exp. Bot.*, **61**, 4197–220.
- Miller, G. and Mittler, R.** (2006) Could heat shock transcription factors function as hydrogen peroxide sensors in plants? *Ann. Bot.*, **98**, 279–88.
- Mittler, R., Vanderauwera, S., Suzuki, N., Miller, G., Tognetti, V.B., Vandepoele, K., Gollery, M., Shulaev, V. and Breusegem, F. Van** (2011) ROS signaling: The new wave? *Trends Plant Sci.*, **16**, 300–309.
- Møller, I.M., Jensen, P.E. and Hansson, A.** (2007) Oxidative modifications to cellular components in plants. *Annu. Rev. Plant Biol.*, **58**, 459–481.
- Møller, I.M. and Sweetlove, L.J.** (2010) ROS signalling--specificity is required. *Trends Plant Sci.*, **15**, 370–4.
- Nelson, E.B. and Tolbert, N.E.** (1970) Glycolate dehydrogenase in green algae. *Arch. Biochem. Biophys.*, **141**, 102–110.
- Nürnberg, T. and Scheel, D.** (2001) Signal transmission in the plant immune response. *Trends Plant Sci.*, **6**, 372–9.
- Ogasawara, Y., Kaya, H., Hiraoka, G., et al.** (2008) Synergistic activation of the *Arabidopsis* NADPH oxidase AtrbohD by Ca<sup>2+</sup> and phosphorylation. *J. Biol. Chem.*, **283**, 8885–8892.
- Ogren, W.L. and Bowes, G.** (1971) Ribulose diphosphate carboxylase regulates soybean photorespiration. *Nat. New Biol.*, **230**, 159–160.



#### 4. References

---

- Pei, Z.M., Murata, Y., Benning, G., Thomine, S., Klüsener, B., Allen, G.J., Grill, E. and Schroeder, J.I.** (2000) Calcium channels activated by hydrogen peroxide mediate abscisic acid signalling in guard cells. *Nature*, **406**, 731–734.
- Petrov, V.D. and Breusegem, F. Van** (2012) Hydrogen peroxide—a central hub for information flow in plant cells. *AoB Plants*, **2012**, pls014.
- Pfalz, M., Vogel, H. and Kroymann, J.** (2009) The gene controlling the indole glucosinolate modifier1 quantitative trait locus alters indole glucosinolate structures and aphid resistance in Arabidopsis. *Plant Cell*, **21**, 985–99.
- Pick, T.R., Bräutigam, A., Schulz, M. a, Obata, T., Fernie, A.R. and Weber, A.P.M.** (2013) PLGG1, a plastidic glycolate glycerate transporter, is required for photorespiration and defines a unique class of metabolite transporters. *Proc. Natl. Acad. Sci. U. S. A.*, **110**, 3185–90.
- Pnueli, L., Liang, H., Rozenberg, M. and Mittler, R.** (2003) Growth suppression, altered stomatal responses, and augmented induction of heat shock proteins in cytosolic ascorbate peroxidase (Apx1)-deficient Arabidopsis plants. *Plant J.*, **34**, 187–203.
- Queval, G., Issakidis-Bourguet, E., Hoerberichts, F. a, Vandorpe, M., Gakière, B., Vanacker, H., Miginiac-Maslow, M., Breusegem, F. Van and Noctor, G.** (2007) Conditional oxidative stress responses in the Arabidopsis photorespiratory mutant cat2 demonstrate that redox state is a key modulator of daylength-dependent gene expression, and define photoperiod as a crucial factor in the regulation of H<sub>2</sub>O<sub>2</sub>-induced cel. *Plant J.*, **52**, 640–57.
- Ramil, E., Agrimonti, C., Shechter, E., Gervais, M. and Guiard, B.** (2000) Regulation of the CYB2 gene expression: transcriptional co-ordination by the Hap1p, Hap2/3/4/5p and Adr1p transcription factors. *Mol. Microbiol.*, **37**, 1116–1132.
- Reumann, S., Babujee, L., Ma, C., et al.** (2007) Proteome analysis of Arabidopsis leaf peroxisomes reveals novel targeting peptides, metabolic pathways, and defense mechanisms. *Plant Cell*, **19**, 3170–93.
- Reumann, S., Ma, C., Lemke, S. and Babujee, L.** (2004) AraPerox. A Database of Putative Arabidopsis Proteins from Plant Peroxisomes. *Plant Physiol.*, **136**, 2587–2608.
- Reumann, S., Quan, S., Aung, K., et al.** (2009) In-depth proteome analysis of Arabidopsis leaf peroxisomes combined with in vivo subcellular targeting verification indicates novel metabolic and regulatory functions of peroxisomes. *Plant Physiol.*, **150**, 125–43.
- Rio, L.A. del, Sandalio, L.M., Corpas, F.J., Palma, J.M. and Barroso, J.B.** (2006) Reactive Oxygen Species and Reactive Nitrogen Species in Peroxisomes . Production , Scavenging , and Role in Cell Signaling. *Plant Physiol.*, **141**, 330–335.
- Rizhsky, L., Liang, H. and Mittler, R.** (2003) The water-water cycle is essential for chloroplast protection in the absence of stress. *J. Biol. Chem.*, **278**, 38921–5.

#### 4. References

---

- Sagi, M. and Fluhr, R.** (2006) Production of Reactive Oxygen Species by Plant NADPH Oxidases. *Plant Physiol.*, **141**, 336–340.
- Sagi, M. and Fluhr, R.** (2001) Superoxide production by plant homologues of the gp91(phox) NADPH oxidase. Modulation of activity by calcium and by tobacco mosaic virus infection. *Plant Physiol.*, **126**, 1281–90.
- Sheen, J.** (1991) Molecular mechanisms underlying the differential expression of maize pyruvate, orthophosphate dikinase genes. *Plant Cell*, **3**, 225–245.
- Somerville, C.R.** (2001) An early Arabidopsis demonstration. Resolving a few issues concerning photorespiration. *Plant Physiol.*, **125**, 20–4.
- Somerville, C.R. and Ogren, W.L.** (1981) Photorespiration-deficient Mutants of Arabidopsis thaliana Lacking Mitochondrial Serine Transhydroxymethylase Activity. *Plant Physiol.*, **67**, 666–671.
- Stabenau, H. and Winkler, U.** (2005) Glycolate metabolism in green algae. *Physiol. Plant.*, **123**, 235–245.
- SUN, J., WANG, M.-J., DING, M.-Q., et al.** (2010) H<sub>2</sub>O<sub>2</sub> and cytosolic Ca<sup>2+</sup> signals triggered by the PM H<sup>+</sup>-coupled transport system mediate K<sup>+</sup>/Na<sup>+</sup> homeostasis in NaCl-stressed Populus euphratica cells. *Plant. Cell Environ.*, **33**, 943–958.
- Timm, S., Mielewczik, M., Florian, A., Frankenbach, S., Dreissen, A., Hocken, N., Fernie, A.R., Walter, A. and Bauwe, H.** (2012) High-to-low CO<sub>2</sub> acclimation reveals plasticity of the photorespiratory pathway and indicates regulatory links to cellular metabolism of Arabidopsis. *PLoS One*, **7**, e42809.
- Timm, S., Nunes-Nesi, A., Pärnik, T., et al.** (2008) A cytosolic pathway for the conversion of hydroxypyruvate to glycerate during photorespiration in Arabidopsis. *Plant Cell*, **20**, 2848–59.
- Tolbert, N.E.** (1997) the C<sub>2</sub> Oxidative Photosynthetic Carbon Cycle. *Annu. Rev. Plant Physiol. Plant Mol. Biol.*, **48**, 1–25.
- Torres, M.A., Dangl, J.L. and Jones, J.D.G.** (2002) Arabidopsis gp91phox homologues AtrbohD and AtrbohF are required for accumulation of reactive oxygen intermediates in the plant defense response. *Proc. Natl. Acad. Sci. U. S. A.*, **99**, 517–522.
- Triantaphylidès, C., Krischke, M., Hoerberichts, F.A., Ksas, B., Gresser, G., Havaux, M., Breusegem, F. Van and Mueller, M.J.** (2008) Singlet oxygen is the major reactive oxygen species involved in photooxidative damage to plants. *Plant Physiol.*, **148**, 960–968.
- Tripathy, B.C. and Oelmüller, R.** (2012) Reactive oxygen species generation and signaling in plants. *Plant Signal. Behav.*, **7**, 1621–33.

#### 4. References

---

- Vandenabeele, S., Vanderauwera, S., Vuylsteke, M., et al.** (2004) Catalase deficiency drastically affects gene expression induced by high light in *Arabidopsis thaliana*. *Plant J.*, **39**, 45–58.
- Vanlerberghe, G.C.** (2013) Alternative Oxidase: A Mitochondrial Respiratory Pathway to Maintain Metabolic and Signaling Homeostasis during Abiotic and Biotic Stress in Plants. *Int. J. Mol. Sci.*, **14**, 6805–47.
- Wagner, A.M.** (1995) A role for active oxygen species as second messengers in the induction of alternative oxidase gene expression in *Petunia hybrida* cells. *{FEBS} Lett.*, **368**, 339–342.
- Weber, A., Menzlaff, E., Arbinger, B., Gutensohn, M., Eckerskorn, C. and Flügge, U.I.** (1995) The 2-oxoglutarate/malate translocator of chloroplast envelope membranes: molecular cloning of a transporter containing a 12-helix motif and expression of the functional protein in yeast cells. *Biochemistry*, **34**, 2621–2627.
- Winter, D., Vinegar, B., Nahal, H., Ammar, R., Wilson, G. V and Provart, N.J.** (2007) An “Electronic Fluorescent Pictograph” browser for exploring and analyzing large-scale biological data sets. *PLoS One*, **2**, e718.
- Wydro, M., Kozubek, E. and Lehmann, P.** (2006) Optimization of transient *Agrobacterium*-mediated gene expression system in leaves of *Nicotiana benthamiana*. *Acta Biochim. Pol.*, **53**, 289–298.
- Xing, Y., Jia, W. and Zhang, J.** (2008) AtMKK1 mediates ABA-induced CAT1 expression and H<sub>2</sub>O<sub>2</sub> production via AtMPK6-coupled signaling in *Arabidopsis*. *Plant J.*, **54**, 440–51.
- Xu, H., Zhang, J., Zeng, J., Jiang, L., Liu, E., Peng, C., He, Z. and Peng, X.** (2009) Inducible antisense suppression of glycolate oxidase reveals its strong regulation over photosynthesis in rice. *J. Exp. Bot.*, **60**, 1799–809.
- Zelitch, I., Schultes, N.P., Peterson, R.B., Brown, P. and Brutnell, T.P.** (2009) High glycolate oxidase activity is required for survival of maize in normal air. *Plant Physiol.*, **149**, 195–204.
- Zhang, A., Jiang, M., Zhang, J., Tan, M. and Hu, X.** (2006) Mitogen-activated protein kinase is involved in abscisic acid-induced antioxidant defense and acts downstream of reactive oxygen species production in leaves of maize plants. *Plant Physiol.*, **141**, 475–487.

## 5. Manuscripts

1. **Salma Balazadeh, Nils Jaspert, Muhammad Arif, Bernd Mueller-Roeber and Veronica G. Maurino (2012).** Expression of ROS-responsive genes and transcription factors after metabolic formation of H<sub>2</sub>O<sub>2</sub> in chloroplasts. *Frontiers in plant science* 2012, Volume 3, Article 234
2. **Nasser Sewelam, Nils Jaspert, Katrien Van Der Kelen, Jessica Schmitz, Henning Frerigmann, Vanesa B. Tognetti, Elia Stahl, Jürgen Zeier, Frank Van Breusegem and Veronica G. Maurino (2014).** Spatial H<sub>2</sub>O<sub>2</sub> Signalling Specificity: H<sub>2</sub>O<sub>2</sub> from Chloroplasts and Peroxisomes Modulates the Plant Transcriptome Differentially. Submitted for publication to *Molecular Plant*
3. **Anke Kuhn, Martin KM Engqvist, Nils Jaspert, Jessica Schmitz and Veronica G Maurino.** Substrate specificities of peroxisomal H<sub>2</sub>O<sub>2</sub>-producing (L)-2 hydroxyacid oxidases. Manuscript

## **Manuscript 1**

Expression of ROS-responsive genes and transcription factors after metabolic formation of H<sub>2</sub>O<sub>2</sub> in chloroplasts.

**Manuscript 1:** Expression of ROS-responsive genes and transcription factors after metabolic formation of H<sub>2</sub>O<sub>2</sub> in chloroplasts.

**Status:** published (November 2012)

Salma Balazadeh, Nils Jaspert, Muhammad Arif, Bernd Mueller-Roeber and Veronica G. Maurino

**Journal:** Frontiers in Plant Science

**Impact factor:** Coming in July 2014

1. Co-author

**Own contribution:** 30 %

- Plant growth
- H<sub>2</sub>O<sub>2</sub> measurement
- Co-writing

## **Manuscript 2**

Spatial H<sub>2</sub>O<sub>2</sub> Signalling Specificity: H<sub>2</sub>O<sub>2</sub> from Chloroplasts and Peroxisomes  
Modulates the Plant Transcriptome Differentially.

## **Spatial H<sub>2</sub>O<sub>2</sub> Signalling Specificity: H<sub>2</sub>O<sub>2</sub> from Chloroplasts and Peroxisomes Modulates the Plant Transcriptome Differentially**

Nasser Sewelam<sup>a,b,2</sup>, Nils Jaspert<sup>a,2</sup>, Katrien Van Der Kelen<sup>c</sup>, Jessica Schmitz<sup>a</sup>, Henning Frerigmann<sup>d,f</sup>, Vanesa B. Tognetti<sup>c,g</sup>, Elia Stahl<sup>e</sup>, Jürgen Zeier<sup>e,f</sup>, Frank Van Breusegem<sup>b</sup> and Veronica G. Maurino<sup>a,1</sup>

**a**Institut of Developmental and Molecular Biology of Plants, Plant Molecular Physiology and Biotechnology Group, Heinrich-Heine-Universität, Universitätsstraße 1, 40225 Düsseldorf, Germany

**b** Botany Department, Faculty of Science, Tanta University, 31527, Tanta, Egypt.

**c** Department of Plant Systems Biology, VIB, and Department of Plant Biotechnology and Bioinformatics, Ghent University, Technologiepark 927, B-9052, Gent, Belgium

**d** Botanical Institute, Cologne Biocenter, University of Cologne, 50674 Cologne, Germany

**e** Molecular Ecophysiology of Plants, Heinrich-Heine-Universität, Universitätsstraße 1, 40225 Düsseldorf, Germany

**f** Cluster of Excellence on Plant Sciences (CEPLAS)

**g** Present address: Mendel Centre for Plant Genomics and Proteomics, CEITEC - Central European Institute of Technology, Masaryk University, Kamenice 5, CZ-62500 Brno, Czech Republic

<sup>1</sup> To whom correspondence should be addressed. E-mail [veronica.maurino@uni-duesseldorf.de](mailto:veronica.maurino@uni-duesseldorf.de), tel. 49-211-8112368, fax 49-211-8113706.

<sup>2</sup> These authors contributed equally to this work.

**Running title:** Source specific H<sub>2</sub>O<sub>2</sub> signalling



## ABSTRACT

Hydrogen peroxide (H<sub>2</sub>O<sub>2</sub>) operates as a signalling molecule in eukaryotes, but the specificity of its signalling capacities remains largely unrevealed. Here, we analysed whether a moderate production of H<sub>2</sub>O<sub>2</sub> from two different plant cellular compartments has divergent effects on the plant transcriptome. *A. thaliana* overexpressing glycolate oxidase in the chloroplast (Balazadeh et al., 2012; Fahnenstich et al., 2008) and plants deficient in peroxisomal catalase (Inze et al., 2012; Queval et al., 2007) were grown under non-photorespiratory conditions and then transferred to photorespiratory conditions to foster the production of H<sub>2</sub>O<sub>2</sub> in both organelles. We show that H<sub>2</sub>O<sub>2</sub> originating in a specific organelle induces two kinds of responses: one that integrates signals independently from the subcellular site of H<sub>2</sub>O<sub>2</sub> production and other, which is dependent of the H<sub>2</sub>O<sub>2</sub> production site. The data indicated that H<sub>2</sub>O<sub>2</sub> produced in peroxisomes induces prevailing protein repair responses, while H<sub>2</sub>O<sub>2</sub> produced in chloroplasts induces early signalling responses through the control of gene transcription and secondary signalling messengers. The comparative analysis indicated that genes involved in responses to wounding and pathogen attack are specifically up-regulated by chloroplastic produced-H<sub>2</sub>O<sub>2</sub>, including indolic glucosinolates-, camalexin- and stigmaterol-biosynthetic genes. Indeed, chloroplastic production of H<sub>2</sub>O<sub>2</sub> induces the accumulation of 4-methoxy-indol-3-ylmethyl glucosinolate and stigmaterol *in planta*.

Keywords: Hydrogen peroxide; Reactive oxygen species, Glycolate oxidase, Catalase, photorespiration; Oxidative signalling.

## INTRODUCTION

Enhanced reactive oxygen species (ROS) production in plant cells is a common physiological event that takes place in response to biotic and abiotic perturbations. Disruption of ROS cellular homeostasis occurs by over-reduction of electron transport activities in chloroplast, mitochondria, plasma membrane, endoplasmic reticulum and peroxisome or as by-product of various metabolic pathways localized in different compartments. For example, upon pathogens, chilling, wounding, heat and ozone stresses H<sub>2</sub>O<sub>2</sub> production is mediated by NADPH oxidase-dependent oxidative burst (Bolwell, 1999; Orozco-Cardenas et al., 2001; Prasad, 1997; Rao and Davis, 2001). In *Arabidopsis*, ABA induced H<sub>2</sub>O<sub>2</sub> lead to stomatal closure by activation of the plasma membrane Ca<sup>2+</sup> channels in guard cells (Pei *et al.*, 2000),

and H<sub>2</sub>O<sub>2</sub> acts both as upstream and downstream component in the cytosolic Ca<sup>2+</sup> signalling network (Sun *et al.*, 2010). In addition, ROS levels are linked with cellular redox networks, for example through thioredoxins, peroxiredoxins, glutaredoxins and/or NADPH (Mittler *et al.*, 2011). Therefore, stress-induced ROS are predicted to perturb redox balance which in turn activates downstream ROS signalling. The importance of ROS compartmentalization during stress responses was recently well exemplified during pathogen recognition. Respiratory burst NADPH oxidases are thought to mediate ROS production in the apoplast for signal propagation to neighbouring cells and for signalling increased intracellular ROS and SA during the establishment of disease resistant (Chaouch *et al.*, 2012).

From the different ROS (including ·O<sub>2</sub>, H<sub>2</sub>O<sub>2</sub>, ·OH and singlet oxygen (<sup>1</sup>O<sub>2</sub>)), H<sub>2</sub>O<sub>2</sub> is the most abundant and stable ROS molecules (cellular half-life ~1 ms, steady-state levels ~10<sup>-7</sup> M) (D'Autreaux and Toledano, 2007, Bienert *et al.*, 2013). Although H<sub>2</sub>O<sub>2</sub> is not charged, due to its larger dipole moment/polarity than water, non-facilitate diffusion across membranes is limited and efficient transport occurs by specific channel proteins referred to as aquaporins. The expression of aquaporins which are permeable for H<sub>2</sub>O<sub>2</sub> in yeast cells shows to be regulated by H<sub>2</sub>O<sub>2</sub> treatments and abiotic stressors in Arabidopsis, indicating a role in stress-adaptation H<sub>2</sub>O<sub>2</sub>-mediated (Hooijmaijers *et al.*, 2012; Jang *et al.*, 2012; Bienert and Chaumont, 2013). The selective reactivity, stability and diffusibility of H<sub>2</sub>O<sub>2</sub> makes it an ideal signalling molecule. The signalling properties are mediated through the capability of H<sub>2</sub>O<sub>2</sub> to directly or indirectly, via the formation of other ROS, affect protein redox status via oxidation of methionine residues and thiol groups of cysteines and either activate, inactivate or alter its function and structure (Møller *et al.*, 2007; Mittler *et al.*, 2011). Moreover, H<sub>2</sub>O<sub>2</sub> modulates carbonylation, which alters protein activity and predominantly increases their susceptibility to proteolysis (Dean *et al.*, 1997; Jain *et al.*, 2008; Debska *et al.*, 2013). Alternatively, H<sub>2</sub>O<sub>2</sub> and other ROS can interact with other non-proteinaceous factors, like lipids or small molecules in the proximity of their synthesis sites, leading to the production or destruction of secondary signalling molecules, e.g., <sup>1</sup>O<sub>2</sub>-mediated non-enzymatic lipid peroxidation or inactivation of iron-sulfur groups (Fridovich, 1997; Triantaphylidès *et al.*, 2008). In addition, phytohormone stability can be altered by unbalanced ROS accumulation. For example, auxin can be inactivated by H<sub>2</sub>O<sub>2</sub>-dependent oxidation via peroxidases (Kokkinakis and Brooks, 1979). On the other hand, large-scale transcriptomic analysis strongly suggests that crosstalk between H<sub>2</sub>O<sub>2</sub> and phytohormone signalling networks governs plant stress growth and development (Mhamdi *et al.*, 2012).

Oxidative stimuli provoke large-scale changes in the transcriptome of prokaryotic and eukaryotic organisms (Vandenbroucke et al., 2008). The first genome-wide expression studies in plants were conducted on *Arabidopsis* cell suspensions treated with  $H_2O_2$  (Desikan et al., 2001a). This study provided the first snapshot of a transcriptome perturbed by oxidative stress. Later, oxidative stress treatments using 3-Aminotriazole (a peroxisomal catalase inhibitor) (Gechev et al., 2005), ozone (Gadjev et al., 2006; Sandermann, 2004) and menadione (Baxter et al., 2007; Sweetlove et al., 2002) provided further insights in gene expression changes by exogenously applied ROS or anti-oxidant inhibitors (Maurino and Flugge, 2008). Similarly, the transcriptomes of tobacco and *Arabidopsis* mutant and transgenic plants that are perturbed in individual genes were assessed (Davletova et al., 2005; Maurino and Flugge, 2008; op den Camp et al., 2003; Rizhsky et al., 2003; Umbach et al., 2005; Vandenabeele et al., 2004; Vanderauwera et al., 2005, Queval et al., 2007; Queval et al., 2012, Gadjev et al., 2006). Analysis of the obtained transcriptomes delivered not only detailed inventories of ROS-dependent gene expression in plants, but also provided first hints for the specific signalling capacities of different ROS and the impact of their subcellular production sites on their specificity. Subsequent meta-analyses (Gadjev et al., 2006; Rosenwasser et al., 2013) disclosed specific transcriptomic footprints underlying ROS signaling in *Arabidopsis*, reinforcing the relevance of the subcellular perturbation site of ROS homeostasis to launch a specific response. Despite the importance for such meta-analyses in providing transcriptional frameworks of the oxidative stress response, they suffer from inherent drawbacks. As individual microarray data sets were obtained from plants grown at variable growth conditions and sampled from different developmental growth stages, an accurate comparative analysis of the different mutant and transgenic lines is impaired.

Although, ROS are known to be highly controlled signalling molecules that are able to transfer the environmental signals together with other signalling intermediates to the genetic machinery (Polidoros et al., 2005, Suzuki et al., 2012), the way in which ROS can provide specific signalling functions is still polemical. The fact that  $H_2O_2$  can be produced in chloroplasts, mitochondria, peroxisomes, at plasma membranes and cell walls raises the question of how plants integrates the multiples  $H_2O_2$  signals from different cellular compartments. To analyse whether compartmentalized photorespiratory  $H_2O_2$  has different signalling roles we assessed transcriptional changes induced by  $H_2O_2$  originating from the chloroplast and the peroxisomes. Transgenic *Arabidopsis* plants that metabolically produce  $H_2O_2$  in chloroplasts (GO5 plants, (Balazadeh et al., 2012; Fahnenstich et al., 2008) and in

peroxisomes (*cat2-2* plants, (Inze et al., 2012; Queval et al., 2007) were grown under non-photorespiratory conditions (high CO<sub>2</sub>) and then transferred to photorespiratory conditions (normal air) to induce the production of H<sub>2</sub>O<sub>2</sub> in the targeted organelle. During photorespiration, ribulose-1,5-bisphosphate oxygenase produces glycolate upon oxygenation of ribulose-1,5-bisphosphate. In wild-type plants, glycolate is transported from the chloroplast to the peroxisomes. In the peroxisomes, glycolate oxidase converts glycolate into glyoxylate and H<sub>2</sub>O<sub>2</sub>. The latter is efficiently scavenged by the highly abundant catalase. In catalase-deficient plants, photorespiration induces peroxisomal perturbation of H<sub>2</sub>O<sub>2</sub> homeostasis. In the transgenic plants overproducing plastid glycolate oxidase, glycolate is efficiently converted already in the chloroplast to glyoxylate and H<sub>2</sub>O<sub>2</sub>, hence providing a genetic system to perturb H<sub>2</sub>O<sub>2</sub> levels in the chloroplasts. We identified responses that are either dependent or independent from the subcellular site of H<sub>2</sub>O<sub>2</sub> production. A moderate H<sub>2</sub>O<sub>2</sub> production from chloroplasts induced early signalling responses through the control of gene transcription and secondary-signalling messengers, while moderate H<sub>2</sub>O<sub>2</sub> production from peroxisomes induced prevailing protein repair responses. Furthermore, the comparative analysis indicated that genes involved in indole glucosinolate, camalexin and stigmasterol biosynthesis are specifically up-regulated by chloroplastic produced-H<sub>2</sub>O<sub>2</sub>. Indeed, chloroplastic production of H<sub>2</sub>O<sub>2</sub> induces the accumulation of 4-methoxy-indol-3-ylmethyl-glucosinolate and stigmasterol *in planta*.

## RESULTS

### H<sub>2</sub>O<sub>2</sub> Accumulation and Photoinhibition in GO5 and *cat2-2* plants

To evaluate the accumulation of H<sub>2</sub>O<sub>2</sub> in GO5 and *cat2-2* plants after transferring long day-grown plants from high CO<sub>2</sub> to normal air conditions at moderate light intensity we use 3,3'-Diaminobenzidine (DAB) staining at different time points after transfer. At the individual time points analysed, we observed similar patterns and intensities of staining in leaves of wild type, GO5 and *cat2-2* (Figure 1A). An increase in H<sub>2</sub>O<sub>2</sub> levels reached a maximum after 8 hours of transfer to normal air and has decreased by 56 hours (Figure 1A). To analyse if the production of H<sub>2</sub>O<sub>2</sub> from chloroplasts or peroxisomes induced changes in the photosystem II (PSII) photosynthetic activity of GO5 and *cat2-2* plants, the maximum efficiency of PSII ( $F_v/F_m$ ) was measured at different time points after transfer. The  $F_v/F_m$  values of all plants were similar under all conditions analysed (Figure 1B and Supplemental Figure 1). These results and the healthy appearance of the plants after four days of induction of H<sub>2</sub>O<sub>2</sub> production

(Supplemental Figure 1A and B) indicate that the plants did not suffer from photoinhibition due to oxidative stress during the course of the experiment. In contrast, when the plants were transferred to conditions in which the flux through the photorespiratory pathways was very high (normal air and high light intensities), GO5 and catalase-deficient mutants showed a higher accumulation of H<sub>2</sub>O<sub>2</sub> (Supplemental Figure 1C) and lower F<sub>v</sub>/F<sub>m</sub> values than the wild type and presented oxidative stress lesion (Fahnenstich et al., 2008; Vandenabeele et al., 2004).

### **Metabolic profiling of plants after shifting from high CO<sub>2</sub> to ambient conditions**

To demonstrate that our experimental design induces photorespiration we compared the plant metabolite levels at 8 and 48 h after transfer from high CO<sub>2</sub> to ambient CO<sub>2</sub> conditions. Comparison to constant high CO<sub>2</sub> conditions indicated that all genotypes behave similarly after 8 h of transfer to ambient air conditions with a strong increase in the amount of photorespiratory intermediates (Figure 2A). This was verified by a principle component analysis of the dataset, which revealed that the most triggering factor separating the different data sets in the first component is the induction of photorespiration after transferring the plants to ambient CO<sub>2</sub> (Figures 2B and C); the amounts of glycerate, glycine, serine and glycolate increased strongly in all genotypes after 8 h of transfer to ambient air conditions. These data are in agreement with the increased H<sub>2</sub>O<sub>2</sub> accumulation at 8 h after transfer to photorespiratory growth conditions (Figure 1A). Moreover, they support our experimental condition as a system to activate photorespiration without inducing photoinhibition. As expected, control plants grown in continuous high CO<sub>2</sub> and harvested at time points 0 h and 48 h showed a similar profile of metabolites (Figure 2B and C).

### **Genome-wide Transcriptome Analysis after Formation of H<sub>2</sub>O<sub>2</sub> from Chloroplasts or Peroxisomes**

To assess transcriptional changes induced by a moderate production of H<sub>2</sub>O<sub>2</sub> from chloroplasts and peroxisomes, GO5 and *cat2-2* plants were grown under non-photorespiratory conditions (high CO<sub>2</sub>) and then transferred to photorespiratory conditions (normal air) while maintaining the same light intensity. RNA isolated from rosettes harvested at 8 h after transfer to normal air, and the corresponding control harvested at the same time point but from plants kept in high CO<sub>2</sub> was hybridised on the ATH1 Genome array (Affymetrics). Genes were

classified according to their fold-change in expression and the threshold for response was set to two-fold change in expression with regards to the wild type. At 8 h after the shift from high CO<sub>2</sub> to ambient conditions, a significant deregulation of the expression of a total of 275 and 118 genes in GO5 and *cat2-2* plants, respectively, was observed (Supplemental Table 1). The data indicated that 259 and 116 genes were induced, while 16 and 2 genes were down-regulated in GO5 and *cat2-2* plants, respectively (Supplemental Table 1).

Comparing both sets of induced genes, we found that 213 genes were induced specifically in GO5 plants, and 70 genes in *cat2-2* plants (Figure 3A, Supplemental Table 2 and 3). We also found that 46 genes were co-induced in GO5 and *cat2-2* plants, although they showed higher induction levels in GO5 plants (Figure 3A; Supplemental Table 4). Tables 1, 2 and 3 show the 20 most highly expressed genes in each genotype.

The identity and functional information of the identified up-regulated genes were investigated using information of TAIR (The Arabidopsis Information Resource; <https://arabidopsis.org>), which was updated with information obtained from the UniProt databases (The Universal Protein Resource; <http://www.uniprot.org/>) and published data on specific genes. This analysis allowed us to classify the set of induced genes in different functional categories (Figure 3B-3D).

Genes encoding proteins with a putative/known function specifically induced by chloroplastic produced H<sub>2</sub>O<sub>2</sub> are distributed in a few categories, such as TFs (14%), proteins with signalling functions (16%), proteins with functions in defence and/or detoxification (14%) and proteins with functions in intermediary metabolism (42%) (Figure 3B, Supplemental Tables 5 to 8). Genes specifically induced by peroxisomal produced H<sub>2</sub>O<sub>2</sub> are mainly distributed in two functional categories: 39% encode proteins with functions in defence and/or detoxification, while 36% encode proteins with functions in protein folding and repair (Figure 3D, Supplemental Table 3). The rest of the genes with a putative/known function belong to the categories signalling (11%), TFs (4%) and metabolism (3%) (Figure 3D, Supplemental Table 3). Finally, the categorisation of genes up-regulated by H<sub>2</sub>O<sub>2</sub> irrespective from its subcellular origin indicated that a high proportion of genes (39%) encode proteins with functions in defence and/or detoxification, 22% of the genes encode proteins with a function in intermediary metabolism and the other genes encode proteins with functions in signalling (13%) and protein folding and repair (11%), and TFs (3%) (Figure 3C, Supplemental Table 4).

### Expression Kinetic Analysis of Selected Genes

Our genome-wide transcriptome analysis provides information about the transcriptional modulation at a specific moment (8 h) after the induction of H<sub>2</sub>O<sub>2</sub> formation in chloroplasts or peroxisomes. To validate those results and analyse the dynamics of the transcriptional responses of selected genes in GO5 and *cat2-2* plants, we performed a timecourse transcriptome analysis (at 0, 0.5, 4, 8 and 24 h after the induction of H<sub>2</sub>O<sub>2</sub> formation) by quantitative real-time (qRT)-PCR (Figure 4). For the analysis, we chose genes that were up-regulated after 8 h of induction of H<sub>2</sub>O<sub>2</sub> production only in chloroplasts (At2g04050, DTX3, a putative Mate efflux carrier; At5g62480, GSTU9, a tau glutathion S-transferase; At3g25250, AGC2-1, a putative protein kinase; At2g38470, WRKY33 and At1g21120, IGTM2, the indole glucosinolate O-methyltransferase2) or only in peroxisomes (At3g28740, CYP81D11, a CYTP450 family protein) (Tables S2 and S3).

The group of genes up-regulated after induction of H<sub>2</sub>O<sub>2</sub> production in chloroplasts showed different expression kinetics: part of the genes showed maximum expression 8 h after the induction of H<sub>2</sub>O<sub>2</sub> production (At5g62480, At3g25250 and At1g21120), while other genes (At2g04050 and At2g38470) showed higher expression levels at two different time points, i.e. at 0.5 h and at 8 h (Figure 4). In the case of At2g04050, the higher expression level was observed at the early time point of 0.5 h in both GO5 and *cat2-2* plants. On the other hand, At3g28740 showed higher relative expression levels than the wild type only in *cat2-2* and already at 4 h after induction of H<sub>2</sub>O<sub>2</sub> production (Figure 4).

### Tryptophan-derived defence compounds and stigmasterol contents

The transcriptome analysis indicated that chloroplastic produced H<sub>2</sub>O<sub>2</sub> results in the specific up-regulation of genes involved in the biosynthesis of the tryptophan-derived defence compounds, i.e. camalexin and glucosinolates. After chloroplastic H<sub>2</sub>O<sub>2</sub> production we observed up-regulation of WRK33 and *HIG1/MYB51*, encoding two transcription factors known to regulate these pathways; *CYP71A12* encoding a cytochrome P450 enzyme that converts indole-3-acetaldoxime to indole-3-acetonitrile during camalexin biosynthesis (Millet et al., 2010), *CYP71B15 (PAD3)*, encoding a cytochrome P450 enzyme that catalyses the conversion of dihydrocamalexin acid to camalexin; *CYP81F2*, encoding a cytochrome P450 enzyme that catalyses the conversion of indole-3-yl-methyl glucosinolate (I3M) to 4-hydroxy-indole-3-yl-methyl glucosinolate (4OHI3M); and *IGTM2*, encoding an enzyme which

catalyses the transfer of a methyl group to 4OH-I3M to form methoxy-indol-3-ylmethyl glucosinolate (4MO-I3M) (Figure 5, Supplemental Table 2). Moreover, chloroplastic produced  $H_2O_2$  induces the expression of *ANAC042*, which was shown to be involved in camalexin biosynthesis induction (Saga et al., 2012). The transcriptional dynamic analysis shown in Figure 4 confirmed that the expression of *IGTM2* is highly induced already after 4 h of production of chloroplastic  $H_2O_2$ . Comparative *in silico* analysis of available microarray data suggested that chloroplastic produced  $H_2O_2$  might induce the expression of indolic glucosinolates and camalexin biosynthetic genes (Balazadeh et al., 2012). Here, we validated and experimentally confirmed this previous observation.

To investigate whether the observed up-regulation of genes involved in indolic glucosinolates and camalexin biosynthesis is enough to modify the levels of these metabolites, we determined the concentration of these defence compounds in leaves of wild type, GO5 and *cat2-2* at different time points after transferring the plants to normal  $CO_2$  conditions. We observed similar concentrations of camalexin and total (aliphatic and indolic) and individual glucosinolates in all genotypes with the exception of a significant enhanced concentration of 4MO-I3M in GO5 after 8 and 56 h of  $H_2O_2$  production with respect to the WT at the respective time points (Table 4 and Table 10).

In addition, the expression of *CYP710A1* (At2g34500), which encodes the cytochrome P450 oxidoreductase that synthesizes the phytosterol stigmasterol from  $\beta$ -sitosterol via C22 desaturation (Arnqvist et al., 2008; Griebel and Zeier, 2010; Morikawa et al., 2006), was specifically highly induced in GO5 plants (Supplemental Table 8). Hence, we determined the concentration of specific phytosterols in wild-type, GO5 and *cat2-2* leaves by GC/MS analysis. The timecourse analysis revealed that stigmasterol accumulates only in leaves of GO5 plants already at 32 h after the induction of  $H_2O_2$  production (Table 4). The concentrations of other phytosterols measured, including  $\beta$ -sitosterol, campesterol, and cholesterol remained unchanged (Supplemental Table 9).

## DISCUSSION

### Using Photorespiration to Modulate the Production of $H_2O_2$ in Different Subcellular Compartments

Here, we present a genome-wide transcriptome analysis in *A. thaliana* after a sustained *in planta* production of  $H_2O_2$  in two different organelles, the chloroplast and the peroxisome.



Previously reported transcriptome studies using catalase-deficient plants (*CAT2AS*, antisense *A. thaliana* plants with 65% residual catalase activity and *CAT2HP1*, RNAi *A. thaliana* plants with 20% residual catalase activity) revealed large modifications of the expression profile at 8 h after induction of H<sub>2</sub>O<sub>2</sub> production (Vandenabeele et al., 2004; Vanderauwera et al., 2005). In contrast, our transcriptome analysis indicated a mild modification of the nuclear gene expression 8 h after induction of H<sub>2</sub>O<sub>2</sub> production in the catalase-deficient *cat2-2* plants. The differences in the results obtained can be easily explained by comparing the approaches used to induce H<sub>2</sub>O<sub>2</sub> production in the catalase-deficient plants. In previous work plants grown in short days (12h/12h) at 100-140  $\mu\text{mol m}^{-2} \text{s}^{-1}$  in normal air (photorespiratory conditions) were exposed to high light of 1600-1800  $\mu\text{mol m}^{-2} \text{s}^{-1}$  to enhance the flux through the photorespiratory pathway resulting in a massive production of H<sub>2</sub>O<sub>2</sub>. Here, plants were grown in long days (16h/8h) at 75  $\mu\text{mol quanta m}^{-2} \text{s}^{-1}$  and high CO<sub>2</sub> concentration (non-photorespiratory conditions) and were transferred to normal air conditions and the same light intensity to induce photorespiration, resulting in a mild H<sub>2</sub>O<sub>2</sub> production. Growth of these plants under ambient growth conditions already provoked differences in gene expression and the high light treatment amplified the effect (Vanderauwera et al., 2005). The phenotype of the plants after the induction of H<sub>2</sub>O<sub>2</sub> production clearly demonstrate the differences in the amount of H<sub>2</sub>O<sub>2</sub> resulting from both approaches; while leaves of catalase-deficient plants developed cell death after 8 h under high light (Vandenabeele et al., 2004), they showed no signs of stress after at least five days in normal air conditions (Figure 1). It is known that H<sub>2</sub>O<sub>2</sub> at low concentrations would act as messenger molecule involved in different signalling pathways (Dat et al., 2000; Karpinski et al., 1999), while at high concentrations it may induce cell death (Vandenabeele et al., 2003). Thus, although Vanderauwera et al. (2005) and this work used enhanced photorespiratory fluxes to induce intraorganellar H<sub>2</sub>O<sub>2</sub> production, a significant variation in the amount of H<sub>2</sub>O<sub>2</sub> produced in each approach, due to differences in the experimental design, might be responsible for the differential modulation of the transcriptome that was observed.

Altogether, our results demonstrate that the induction of photorespiration in the GO5 and *cat2-2* plants in our experimental system triggers a moderate production of H<sub>2</sub>O<sub>2</sub> in chloroplasts and peroxisomes, respectively, which does not induce early oxidative stress responses and can thus be exploited to perform a comparative analysis of H<sub>2</sub>O<sub>2</sub> signalling effects originating from these organelles.

## **H<sub>2</sub>O<sub>2</sub> from Chloroplasts Specifically Modulate the Expression of Many Genes Encoding Transcription Factors and Protein/Receptor Kinases**

Gene regulatory signalling pathways converge at the level of transcription. Interactions among regulatory genes and between regulators and target genes can result in a spatio-temporal regulation of gene expression (Palaniswamy et al., 2006). Transcription factors represent a crucial interface between stress receptors/sensors and the downstream responsive signalling and metabolic genes. The results presented in Supplemental Table 2 show that 14% of genes induced as a result of H<sub>2</sub>O<sub>2</sub> production in chloroplasts encode TFs, which are primary candidates to govern the H<sub>2</sub>O<sub>2</sub>-responsiveness of the other genes, whose expression was up-regulated in the GO5 plants. These 30 TF-encoding genes belong to many different TF gene families (Supplemental Table 5). While several of these TFs are related to different stress responses, their involvement in plant stress responses is still unknown for many. Interestingly, we found only three TFs-encoding genes whose transcription was up-regulated in *cat2-2* plants as a result of H<sub>2</sub>O<sub>2</sub> production in peroxisomes (Supplemental Table 3). Thus, the relatively large number of TF-encoding genes induced in GO5 plants indicates that H<sub>2</sub>O<sub>2</sub> originating from chloroplasts has a critical specific signalling role controlling gene transcription.

Using data from ROS-related microarray studies, Gadjev et al. (2006) examined the expression of 1,500 TFs of *A. thaliana* in response to different ROS, including singlet oxygen, H<sub>2</sub>O<sub>2</sub> and <sup>•</sup>OH. When comparing the TFs significantly up-regulated in the GO5 plants with the 30 most highly up-regulated in the *flu* mutant (op den Camp et al., 2003) and in *CAT2HP1* plants after exposition to high light (Vanderauwera et al., 2005) a very low overlap of the genes was found. Only four TF-encoding genes were up-regulated in both GO5 and *flu* mutants, while two TF-encoding genes were up-regulated in GO5 and in *CAT2HP1* plants after exposition to high light. This comparison clearly emphasize that not only the type of ROS but also its subcellular origin is determining specific signalling responses.

Furthermore, the data presented here showed that 13.6% of the genes significantly and only induced in GO5 plants (29 genes) encode for protein kinases/receptor kinases (Figure 3A and 3B; Supplemental Tables 2 and 6). Interestingly, most of these kinase genes code for extracellular or plasma membrane-bound proteins (Supplemental Table 6), i.e. they represent a group of receptor-like kinases. Receptor-like kinases are transmembrane proteins that control a wide range of physiological responses in plants (Shiu and Bleecker, 2001; Shiu and Bleecker, 2003). The microdomain organisation and physical state of cell membranes is

known to be a very sensitive monitor of different environmental challenges (Horvath et al., 1998). Accordingly, the large number of the induced membrane-bound kinases in GO5 plants suggests that H<sub>2</sub>O<sub>2</sub> originating from chloroplasts play an important role in the perception and early signalling events that would in turn control numerous downstream secondary signalling messengers. Joo et al. (2005) proposed that plastid derived ROS signals activate the membrane associated NADPH oxidases during the early component of the oxidative burst in ozone-treated *A. thaliana* leaves. Accordingly, they suggested that signalling from the chloroplast is central for oxidative stress induction by ozone. Other studies also found that induction of light and wounding stress response requires chloroplast signalling mediated by ROS (Fryer et al., 2003; Fryer et al., 2002). Our data show that only a few protein/receptor kinases-encoding genes were induced after production of H<sub>2</sub>O<sub>2</sub> in peroxisomes in the *cat2-2* plants (Figure 3D and Supplemental Table 3). Together, these findings suggest that H<sub>2</sub>O<sub>2</sub> originating from chloroplasts has a crucial role in activating specific early signalling components compared to H<sub>2</sub>O<sub>2</sub> produced in peroxisomes.

### **Various Detoxification and Defence genes are specifically Highly Induced by H<sub>2</sub>O<sub>2</sub> from Chloroplasts**

Our results showed that many genes induced by metabolically produced H<sub>2</sub>O<sub>2</sub> in chloroplasts encode detoxification and defence proteins (Supplemental Table 7). For example, many members of the MATE (multidrug and toxic compound extrusion) family were highly induced in GO5 plants. MATE transporters are widespread in plants, with 58 paralogues found in *A. thaliana* (Hvorup et al., 2003), and they provide a defence mechanism against herbivores and microbial pathogens through the secretion of a diverse range of secondary metabolites (Morita et al., 2009; Omote et al., 2006).

In addition various Tau-class Glutathione-S-Transferases (GST) genes and a gene encoding an ABC transporter known to transport glutathione-conjugates were highly induced in GO5 plants (Supplemental Table 7). Tau-GSTs are plant-specific enzymes involved in detoxification of several compounds by catalysing their conjugation to GSH, thereby facilitating their vacuolar sequestration. Besides the formation of glutathione-conjugates, GSTs act as flavonoid-binding proteins, and indirectly facilitate the vacuolar uptake of anthocyanins (Kitamura et al., 2004; Mueller et al., 2000). They also act as phytohormone-binding proteins and thus participate in the modulation of hormone activities (Gonneau et al., 2001; Smith et al., 2003).

The high induction of genes involved in transport and conjugation (detoxification) of several compounds in the GO5 plants suggests that H<sub>2</sub>O<sub>2</sub> produced in chloroplasts may play a specific role in the modulation of secondary metabolites and hormone levels.

Production of H<sub>2</sub>O<sub>2</sub> in the chloroplasts induces the expression of an important number of genes encoding proteins involved in metabolic functions (Supplemental Table 8). The group of most highly regulated genes contain many enzymes with an oxidoreductase function, which might be involved in the modification of secondary metabolites and hormones involved in defence pathways. Furthermore, many enzymes involved in glycolysis and the oxidative pentose-phosphate pathway are upregulated in the GO5 plants after the production of H<sub>2</sub>O<sub>2</sub>, suggesting that these plants have a higher demand of reductive power, a fact that is in line with the higher number of up-regulated oxidoreductases that were found in these plants.

### **A Cell Repair Response is Specifically Induced by Peroxisomal Produced-H<sub>2</sub>O<sub>2</sub>**

A relatively large number of heat shock proteins (HSPs), 26S proteasome-related proteins and proteins involved in ubiquitin-dependent protein degradation were induced specifically in *cat2-2* plants as a result of H<sub>2</sub>O<sub>2</sub> production in peroxisomes (Supplemental Table 3). In accordance with this finding, many small HSP, together with other HSPs and heat shock factors, were reported to be up-regulated in other catalase-deficient plants subjected to high light stress (Inze et al., 2012; Vandenabeele et al., 2003; Vandenabeele et al., 2004). As a lower number of genes were significantly differentially regulated in *cat2-2* versus wild type compared to GO5 versus wild type, and as only a few HSPs showed modified expression in the GO5 plants, we postulate that an increased H<sub>2</sub>O<sub>2</sub> production in peroxisomes induces foremost stress responses such as the refolding and degradation of damaged/misfolded proteins from the cellular environment. The degradation of oxidatively damaged proteins may also contribute to retrograde H<sub>2</sub>O<sub>2</sub> signalling through the production of oxidized peptides that can act as source-specific secondary messengers (Moller and Sweetlove, 2010).

### **Co-induced genes in GO5 and *cat2-2* plants are dominated by UDP-glucuronosyl/UDP-glucosyl transferases**

A group of 46 genes were induced both in GO5 and *cat2-2* plants after transfer to photorespiratory conditions (Supplemental Table 4), indicating the existence of pathways induced by H<sub>2</sub>O<sub>2</sub> independently from its subcellular site of production. These H<sub>2</sub>O<sub>2</sub>-

responding genes include a relative large number of genes encoding UDP-glucuronosyl/UDP-glucosyl transferases (UGT). UGT catalyses the transfer of glucose using UDP-glucose to a wide range of acceptor molecules, including plant hormones (Bandurski et al., 1995) and all major classes of plant secondary metabolites (Harborne and Grayer, 1988; Vogt and Jones, 2000; Wollenweber and Jay, 1988). Glycosylation of small molecules involved in defence and signalling plays an important role in creating a high diversity, as well as in regulating the biological activity of these compounds (Ross et al., 2001). In the case of phytohormones, glycosyl conjugates might act as reversible deactivated storage forms, hence, glycosylation might have a role in the regulation of physiologically active hormone levels (Bandurski et al., 1995).

We found that the expression of *UGT74E2*, *UGT73C5*, *UGT73C1*, *UGT73B3*, *UGT73B5*, *UGT75B1*, *UGT87A2*, *UGT75D1* and *UGT73B1* is modulated by H<sub>2</sub>O<sub>2</sub> independently of the site of its production. In our assay, the most highly co-up-regulated gene (185.15 and 20.71 FC in GO5 and *cat2-2*, respectively; Supplemental Table 4) encodes the UDP-glucosyl transferase UGT74E2. It was already shown in catalase-deficient *CAT2HPI* plants (with 20% residual catalase activity) that *UGT74E2* was one of the strongly induced genes after high light induction of H<sub>2</sub>O<sub>2</sub> formation (Vanderauwera et al., 2005). This enzyme produces indole-3-butyric acid-Glc and is involved in auxin homeostasis (Tognetti et al., 2010). UGT73C5 (At2g36800) glucosylates the steroid hormones brassinolide and castasterone (Poppenberger et al., 2005) and was shown to be necessary during the hypersensitive response (Langlois-Meurinne et al., 2005). UGT75B1 catalyses the formation of the p-aminobenzoate-glucose. Plants produce p-aminobenzoate (pABA) in chloroplasts and use it for folate synthesis in mitochondria (Eudes et al., 2008). UGT87A2 is involved in the regulation of flowering time (Wang et al., 2012). UGT75D1 is involved in the metabolism of indole-3-acetic acid (Ostin et al., 1998).

These results suggest that the modulation of expression of a high number of UGTs by H<sub>2</sub>O<sub>2</sub> is independent from the subcellular site of H<sub>2</sub>O<sub>2</sub> production and indicate the existence of convergent signalling routes for H<sub>2</sub>O<sub>2</sub>.

### **Chloroplastic and Peroxisomal H<sub>2</sub>O<sub>2</sub> Signals Modulate the Transcription of Genes Involved in Mitochondrial Retrograde Regulation**

Genes recently identified to be involved in mitochondrial retrograde regulation (MMR) (De Clercq et al., 2013; Ng et al., 2013) were found to be highly induced by H<sub>2</sub>O<sub>2</sub> produced either in chloroplasts or in chloroplasts and peroxisomes simultaneously (Supplemental Tables 2 and 4). Interestingly, in the set of commonly induced genes in GO5 and *cat2-2* plants, the expression of MMR genes is much more pronounced by chloroplastic produced H<sub>2</sub>O<sub>2</sub> (Supplemental Table 4). This suggests that H<sub>2</sub>O<sub>2</sub> signals coming from chloroplasts or from chloroplasts and peroxisomes might also converge with mitochondrial retrograde signalling after mitochondrial perturbation. In general, these signals originating from different organelles, can be induced under different environmental or metabolic perturbations and may induce nuclear responses that are key to maintain the integrity of cellular function.

### **The Biosynthesis of Camalexin, Indole Glucosinolates and Stigmasterol is Specifically Deregulated by Chloroplastic Produced-H<sub>2</sub>O<sub>2</sub>**

Chloroplastic produced H<sub>2</sub>O<sub>2</sub> results in the specific up-regulation of genes involved in the biosynthesis of camalexin and indolic glucosinolates (Figure 5, Supplemental Table 2). Indeed, we found a low but significant enhanced concentration of the indolic glucosinolate 4MO-I3M only in the GO5 plants after 8 and 56 h of induction of H<sub>2</sub>O<sub>2</sub> production (Table 4), indicating that 4MO-I3M formation is specifically triggered by chloroplastic produced H<sub>2</sub>O<sub>2</sub>. Nevertheless, the content of camalexin and other glucosinolates was unchanged after chloroplastic H<sub>2</sub>O<sub>2</sub> production (Supplemental Table 10). These results suggest that it is possible that other genes essential for the regulation of glucosinolate and camalexin biosynthesis are not induced by chloroplastic produced H<sub>2</sub>O<sub>2</sub> and/or some enzymes of the pathway are subjected to posttranscriptional regulation and this is not occurring in the GO5 plants. Thus, the transcriptional upregulation of many genes of the pathways did not result in an increased level of all these metabolites *in planta*. We can also not exclude the possibility that glucosinolate/camalexin catabolic pathways/reactions might be upregulated in the GO5 plants at a later time point than that analyzed in our transcriptome analysis (8 h after induction of H<sub>2</sub>O<sub>2</sub> production).

Our data revealed that chloroplastic produced H<sub>2</sub>O<sub>2</sub> induces accumulation of stigmasterol, while the levels of the CYP710A1 substrate  $\beta$ -sitosterol remain unchanged (Table 4 and Supplemental Table 9). The conversion of  $\beta$ -sitosterol to stigmasterol is also triggered after bacterial and fungal pathogen infection (between 10 and 48 h after inoculation), treatment with elicitor molecules, such as flagellin 22 (flg22) and lipopolysaccharides (LPS), and

application of ROS (Griebel and Zeier, 2010). In all these cases, the cellular concentrations of  $\beta$ -sitosterol also remained constant (Griebel and Zeier, 2010). In leaves, the stigmasterol synthesized after pathogen assault in wild-type leaves is predominantly incorporated into plant membranes and might reduce their fluidity and permeability (Griebel and Zeier, 2010; Schaller, 2003). Enhanced stigmasterol formation after infection with the bacterial pathogen *Pseudomonas syringae* promotes the susceptibility of *A. thaliana* to bacterial attack (Griebel and Zeier, 2010). As in the case of pathogen contact, the increased level of stigmasterol after  $H_2O_2$  production in chloroplasts may be a response to modulate plant defence signalling by influencing the properties of ordered membrane (micro)domains. In this context it was shown that lipid rafts may play a role as platforms for the recruitment of molecular components involved in plant defence signalling (Bhat et al., 2005). These results support previous findings showing that chloroplast-derived ROS are essential during non-host interactions (Zurbriggen et al., 2009).

### **$H_2O_2$ Originating in a Specific Organelle Induces at Least two Different Spatial Signalling Effects**

In this work we identified genes whose expression is specifically modulated by either chloroplastic or peroxisomal produced  $H_2O_2$ . At the same time we identified a group of genes, whose expression is modulated by both chloroplastic and peroxisomal produced  $H_2O_2$ . These results clearly provide additional evidence that  $H_2O_2$  originating in a specific organelle can induce two different kinds of responses: one depending on the subcellular site of  $H_2O_2$  production and the other integrating  $H_2O_2$  signals independently from the subcellular site of its production (Figure 6). It is a future challenge to clarify the structure of gene networks and identify downstream responses induced by  $H_2O_2$  originating from specific organelles. Furthermore, the data presented here showed that the induced genes in GO5 plants were dominated by TFs-, protein kinases- and defence proteins-encoding genes, indicating that  $H_2O_2$  from chloroplasts induces signalling responses through the control of gene transcription and secondary signalling messengers. On the other hand, a relatively large number of genes encoding proteins involved in protein refolding, repair and degradation were induced specifically in *cat2-2* plants, suggesting that  $H_2O_2$  production in peroxisomes induced prevailing stress acclimation and/or tolerance responses.

## METHODS

### Plant material and growth conditions

*Arabidopsis thaliana* (L.) Heynh. ecotype Columbia-0 (Col-0, wild type), catalase-deficient Salk plants having 10-15% of wild-type catalase activity (*cat2-2*; N576998; (Queval et al., 2007) and *A. thaliana* plants expressing glycolate oxidase in chloroplasts (GO5 plants; (Fahnenstich et al., 2008)) were grown in pots containing three parts of soil (Gebr. Patzer KG, Sinntal-Jossa, Germany) and one part of vermiculite (Basalt Feuerfest, Linz, Austria) under a 16h light/8h dark regime at photosynthetically active photon flux densities (PPFD) of 75  $\mu\text{mol quanta m}^{-2} \text{ s}^{-1}$  at 22°C day/18°C night temperatures and a CO<sub>2</sub> concentration of 3,000 ppm. After three weeks of growth, plants were transferred to ambient CO<sub>2</sub> concentration (380 ppm) and the same PPFD. Plant material (whole rosettes or rosette leaves) were harvested at different time points after transfer, immediately frozen in liquid nitrogen and stored at -80°C until use for RNA isolation and metabolite and hormone measurements.

### Microarray analysis

For genome-wide transcriptome analysis whole rosettes from Col-0, GO5 and *cat2-2* plants were harvested at 0 and 8 h after transferring the plants to normal air conditions. Control samples were harvested at 8 h from plants continuously maintained in high CO<sub>2</sub>. RNA was isolated from samples using TRIzol Reagent (Invitrogen, Carlsbad, CA, USA). Triplicate samples were hybridised to 27 GeneChip *Arabidopsis* ATH1 Genome Arrays (Affymetrix, Santa Clara, CA, USA) at the VIB Nucleomics core facility following standard protocols (Leuven, Belgium). Quality control and Robust Multi-array Average (RMA) normalisation were performed using the R package *affy* (Bioconductor). Using the R package *limma* (Bioconductor), pair-wise comparisons between conditions or genotypes were performed using Student's *t*-test on the log<sub>2</sub> transformed values, and genes with *P* values <0.01 were retained for further analysis. To exclude changes in gene expression due to circadian effects, we compared the changes in gene expression in Col-0, GO5 and *cat2-2* in high and ambient CO<sub>2</sub> at time points 0 and 8h. Accordingly, we excluded the genes that showed changes in their expression not only due to the shift from high CO<sub>2</sub> to ambient air conditions, but also due to differences of the sampling time.

### Isolation of RNA and quantitative RT-PCR analysis



For RNA extraction rosette leaves were harvested at 0, 0.5, 4, 8 and 24 h after transferring the plants from high CO<sub>2</sub> to ambient air conditions and kept immediately in liquid nitrogen. Total RNA was extracted according to the method of (Logemann et al., 1987). RNA integrity has been tested by gel electrophoresis and its quantity was measured by NanoDrop spectrophotometer (ND-1000 spectrophotometer). First-strand cDNA synthesis was performed using SuperScriptII reverse transcriptase system (Invitrogen) following the supplier's instructions.

The relative expression levels of selected genes were analysed by qRT-PCR. The sequences of the used primers are listed in Supplemental Table 11. Quantitative RT-PCR was performed with a StepOnePlus Real Time PCR System (Applied Biosystems) on 96-well plates using SYBR Green to monitor the real-time synthesis of double-stranded DNA. Each 10- $\mu$ l reaction contained 5  $\mu$ l SYBR Green master mix reagent (Applied Biosystems), 1  $\mu$ l primer mixture (forward and reverse, 5  $\mu$ M), 1  $\mu$ l cDNA (10 ng/ $\mu$ l) and 3  $\mu$ l MilliQ water. The primer efficiency (E value) of each primer pair was determined using a standard curve. The relative expression of each gene (compared to actin, At3g18780) was calculated using the following equation:  $E_S^{-(C_{tS})}/E_A^{-(C_{tA})}$ , where  $E_S$  is the primer efficiency of the primer pair for the studied gene,  $E_A$  is that for actin,  $C_{tS}$  is the threshold cycle for the studied gene and  $C_{tA}$  is that for actin. Standard deviation has been calculated from three replicates of each treatment (Czechowski et al., 2004).

### **Metabolite analysis by GC-EI-TOF-MS**

For metabolite analysis whole rosettes from 4-week-old plants were harvested at 0, 8 and 48 h after transferring the plants to normal CO<sub>2</sub> conditions. As controls, samples were also harvested at the same time points from plants kept in the CO<sub>2</sub> chamber. Samples were quickly frozen in liquid nitrogen as described by (Lisec et al., 2006) and stored at -80°C until analysis. Three independent biological replicates consisting of three independent plants each (9 biological samples) were used. The plant material was ground in a mortar and an aliquot (50 mg fresh weight) was used for the extraction using the procedure described by (Lee and Fiehn, 2008). Ribitol was used as an internal standard for data normalisation. For GC-EI-TOF analysis, samples were processed and analysed according to (Lee and Fiehn, 2008).

Relative metabolite levels from the 9 biological samples were averaged and compared between ambient CO<sub>2</sub> and constant high CO<sub>2</sub> at the corresponding time points. Log<sub>2</sub> fold

changes in metabolite levels of ambient CO<sub>2</sub> versus constant high CO<sub>2</sub> were colour-coded and visualised as heat map. For multivariate analysis a principle component analysis (PCA, single value decomposition) was performed using the R tool (R Core Team, 2013, <http://www.R-project.org/>). The dataset was centred and autoscaled by default.

### **H<sub>2</sub>O<sub>2</sub> staining**

To visualise H<sub>2</sub>O<sub>2</sub> accumulation whole rosettes were gently vacuum infiltrated with 0.1% diaminobenzidine (DAB) in 10 mM 2-(N-morpholino)ethane-sulfonic acid (MES, pH 6.5) as described in (Thordal-Christensen et al., 1997). After 1 h of incubation the leaves were de-stained with ethanol and photographed.

### **Glucosinolate and camalexin measurements**

Whole rosettes of Col-0, GO5 and *cat2-2* plants harvested at different time points were immediately frozen in liquid nitrogen. For glucosinolate analysis the samples were lyophilised and aliquots (50-100 mg) were ground to a fine powder with a glass bead in a ball mill. After addition of 20 µl of 4 mM benzyl glucosinolate as an internal standard, glucosinolates were extracted with 1 ml 80% Methanol. Extracts were loaded on DEAE Sephadex column (0.1 g equilibrated in 0.5 M acetic acid/NaOH pH 5). Purification of desulfo glucosinolates was performed by conversion through an overnight incubation with purified sulfatase from *Helix pomatia* (Thies, 1979). For analysis of the desulfo glucosinolates the samples were subjected to an Acquity UPLC-System (Waters, Eschborn). Separation was performed with a gradient of A = 10 % Acetonitrile (100 % - 5 % (9.6 min)) and B = 90 % Acetonitrile (0 % - 95 % (9.6 min)) and a flow rate of 0.225 ml/min. UV-detection was performed at 229 nm after elution of the BEH-C18-Column (1,7 µm; 2,1 x 150 mm; Waters, Eschborn). The amount of glucosinolates was calculated as per gram of dry weight using known response factors (Muller et al., 2001) and the amount of internal standard (IS).

Isolation and analysis of camalexin was performed as described previously (Bednarek et al., 2009). For camalexin analysis, whole rosettes from Col-0, GO5 and *cat2-2* were harvested, immediately frozen in liquid nitrogen and lyophilised. After extraction with 25 µl DMSO per mg fresh weight (FW), samples were subjected to HPLC analysis using a Hyperclone C18 ODS column (Phenomenex) connected to a HPLC system (Dionex). The sample separation was performed with a gradient of A = Water (96 % - 0 %) and B = 98 % Acetonitrile (4 % - 100 %) and at a flow rate of 0.3 ml/min at 22°C. Camalexin was detected at 318 nm after

elution and calculated as relative camalexin content per g fresh weight. Camalexin standard was kindly provided by Dirk Scheel (University Halle).

### **Phytosterols measurements**

Phytosterols were extracted from around 100 mg frozen leaf material according to a method described by Griebel and Zeier (2010) with minor modifications. Frozen leaf tissue was homogenised and mixed with 600 µl extraction buffer (water:1-propanole:HCl = 1:2:0.005). After addition of 10 µg ergosterol as an internal standard and 1 ml of CH<sub>2</sub>Cl<sub>2</sub>, the mixture was shaken thoroughly and centrifuged for 1 min at 14.000 rpm for phase separation. The lower, organic phase was removed, dried over Na<sub>2</sub>SO<sub>4</sub> and subject to a vapour-phase extraction procedure described previously (Navarova et al., 2012). Vapour-phase extraction was performed with Porapak-Q absorbent (VCT-1/4X3-POR-Q; Analytical Research Systems) and the final vapourisation step at 200 °C was set up to 3 min. Samples were eluted from the vapour-phase extraction column using 1 ml of CH<sub>2</sub>Cl<sub>2</sub>, and the sample volume was subsequently reduced to 30 µl in a stream of nitrogen. The sterols were converted to trimethylsilyl derivatives by adding 10 µl of pyridine and 10 µl of BSTFA (N,N-bis-trimethylsilyl-trifluoroacetamide) and sample incubation for 30 min at 70 °C. Samples were diluted to 100 µl and a 4 µl aliquot was subjected to GC/MS analysis. The injected sample mixture was separated on a gas chromatograph (GC 7890A; Agilent Technologies) equipped with a fused silica capillary column (HP-1MS 30 m x 0.25 mm; J&W Scientific, Agilent Technologies), and mass spectra were recorded with a combined 5975C mass spectrometric detector (Agilent Technologies) in the electron ionisation mode. For GC separation, the injector temperature was 250 °C. A constant flow of helium (1.2 ml/min) and the following temperature program were used: 50 °C for 3 min, with 8 °C/min to 240 °C, with 20 °C/min to 320 °C, 320 °C for 10 min. For quantification of sterols, peaks emanating from selected ion chromatograms were integrated [m/z 368 for cholesterol, m/z 363 for ergosterol, m/z 394 for stigmasterol, m/z 382 for campesterol, m/z 396 for β-sitosterol]. The corresponding peak areas were expressed relative to the peak area of the internal standard ergosterol.

### **F<sub>v</sub>/F<sub>m</sub> measurements**

PSII Chlorophyll a fluorescence was determined with a pulse amplitude modulation fluorometer (Imaging-PAM; Walz, Effeltrich, Germany; (Schreiber et al., 1986).

The maximum quantum yield efficiency of PSII ( $F_v/F_m = [F_m - F_0]/F_m$ ) were recorded after 20 min of dark adaptation and taken as a measure of PSII integrity and plant fitness.

## SUPPLEMENTARY DATA

Supplementary Data are available at Molecular Plant Online.

## FUNDING

Financial support was provided by the Deutsche Forschungsgemeinschaft (DFG) through grant MA2379/11-1 to V.G.M., and by the Ghent University Multidisciplinary Research Partnership “Biotechnology for a Sustainable Economy” (Grant 01MRB510W) and the Interuniversity Attraction Poles Programme (IUAP P7/29 “MARS”), initiated by the Belgian Science Policy Office to F.V.B. V.B.T. was a recipient of Marie Curie Intra-European Fellowship for Career Development (PIEF-GA-2008-221427). The work of N.S. was supported by the Ministry of Higher Education of the Arab Republic of Egypt (MoHE) and the Deutscher Akademischer Austauschdienst (DAAD).

## FIGURE LEGENDS

**Figure 1.** (A) DAB staining showing H<sub>2</sub>O<sub>2</sub> production in wild type (Col-0), GO5 and *cat2-2* after transfer of high CO<sub>2</sub> grown plants to normal air at 75  $\mu\text{mol quanta m}^{-2} \text{s}^{-1}$ . (B) Maximum quantum yield of PSII ( $F_v/F_M$ ) determined in Col-0, GO5 and *cat2-2* at different time points after transfer of high CO<sub>2</sub> grown plants to normal air and of the same plants maintained in high CO<sub>2</sub> conditions.

**Figure 2.** (A) Heat map of individual metabolites comparing ambient CO<sub>2</sub> and high CO<sub>2</sub> in wild-type (Col-0), GO5 and *cat2-2* plants ( $\log_2$  fold change). (B) PCA score plot of GC/MS metabolite data. (C) PCA loadings plot of GC-EI-TOF-MS metabolite data.

**Figure 3.** (A) Venn diagram of the number of H<sub>2</sub>O<sub>2</sub>-responsive genes up-regulated only in GO5 or *cat2-2* and in both, GO5 and *cat2-2*, after 8 h of H<sub>2</sub>O<sub>2</sub> production. (B) Pie chart of the functional categories of genes whose expression was up-regulated specifically by chloroplastic produced H<sub>2</sub>O<sub>2</sub>. (C) Pie chart of the functional categories of genes whose expression was up-regulated by both, chloroplastic and peroxisomal produced H<sub>2</sub>O<sub>2</sub>. (D) Pie

chart of the functional categories of genes whose expression was up-regulated specifically by peroxisomal produced H<sub>2</sub>O<sub>2</sub>.

**Figure 4.** Dynamics of the transcriptional responses of selected genes in GO5 and *cat2-2* plants analysed by qRT-PCR. The asterisk (\*) indicates statistically significant difference to the time point t=0.

**Figure 5.** Schematic representation of the camalexin and indole glucosinolate biosynthetic pathways showing the genes upregulated by chloroplastic produced H<sub>2</sub>O<sub>2</sub>. FC indicates the fold change induction of gene expression with respect to the wild type. I3M = indol-3-ylmethyl glucosinolate = Glucobrassicin; 4OH-I3M = 4-hydroxy-indol-3-ylmethyl glucosinolate = 4-hydroxyglucobrassicin; 4MO-I3M = methoxy-indol-3-ylmethyl glucosinolate = 4-methoxyglucobrassicin.

**Figure 6.** Diagram showing spatial H<sub>2</sub>O<sub>2</sub> signalling effects. H<sub>2</sub>O<sub>2</sub> originating from chloroplasts or peroxisomes can induce two different kinds of responses: one that is dependent of the subcellular H<sub>2</sub>O<sub>2</sub> production site and the other that integrates H<sub>2</sub>O<sub>2</sub> signals independently from the subcellular site of its production.

## TABLES

**Table 1.** List of the top 20 genes, whose expression is specifically up-regulated after 8 h of H<sub>2</sub>O<sub>2</sub> production in chloroplasts. Cat, category; DD, detoxification and defence; M, metabolism; PFR, protein folding and repair; S, signalling; TF, transcription factor; -, unknown; FC, fold change.

**Table 2.** List of the top 20 genes, whose expression is specifically up-regulated after 8 h of H<sub>2</sub>O<sub>2</sub> production in peroxisomes. Cat, category; DD, detoxification and defence; M, metabolism; PFR, protein folding and repair; S, signalling; TF, transcription factor; -, unknown; FC, fold change.

**Table 3.** List of the top 20 genes, whose expression is up-regulated after 8 h of H<sub>2</sub>O<sub>2</sub> production in chloroplasts and peroxisomes. Cat, category; DD, detoxification and defence; M, metabolism; PFR, protein folding and repair; S, signalling; TF, transcription factor; -, unknown; FC, fold change.

**Table 4.** Timecourse analysis of 4MO-I3M and stigmaterol concentrations in leaves of wild type (WT, Col-0), GO5 and *cat2-2* plants under non photorespiratory and photorespiratory

conditions. The samples were harvested at 0, 8, 32 and 56 h after transferring long day-grown plants from high CO<sub>2</sub> to normal air conditions. Values are means ± standard error from three samples, each consisting of six leaves. H, High CO<sub>2</sub> concentration (3,000 ppm CO<sub>2</sub>); non-photorespiratory conditions. A, Ambient CO<sub>2</sub> concentration (380 ppm CO<sub>2</sub>); photorespiratory conditions. DW, dry weight; FW, fresh weight. Values statistically different from the wild type are highlighted in bold case.

## REFERENCES

- Arnqvist L., Persson M., Jonsson L., Dutta P.C., Sitbon F. (2008). Overexpression of CYP710A1 and CYP710A4 in transgenic Arabidopsis plants increases the level of stigmasterol at the expense of sitosterol. *Planta* 227: 309-317.
- Balazadeh S., Jaspert N., Arif M., Mueller-Roeber B., Maurino V.G. (2012). Expression of ROS-responsive genes and transcription factors after metabolic formation of H<sub>2</sub>O<sub>2</sub> in chloroplasts. *Front Plant Sci* 3: 234.
- Bandurski R.S., Cohen J.D., Slovin J.P., Reinecke D.M. (1995). Auxin biosynthesis and metabolism. In: *Plant Hormones: Physiology, Biochemistry and Molecular Biology*-- Davies, P.J., ed. Dordrecht, The Netherlands: Kluwer Academic Press. 39–65.
- Baxter C.J., Redestig H., Schauer N., Reipsilber D., Patil K.R., Nielsen J., Selbig J., Liu J., Fernie A.R., Sweetlove L.J. (2007). The metabolic response of heterotrophic Arabidopsis cells to oxidative stress. *Plant Physiol* 143: 312-325.
- Bednarek P., Pislewska-Bednarek M., Svatos A., Schneider B., Doubtsky J., Mansurova M., Humphry M., Consonni C., Panstruga R., Sanchez-Vallet A., et al. (2009). A glucosinolate metabolism pathway in living plant cells mediates broad-spectrum antifungal defense. *Science* 323: 101-106.
- Bhat R.A., Miklis M., Schmelzer E., Schulze-Lefert P., Panstruga R. (2005). Recruitment and interaction dynamics of plant penetration resistance components in a plasma membrane microdomain. *Proc Natl Acad Sci U S A* 102: 3135-3140.
- Bienert, G.P. and Chaumont, F. (2013). Aquaporin-facilitated transmembrane diffusion of hydrogen peroxide. *Biochim. Biophys. Acta - Gen. Subj.*
- Bolwell G.P. (1999). Role of active oxygen species and NO in plant defence responses. *Curr Opin Plant Biol* 2: 287-294.
- Chaouch, S., Queval, G. and Noctor, G. (2012). AtRbohF is a crucial modulator of defence-associated metabolism and a key actor in the interplay between intracellular oxidative stress and pathogenesis responses in Arabidopsis. *Plant J.* 69:613–627.
- Czechowski T., Bari R.P., Stitt M., Scheible W.R., Udvardi M.K. (2004). Real-time RT-PCR profiling of over 1400 Arabidopsis transcription factors: unprecedented sensitivity reveals novel root- and shoot-specific genes. *Plant J* 38: 366-379.

- D'Autreaux B., Toledano M.B. (2007). ROS as signalling molecules: mechanisms that generate specificity in ROS homeostasis. *Nat Rev Mol Cell Biol* 8: 813-824.
- Dat J., Vandenameele S., Vranova E., Van Montagu M., Inze D., Van Breusegem F. (2000). Dual action of the active oxygen species during plant stress responses. *Cell Mol Life Sci* 57: 779-795.
- Davletova S., Rizhsky L., Liang H., Shengqiang Z., Oliver D.J., Coutu J., Shulaev V., Schlauch K., Mittler R. (2005). Cytosolic ascorbate peroxidase 1 is a central component of the reactive oxygen gene network of Arabidopsis. *Plant Cell* 17: 268-281.
- Dean, R.T., Fu, S., Stocker, R. and Davies, M.J. (1997). Biochemistry and pathology of radical-mediated protein oxidation. *Biochem. J.* 324 ( Pt 1):1–18.
- Debska, K., Krasuska, U., Budnicka, K., Bogatek, R. and Gniazdowska, A. (2013). Dormancy removal of apple seeds by cold stratification is associated with fluctuation in H<sub>2</sub>O<sub>2</sub>, NO production and protein carbonylation level. *J. Plant Physiol.* 170:480–488.
- De Clercq I., Vermeirssen V., Van Aken O., Vandepoele K., Murcha M.W., Law S.R., Inze A., Ng S., Ivanova A., Rombaut D., et al. (2013). The membrane-bound NAC transcription factor ANAC013 functions in mitochondrial retrograde regulation of the oxidative stress response in Arabidopsis. *Plant Cell* 25: 3472-3490.
- Delaunay A., Isnard A.D., Toledano M.B. (2000). H<sub>2</sub>O<sub>2</sub> sensing through oxidation of the Yap1 transcription factor. *EMBO J* 19: 5157-5166.
- Desikan R., Hancock J.T., Bright J., Harrison J., Weir I., Hooley R., Neill S.J. (2005). A role for ETR1 in hydrogen peroxide signaling in stomatal guard cells. *Plant Physiol* 137: 831-834.
- Desikan R., Hancock J.T., Ichimura K., Shinozaki K., Neill S.J. (2001a). Harpin induces activation of the Arabidopsis mitogen-activated protein kinases AtMPK4 and AtMPK6. *Plant Physiol* 126: 1579-1587.
- Desikan R., Mackerness S.A., Hancock J.T., Neill S.J. (2001b). Regulation of the Arabidopsis transcriptome by oxidative stress. *Plant Physiol* 127: 159-172.



- Eudes A., Bozzo G.G., Waller J.C., Naponelli V., Lim E.K., Bowles D.J., Gregory J.F., 3rd, Hanson A.D. (2008). Metabolism of the folate precursor p-aminobenzoate in plants: glucose ester formation and vacuolar storage. *J Biol Chem* 283: 15451-15459.
- Fahnenstich H., Scarpeci T.E., Valle E.M., Flugge U.I., Maurino V.G. (2008). Generation of hydrogen peroxide in chloroplasts of Arabidopsis overexpressing glycolate oxidase as an inducible system to study oxidative stress. *Plant Physiol* 148: 719-729.
- Finkel T. (2000). Redox-dependent signal transduction. *FEBS Lett* 476: 52-54.
- Fridovich, I. (1997). Superoxide anion radical, superoxide dismutases, and related matters. *J. Biol. Chem.* 272:18515–18517.
- Fryer M.J., Ball L., Oxborough K., Karpinski S., Mullineaux P.M., Baker N.R. (2003). Control of Ascorbate Peroxidase 2 expression by hydrogen peroxide and leaf water status during excess light stress reveals a functional organisation of Arabidopsis leaves. *Plant J* 33: 691-705.
- Fryer M.J., Oxborough K., Mullineaux P.M., Baker N.R. (2002). Imaging of photo-oxidative stress responses in leaves. *J Exp Bot* 53: 1249-1254.
- Gadjev I., Vanderauwera S., Gechev T.S., Laloi C., Minkov I.N., Shulaev V., Apel K., Inze D., Mittler R., Van Breusegem F. (2006). Transcriptomic footprints disclose specificity of reactive oxygen species signaling in Arabidopsis. *Plant Physiol* 141: 436-445.
- Gechev T.S., Minkov I.N., Hille J. (2005). Hydrogen peroxide-induced cell death in Arabidopsis: transcriptional and mutant analysis reveals a role of an oxoglutarate-dependent dioxygenase gene in the cell death process. *IUBMB Life* 57: 181-188.
- Gonneau M., Pagant S., Brun F., Laloue M. (2001). Photoaffinity labelling with the cytokinin agonist azido-CPPU of a 34 kDa peptide of the intracellular pathogenesis-related protein family in the moss *Physcomitrella patens*. *Plant Mol Biol* 46: 539-548.
- Griebel T., Zeier J. (2010). A role for beta-sitosterol to stigmasterol conversion in plant-pathogen interactions. *Plant J* 63: 254-268.
- Harborne J.B., Grayer R.J. (1988). The anthocyanins. In: *The Flavonoids: Advances in Research since 1980*--J.B., H., ed. London: Chapman and Hall. 1–20.

- Hooijmaijers, C., Rhee, J.Y., Kwak, K.J., Chung, G.C., Horie, T., Katsuhara, M. and Kang, H. (2012). Hydrogen peroxide permeability of plasma membrane aquaporins of *Arabidopsis thaliana*. *J. Plant Res.* 125:147–153.
- Horvath I., Glatz A., Varvasovszki V., Torok Z., Pali T., Balogh G., Kovacs E., Nadasdi L., Benko S., Joo F., et al. (1998). Membrane physical state controls the signaling mechanism of the heat shock response in *Synechocystis* PCC 6803: identification of hsp17 as a "fluidity gene". *Proc Natl Acad Sci U S A* 95: 3513-3518.
- Hvorup R.N., Winnen B., Chang A.B., Jiang Y., Zhou X.F., Saier M.H., Jr. (2003). The multidrug/oligosaccharidyl-lipid/polysaccharide (MOP) exporter superfamily. *Eur J Biochem* 270: 799-813.
- Inze A., Vanderauwera S., Hoerberichts F.A., Vandorpe M., Van Gaeveer T., Van Breusegem F. (2012). A subcellular localization compendium of hydrogen peroxide-induced proteins. *Plant Cell Environ* 35: 308-320.
- Jain, V., Kaiser, W. and Huber, S.C. (2008). Cytokinin inhibits the proteasome-mediated degradation of carbonylated proteins in *Arabidopsis* leaves. *Plant Cell Physiol.* 49:843–852.
- Jang, J.Y., Rhee, J.Y., Chung, G.C. and Kang, H. (2012). Aquaporin as a membrane transporter of hydrogen peroxide in plant response to stresses. *Plant Signal. Behav.* 7:1180–1181.
- Joo J.H., Wang S., Chen J.G., Jones A.M., Fedoroff N.V. (2005). Different signaling and cell death roles of heterotrimeric G protein alpha and beta subunits in the *Arabidopsis* oxidative stress response to ozone. *Plant Cell* 17: 957-970.
- Karpinski S., Reynolds H., Karpinska B., Wingsle G., Creissen G., Mullineaux P. (1999). Systemic signaling and acclimation in response to excess excitation energy in *Arabidopsis*. *Science* 284: 654-657.
- Kim J.R., Yoon H.W., Kwon K.S., Lee S.R., Rhee S.G. (2000). Identification of proteins containing cysteine residues that are sensitive to oxidation by hydrogen peroxide at neutral pH. *Anal Biochem* 283: 214-221.

- Kitamura S., Shikazono N., Tanaka A. (2004). TRANSPARENT TESTA 19 is involved in the accumulation of both anthocyanins and proanthocyanidins in *Arabidopsis*. *Plant J* 37: 104-114.
- Kokkinakis D.M., Brooks J.L. (1979). Hydrogen Peroxide-mediated Oxidation of Indole-3-acetic Acid by Tomato Peroxidase and Molecular Oxygen. *Plant Physiol* 64: 220-223.
- Kovtun Y., Chiu W.L., Tena G., Sheen J. (2000). Functional analysis of oxidative stress-activated mitogen-activated protein kinase cascade in plants. *Proc Natl Acad Sci U S A* 97: 2940-2945.
- Langlois-Meurinne M., Gachon C.M., Saindrenan P. (2005). Pathogen-responsive expression of glycosyltransferase genes UGT73B3 and UGT73B5 is necessary for resistance to *Pseudomonas syringae* pv tomato in *Arabidopsis*. *Plant Physiol* 139: 1890-1901.
- Lee D.Y., Fiehn O. (2008). High quality metabolomic data for *Chlamydomonas reinhardtii*. *Plant Methods* 4: 7.
- Lisec J., Schauer N., Kopka J., Willmitzer L., Fernie A.R. (2006). Gas chromatography mass spectrometry-based metabolite profiling in plants. *Nat Protoc* 1: 387-396.
- Logemann J., Schell J., Willmitzer L. (1987). Improved method for the isolation of RNA from plant tissues. *Anal Biochem* 163: 16-20.
- Maurino V.G., Flugge U.I. (2008). Experimental systems to assess the effects of reactive oxygen species in plant tissues. *Plant Signal Behav* 3: 923-928.
- Meinhard M., Rodriguez P.L., Grill E. (2002). The sensitivity of ABI2 to hydrogen peroxide links the abscisic acid-response regulator to redox signalling. *Planta* 214: 775-782.
- Mhamdi, A., Noctor, G. and Baker, A. (2012). Plant catalases: Peroxisomal redox guardians. *Arch. Biochem. Biophys.* 525:181–194.
- Millet Y.A., Danna C.H., Clay N.K., Songnuan W., Simon M.D., Werck-Reichhart D., Ausubel F.M. (2010). Innate immune responses activated in *Arabidopsis* roots by microbe-associated molecular patterns. *Plant Cell* 22: 973-990.

- Mittler, R., Vanderauwera, S., Suzuki, N., Miller, G., Tognetti, V.B., Vandepoele, K., Gollery, M., Shulaev, V. and Breusegem, F. Van (2011). ROS signaling: The new wave? *Trends Plant Sci.* 16:300–309.
- Moller, I.M., Jensen, P.E. and Hansson, A. (2007). Oxidative modifications to cellular components in plants. *Annu. Rev. Plant Biol.* 58:459–481.
- Moller I.M., Sweetlove L.J. (2010). ROS signalling--specificity is required. *Trends Plant Sci* 15: 370-374.
- Morikawa T., Mizutani M., Aoki N., Watanabe B., Saga H., Saito S., Oikawa A., Suzuki H., Sakurai N., Shibata D. (2006). Cytochrome P450 CYP710A encodes the sterol C-22 desaturase in Arabidopsis and tomato. *Plant Cell* 18: 1008-1022.
- Morita M., Shitan N., Sawada K., Van Montagu M.C., Inze D., Rischer H., Goossens A., Oksman-Caldentey K.M., Moriyama Y., Yazaki K. (2009). Vacuolar transport of nicotine is mediated by a multidrug and toxic compound extrusion (MATE) transporter in *Nicotiana tabacum*. *Proc Natl Acad Sci U S A* 106: 2447-2452.
- Mueller L.A., Goodman C.D., Silady R.A., Walbot V. (2000). AN9, a petunia glutathione S-transferase required for anthocyanin sequestration, is a flavonoid-binding protein. *Plant Physiol* 123: 1561-1570.
- Muller C., Agerbirk N., Olsen C.E., Boeve J.L., Schaffner U., Brakefield P.M. (2001). Sequestration of host plant glucosinolates in the defensive hemolymph of the sawfly *Athalia rosae*. *J Chem Ecol* 27: 2505-2516.
- Navarova H., Bernsdorff F., Doring A.C., Zeier J. (2012). Pipecolic acid, an endogenous mediator of defense amplification and priming, is a critical regulator of inducible plant immunity. *Plant Cell* 24: 5123-5141.
- Ng S., Ivanova A., Duncan O., Law S.R., Van Aken O., De Clercq I., Wang Y., Carrie C., Xu L., Kmiec B., et al. (2013). A membrane-bound NAC transcription factor, ANAC017, mediates mitochondrial retrograde signaling in Arabidopsis. *Plant Cell* 25: 3450-3471.
- Omote H., Hiasa M., Matsumoto T., Otsuka M., Moriyama Y. (2006). The MATE proteins as fundamental transporters of metabolic and xenobiotic organic cations. *Trends Pharmacol Sci* 27: 587-593.

- op den Camp R.G., Przybyla D., Ochsenbein C., Laloi C., Kim C., Danon A., Wagner D., Hideg E., Gobel C., Feussner I., et al. (2003). Rapid induction of distinct stress responses after the release of singlet oxygen in *Arabidopsis*. *Plant Cell* 15: 2320-2332.
- Orozco-Cardenas M.L., Narvaez-Vasquez J., Ryan C.A. (2001). Hydrogen peroxide acts as a second messenger for the induction of defense genes in tomato plants in response to wounding, systemin, and methyl jasmonate. *Plant Cell* 13: 179-191.
- Ostin A., Kowalyczk M., Bhalerao R.P., Sandberg G. (1998). Metabolism of indole-3-acetic acid in *Arabidopsis*. *Plant Physiol* 118: 285-296.
- Palaniswamy S.K., James S., Sun H., Lamb R.S., Davuluri R.V., Grotewold E. (2006). AGRIS and AtRegNet. a platform to link cis-regulatory elements and transcription factors into regulatory networks. *Plant Physiol* 140: 818-829.
- Pei, Z.M., Murata, Y., Benning, G., Thomine, S., Klüsener, B., Allen, G.J., Grill, E. and Schroeder, J.I. (2000). Calcium channels activated by hydrogen peroxide mediate abscisic acid signalling in guard cells. *Nature*. 406:731–734.
- Polidoros A.N., Mylona P.V., Pasentsis K., Scandalios J.G., Tsaftaris A.S. (2005). The maize alternative oxidase 1a (*Aox1a*) gene is regulated by signals related to oxidative stress. *Redox Rep* 10: 71-78.
- Poppenberger B., Fujioka S., Soeno K., George G.L., Vaistij F.E., Hiranuma S., Seto H., Takatsuto S., Adam G., Yoshida S., et al. (2005). The *UGT73C5* of *Arabidopsis thaliana* glucosylates brassinosteroids. *Proc Natl Acad Sci U S A* 102: 15253-15258.
- Prasad T.K. (1997). Role of Catalase in Inducing Chilling Tolerance in Pre-Emergent Maize Seedlings. *Plant Physiol* 114: 1369-1376.
- Queval G., Issakidis-Bourguet E., Hoerberichts F.A., Vandorpe M., Gakiere B., Vanacker H., Miginiac-Maslow M., Van Breusegem F., Noctor G. (2007). Conditional oxidative stress responses in the *Arabidopsis* photorespiratory mutant *cat2* demonstrate that redox state is a key modulator of daylength-dependent gene expression, and define photoperiod as a crucial factor in the regulation of H<sub>2</sub>O<sub>2</sub>-induced cell death. *Plant J* 52: 640-657.

- Rao M.V., Davis K.R. (2001). The physiology of ozone induced cell death. *Planta* 213: 682-690.
- Rizhsky L., Liang H., Mittler R. (2003). The water-water cycle is essential for chloroplast protection in the absence of stress. *J Biol Chem* 278: 38921-38925.
- Rosenwasser S., Fluhr R., Joshi J.R., Leviatan N., Sela N., Hetzroni A., Friedman H. (2013). ROSMETER: a bioinformatic tool for the identification of transcriptomic imprints related to reactive oxygen species type and origin provides new insights into stress responses. *Plant Physiol* 163: 1071-1083.
- Ross J., Li Y., Lim E., Bowles D.J. (2001). Higher plant glycosyltransferases. *Genome Biol* 2: 3004.3001-3004.3006
- Saga H., Ogawa T., Kai K., Suzuki H., Ogata Y., Sakurai N., Shibata D., Ohta D. (2012). Identification and Characterization of ANAC042, a Transcription Factor Family Gene Involved in the Regulation of Camalexin Biosynthesis in Arabidopsis. *Mol Plant Microbe Interact* 25: 684-696.
- Sandermann H., Jr. (2004). Molecular ecotoxicology of plants. *Trends Plant Sci* 9: 406-413.
- Schaller H. (2003). The role of sterols in plant growth and development. *Prog Lipid Res* 42: 163-175.
- Schreiber U., Schliwa U., Bilger W. (1986). Continuous recording of photochemical and non-photochemical chlorophyll fluorescence quenching with a new type of modulation fluorometer. *Photosynth Res* 10: 51-62.
- Shiu S.H., Bleecker A.B. (2001). Plant receptor-like kinase gene family: diversity, function, and signaling. *Sci STKE* 2001: re22.
- Shiu S.H., Bleecker A.B. (2003). Expansion of the receptor-like kinase/Pelle gene family and receptor-like proteins in Arabidopsis. *Plant Physiol* 132: 530-543.
- Smith A.P., Nourizadeh S.D., Peer W.A., Xu J., Bandyopadhyay A., Murphy A.S., Goldsbrough P.B. (2003). Arabidopsis AtGSTF2 is regulated by ethylene and auxin, and encodes a glutathione S-transferase that interacts with flavonoids. *Plant J* 36: 433-442.

- SUN, J. et al. (2010). H<sub>2</sub>O<sub>2</sub> and cytosolic Ca<sup>2+</sup> signals triggered by the PM H<sup>+</sup>-coupled transport system mediate K<sup>+</sup>/Na<sup>+</sup> homeostasis in NaCl-stressed *Populus euphratica* cells. *Plant. Cell Environ.* 33:943–958.
- Sweetlove L.J., Heazlewood J.L., Herald V., Holtzapffel R., Day D.A., Leaver C.J., Millar A.H. (2002). The impact of oxidative stress on *Arabidopsis* mitochondria. *Plant J* 32: 891-904.
- Thies W. (1979). Detection and utilisation of a glucosinolate sulfohydrolase in the edible snail *Helix pomatia*. *Naturwissenschaften* 66: 364-365.
- Thordal-Christensen H., Zhang Z., Wei Y., Collinge D.B. (1997). Subcellular localization of H<sub>2</sub>O<sub>2</sub> in plants: H<sub>2</sub>O<sub>2</sub> accumulation in papillae and hypersensitive response during the barley-powdery mildew interaction. *Plant J* 11: 1187–1194.
- Tognetti V.B., Van Aken O., Morreel K., Vandenbroucke K., van de Cotte B., De Clercq I., Chiwocha S., Fenske R., Prinsen E., Boerjan W., et al. (2010). Perturbation of indole-3-butyric acid homeostasis by the UDP-glucosyltransferase UGT74E2 modulates *Arabidopsis* architecture and water stress tolerance. *Plant Cell* 22: 2660-2679.
- Triantaphylides C., Krischke M., Hoeberichts F.A., Ksas B., Gresser G., Havaux M., Van Breusegem F., Mueller M.J. (2008). Singlet oxygen is the major reactive oxygen species involved in photooxidative damage to plants. *Plant Physiol* 148: 960-968.
- Umbach A.L., Fiorani F., Siedow J.N. (2005). Characterization of transformed *Arabidopsis* with altered alternative oxidase levels and analysis of effects on reactive oxygen species in tissue. *Plant Physiol* 139: 1806-1820.
- Vandenabeele S., Van Der Kelen K., Dat J., Gadjev I., Boonefaes T., Morsa S., Rottiers P., Slooten L., Van Montagu M., Zabeau M., et al. (2003). A comprehensive analysis of hydrogen peroxide-induced gene expression in tobacco. *Proc Natl Acad Sci U S A* 100: 16113-16118.
- Vandenabeele S., Vanderauwera S., Vuylsteke M., Rombauts S., Langebartels C., Seidlitz H.K., Zabeau M., Van Montagu M., Inze D., Van Breusegem F. (2004). Catalase deficiency drastically affects gene expression induced by high light in *Arabidopsis thaliana*. *Plant J* 39: 45-58.

- Vandenbroucke K., Robbens S., Vandepoele K., Inze D., Van de Peer Y., Van Breusegem F. (2008). Hydrogen peroxide-induced gene expression across kingdoms: a comparative analysis. *Mol Biol Evol* 25: 507-516.
- Vanderauwera S., Zimmermann P., Rombauts S., Vandenabeele S., Langebartels C., Gruissem W., Inze D., Van Breusegem F. (2005). Genome-wide analysis of hydrogen peroxide-regulated gene expression in *Arabidopsis* reveals a high light-induced transcriptional cluster involved in anthocyanin biosynthesis. *Plant Physiol* 139: 806-821.
- Vogt T., Jones P. (2000). Glycosyltransferases in plant natural product synthesis: characterization of a supergene family. *Trends Plant Sci* 5: 380-386.
- Wang B., Jin S.H., Hu H.Q., Sun Y.G., Wang Y.W., Han P., Hou B.K. (2012). UGT87A2, an *Arabidopsis* glycosyltransferase, regulates flowering time via FLOWERING LOCUS C. *New Phytol* 194: 666-675.
- Wollenweber E., Jay M. (1988). Flavones and flavonols. In: *The Flavonoids: Advances in Research since 1980*--Harborne, J.B., ed. 233–302.
- Zurbriggen M.D., Carrillo N., Tognetti V.B., Melzer M., Peisker M., Hause B., Hajirezaei M.R. (2009). Chloroplast-generated reactive oxygen species play a major role in localized cell death during the non-host interaction between tobacco and *Xanthomonas campestris* pv. *vesicatoria*. *Plant J* 60: 962-973.



**Table 1.** List of the top 20 genes, whose expression is specifically up-regulated after 8 h of H<sub>2</sub>O<sub>2</sub> production in chloroplasts. Cat, category; DD, detoxification and defence; M, metabolism; PFR, protein folding and repair; S, signalling; TF, transcription factor; -, unknown; FC, fold change.

Locus	Description	Molecular/Biological function	Cat	FC
At2g04050	DTX3	MATE efflux carrier, putative/ Mitochondrial retrograde regulation of oxidative stress response	DD	124.0
At5g62480	GSTU9	Tau glutathione S-transferase	DD	54.9
At2g04040	DTX1	MATE efflux carrier /Detoxification of Cd <sup>2+</sup>	DD	31.7
At2g04070	DTX4	MATE efflux carrier, putative/ Mitochondrial retrograde regulation of oxidative stress response	DD	28.3
At3g26830	PAD3; CYP71B15	Cytochrome P450/Camalexin synthase	DD	25.9
At5g61160	AACT1	Agmatine coumaroyltransferase/ Biosynthesis of hydroxycinnamic acid amides. Defence against pathogens.	M	23.1
At1g66690	-	S-adenosyl-L-methionine methyltransferase, putative	M	21.8
At1g32350	AOX1D	Alternative oxidase	DD	20.7
At2g18190	-	AAA-type ATPase, putative	M	19.1
At2g32020	-	Alanine acetyl transferase, putative/ Mitochondrial retrograde regulation of oxidative stress response	M	18.9
At2g20720	-	-	-	18.5
At1g26380	-	ATP-binding reticuline dehydrogenase, putative	M	15.7
At3g28580	-	AAA-type ATPase, putative	M	15.6
At3g45730	-	-	-	15.4
At3g50930	-	AAA-type ATPase, putative	M	15.3
At3g61630	CRF6	Upregulated by cytokinin; Regulator of senescence	TF	15.1
At3g48850	-	phosphate transporter, putative	M	14.8

---

At3g25250	AGC2-1; OXI1	Protein kinase, putative/ Mitochondrial retrograde regulation of oxidative stress response	S	14.5
At2g26560	PLP2	Phospholipase; lipid acyl hydrolase/ role in cell death; affects the accumulation of oxylipins; resistance to virus	M	14.0
At2g16060	AHB1	Nonsymbiotic hemoglobin/Oxygen sensor or electron transfer	M	13.2

---

**Table 2.** List of the top 20 genes, whose expression is specifically up-regulated after 8 h of H<sub>2</sub>O<sub>2</sub> production in peroxisomes. Cat, category; DD, detoxification and defence; M, metabolism; PFR, protein folding and repair; S, signalling; TF, transcription factor; -, unknown; FC, fold change.

Locus	Description	Molecular/Biological function	Cat	FC
At3g28740	CYP81D11	Cytochrome P450 protein/Defence to insects	DD	21.8
At1g59860	HSP17.6A-CI	Heat shock protein. HSP20-like chaperone	PFR	16.6
At3g28210	SAP12	Stress response; Unknown function	DD	13.4
At5g12020	HSP17.6-CII	Heat shock protein. HSP20-like chaperone	PFR	11.3
At2g29500	HSP17.6B-CI	Heat shock protein. HSP20-like chaperone	PFR	10.5
At5g12030	HSP17.6A	Heat shock protein. HSP20-like chaperone	PFR	9.9
At5g52640	HSP90.1	Heat shock protein	PFR	9.0
At3g12580	HSP70	Heat shock protein/Regulation of transcription; Stabilization of proteins	PFR	7.7
At3g46230	HSP17.4-CI	Heat shock protein	PFR	6.9
At1g53540	HSP17.6C-CI	Heat shock protein. HSP20-like chaperone	PFR	6.9
At3g53230	CDC48	AAA-typeATPase, putative/Cell division and growth processes; Protein catabolism	PFR	6.6
At4g12400	HOP3	Co-chaperone, putative	PFR	5.4
At4g37990	CAD8, ELI3-2	Aromatic alcohol:NADP oxidoreductase/Lignin biosynthesis	DD	5.2
At3g20340	-	Unknown protein	-	5.1
At5g48570	FKBP65, ROF2	Co-chaperone	PFR	4.8
At1g71000	-	DNAJ heat shock protein /Chaperone, putative	PFR	4.8
At5g16980	-	Oxidoreductase, putative	M	4.5
At1g09080	BiP-3	Heat shock protein. HSP70-like chaperone/ Regulation of transcription; Stabilization of proteins	PFR	4.1

## Manuscript 2

---

---

At2g17500	PILS5	Auxin efflux carrier, putative	S	4.0
At1g10585	-	bHLH transcription factor. unkonwn	TF	4.0

---

**Table 3.** List of the top 20 genes, whose expression is up-regulated after 8 h of H<sub>2</sub>O<sub>2</sub> production in chloroplasts and peroxisomes. Cat, category; DD, detoxification and defence; M, metabolism; PFR, protein folding and repair; S, signalling; TF, transcription factor; -, unknown; FC, fold change.

Locus	Description	Molecular/Biological function	Cat	FC GO5	FC <i>cat2-2</i>
At1g05680	UGT74E2	UDP-glucosyltransferase /Acts on IBA; Responses to abiotic stress by regulating auxin homeostasis; Mitochondrial retrograde regulation of oxidative stress response	DD, S	185.2	20.7
At2g47000	PGP4	ABC transporter/Auxin transmembrane transporter	DD	78.2	4.5
At2g41730	-	Unknown; Mitochondrial retrograde regulation of oxidative stress response	DD, S	53.9	3.6
At1g17170	GSTU24	Tau Glutathione S-transferase	DD	46.3	40.4
At5g51440	HSP23.5-M	Heat shock protein; chaperone/ Mitochondrial retrograde regulation of oxidative stress response	PFR, S	25.9	14.6
At2g36800	UGT73C5	UDP-glucosyltransferase/Acts on brassinolides and trans-zeatin	DD	25.1	4.6
At4g37370	CYP81D8	Cytochrome P450	-	20.8	3.3
At2g03760	SOT12	Brassinosteroid sulfotransferase/Involved in detoxification	DD	20.0	2.8
At3g63380	ACA12	Ca <sup>2+</sup> -transporting ATPase	S	19.9	2.7
At5g43450	-	2OG-Fe(II) oxygenase; Similar to ACC oxidase/ Mitochondrial retrograde regulation of oxidative stress response	S	14.0	2.1
At4g01870	-	Contains WD40-like Beta propeller repeat	-	13.7	10.0
At5g14730	-	Unknown/ Mitochondrial retrograde regulation of oxidative stress response	S	13.1	3.0

---

At3g55920	CYP21-2	Peptidyl-prolyl isomerase, putative/ folding	Protein	PFR	12.6	16.0
At1g67810	SUFE2	Activates cysteine desulfurase; involved in iron- sulfur cluster assembly		PFR	11.8	3.1
At2g41380	-	S-adenosyl-L-methionine-dependent methyltransferase-like		M	10.7	4.5
At2g36750	UGT73C1	UDP-glucosyltransferase/Acts on trans-zeatin and dihydrozeatin		M	10.5	4.7
At1g17180	GSTU25	Tau Glutathione S-transferase		DD	10.0	32.5
At2g38340	DRE2B	AP2 domain-transcription factor, putative		TF	9.6	2.5
At3g22370	AOX1A	Alternative oxidase/Reduction of ROS production; Mitochondrial retrograde regulation of oxidative stress response		DD, S	9.5	2.1
At4g34131	UGT73B3	UDP-glucosyl transferase/Resistance to pathogens		DD	9.4	7.4

---

**Table 4.** Timecourse analysis of 4MO-I3M and stigmasterol concentrations in leaves of wild type (WT, Col-0), GO5 and *cat2-2* plants under non photorespiratory and photorespiratory conditions. The samples were harvested at 0, 8, 32 and 56 h after transferring long day-grown plants from high CO<sub>2</sub> to normal air conditions. Values are means  $\pm$  standard error from three samples, each consisting of six leaves. H, High CO<sub>2</sub> concentration (3,000 ppm CO<sub>2</sub>); non-photorespiratory conditions. A, Ambient CO<sub>2</sub> concentration (380 ppm CO<sub>2</sub>); photorespiratory conditions. DW, dry weight; FW, fresh weight. Values statistically different from the wild type are highlighted in bold case.

		4MO-I3M ( $\mu\text{mol/g DW}$ )		Stigmasterol ( $\mu\text{g/g FW}$ )	
		H	A	H	A
<b>WT</b>	0	2.1 $\pm$ 0.2	-	1.0 $\pm$ 0.1	-
	8	2.2 $\pm$ 0.2	1.7 $\pm$ 0.1	1.7 $\pm$ 0.7	1.0 $\pm$ 0.0
	32	1.9 $\pm$ 0.2	1.1 $\pm$ 0.1	1.2 $\pm$ 0.2	0.4 $\pm$ 0.0
	56	1.2 $\pm$ 0.1	0.9 $\pm$ 0.1	0.5 $\pm$ 0.2	1.0 $\pm$ 0.3
<b>GO5</b>	0	2.2 $\pm$ 0.1	-	1.2 $\pm$ 0.8	-
	8	<b>1.6 <math>\pm</math> 0.1</b>	<b>2.1 <math>\pm</math> 0.1</b>	1.2 $\pm$ 0.4	0.8 $\pm$ 0.1
	32	2.1 $\pm$ 0.1	<b>1.5 <math>\pm</math> 0.1</b>	0.8 $\pm$ 0.1	<b>5.3 <math>\pm</math> 2.0</b>
	56	1.2 $\pm$ 0.1	0.9 $\pm$ 0.1	0.7 $\pm$ 0.2	<b>5.4 <math>\pm</math> 0.7</b>
<b><i>cat2-2</i></b>	0	2.2 $\pm$ 0.3	-	0.9 $\pm$ 0.1	-
	8	<b>1.6 <math>\pm</math> 0.1</b>	1.8 $\pm$ 0.1	0.6 $\pm$ 0.1	3.7 $\pm$ 2.7
	32	2.0 $\pm$ 0.2	<b>1.5 <math>\pm</math> 0.1</b>	1.3 $\pm$ 0.4	0.6 $\pm$ 0.2
	56	<b>1.4 <math>\pm</math> 0.0</b>	1.0 $\pm$ 0.0	0.7 $\pm$ 0.2	1.5 $\pm$ 0.5

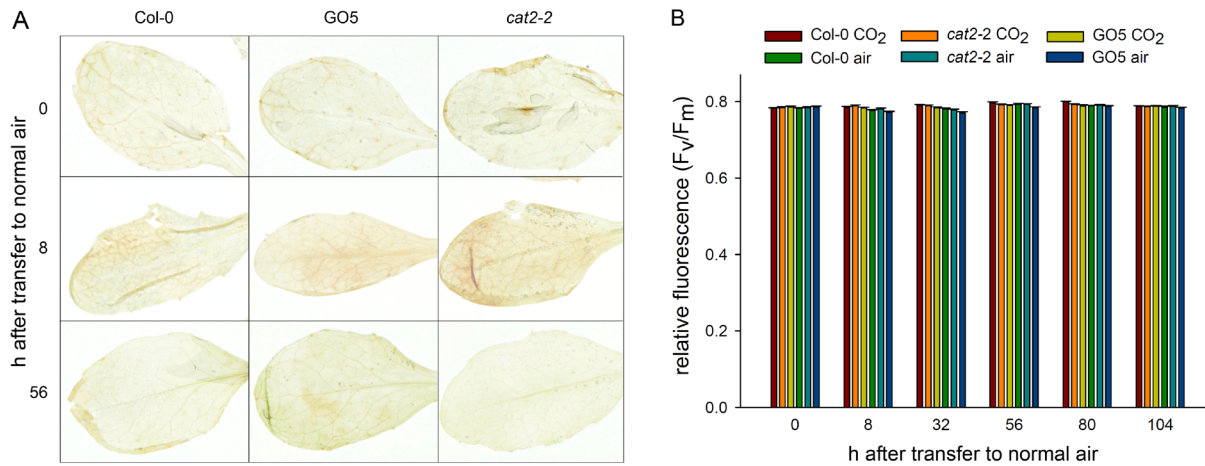


**Figure 1.** (A) DAB staining showing H<sub>2</sub>O<sub>2</sub> production in wild type (Col-0), GO5 and *cat2-2* after transfer of high CO<sub>2</sub> grown plants to normal air at 75  $\mu\text{mol quanta m}^{-2} \text{s}^{-1}$ . (B) Maximum quantum yield of PSII ( $F_v/F_M$ ) determined in Col-0, GO5 and *cat2-2* at different time points after transfer of high CO<sub>2</sub> grown plants to normal air and of the same plants maintained in high CO<sub>2</sub> conditions.



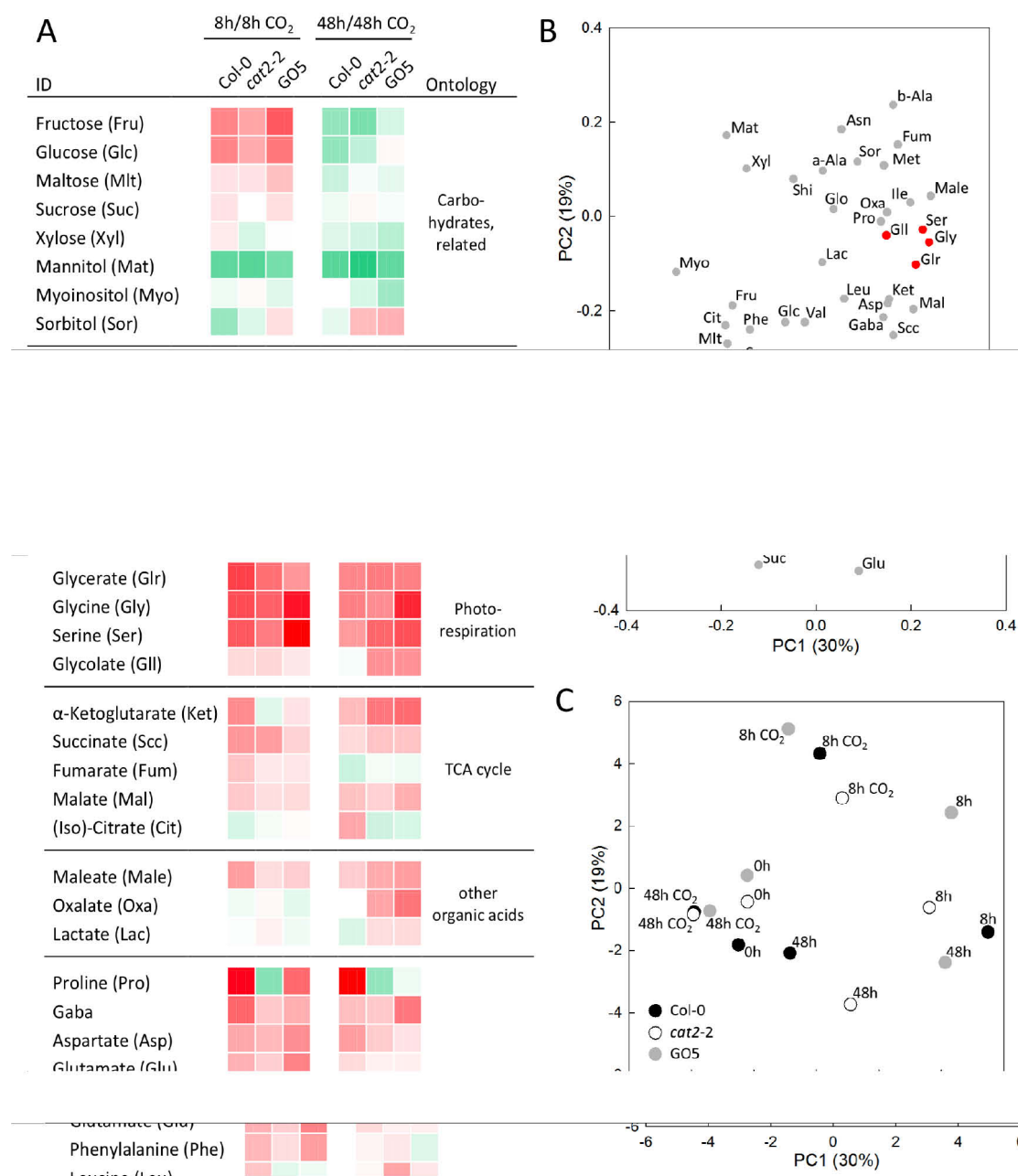


**Figure 2.** (A) Heat map of individual metabolites comparing ambient CO<sub>2</sub> and high CO<sub>2</sub> in wild-type (Col-0), GO5 and *cat2-2* plants (log<sub>2</sub> fold change). (B) PCA score plot of GC/MS metabolite data. (C) PCA loadings plot of GC-EI-TOF-MS metabolite data.

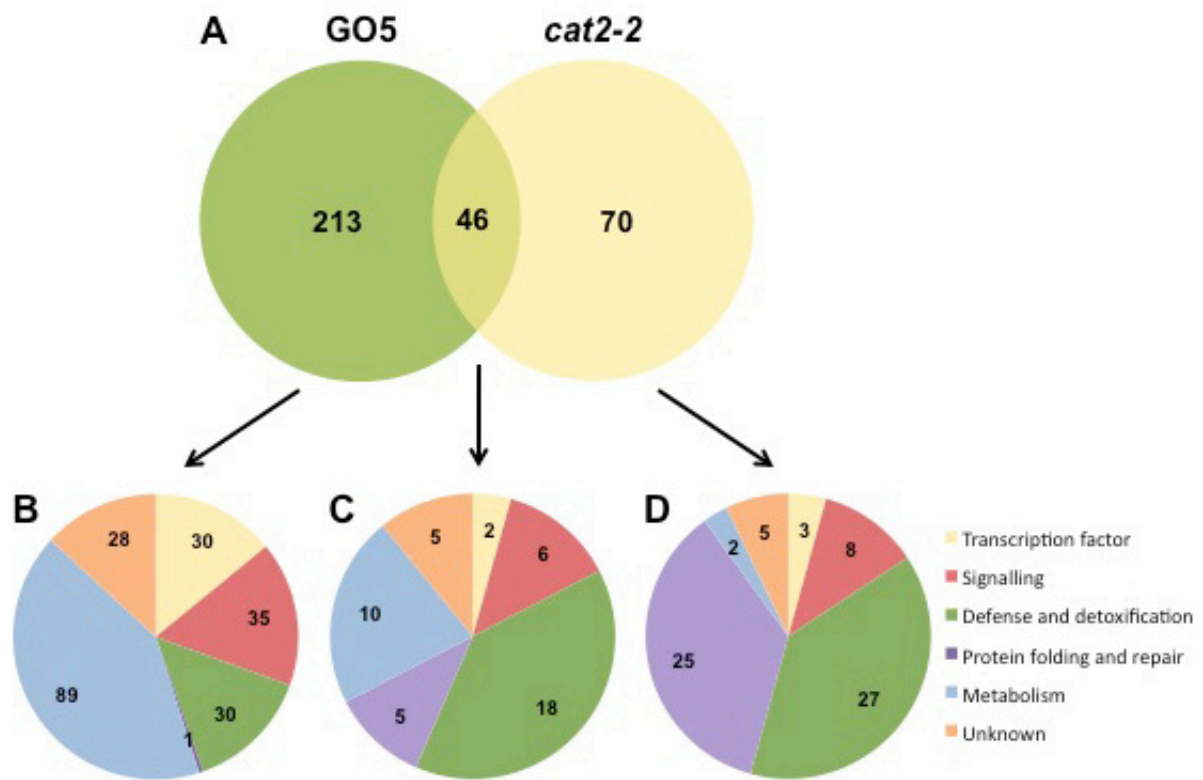


**Figure 3.** (A) Venn diagram of the number of  $H_2O_2$ -responsive genes up-regulated only in GO5 or *cat2-2* and in both, GO5 and *cat2-2*, after 8 h of  $H_2O_2$  production. (B) Pie chart of the functional categories of genes whose expression was up-regulated specifically by chloroplastically produced  $H_2O_2$ . (C) Pie chart of the functional categories of genes whose expression was up-regulated by both, chloroplastic and peroxisomal produced  $H_2O_2$ . (D) Pie chart of the functional categories of genes whose expression was up-regulated specifically by peroxisomally produced  $H_2O_2$ .

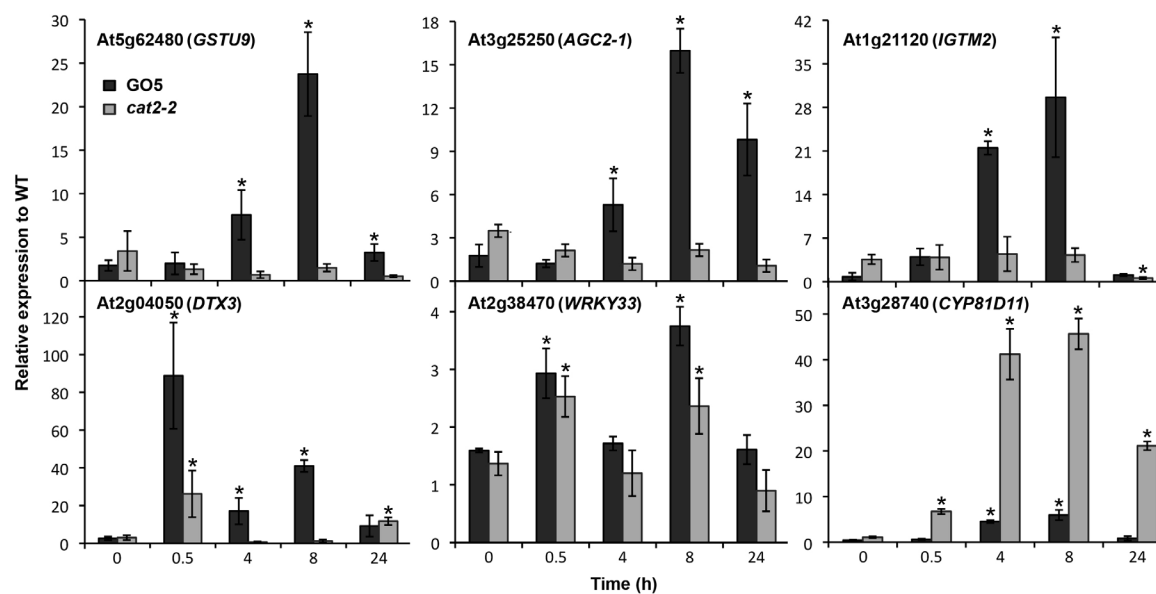


**Figure 4.** Dynamics of the transcriptional responses of selected genes in GO5 and *cat2-2* plants analysed by qRT-PCR. The asterisk (\*) indicates statistically significant difference to the time point t=0.

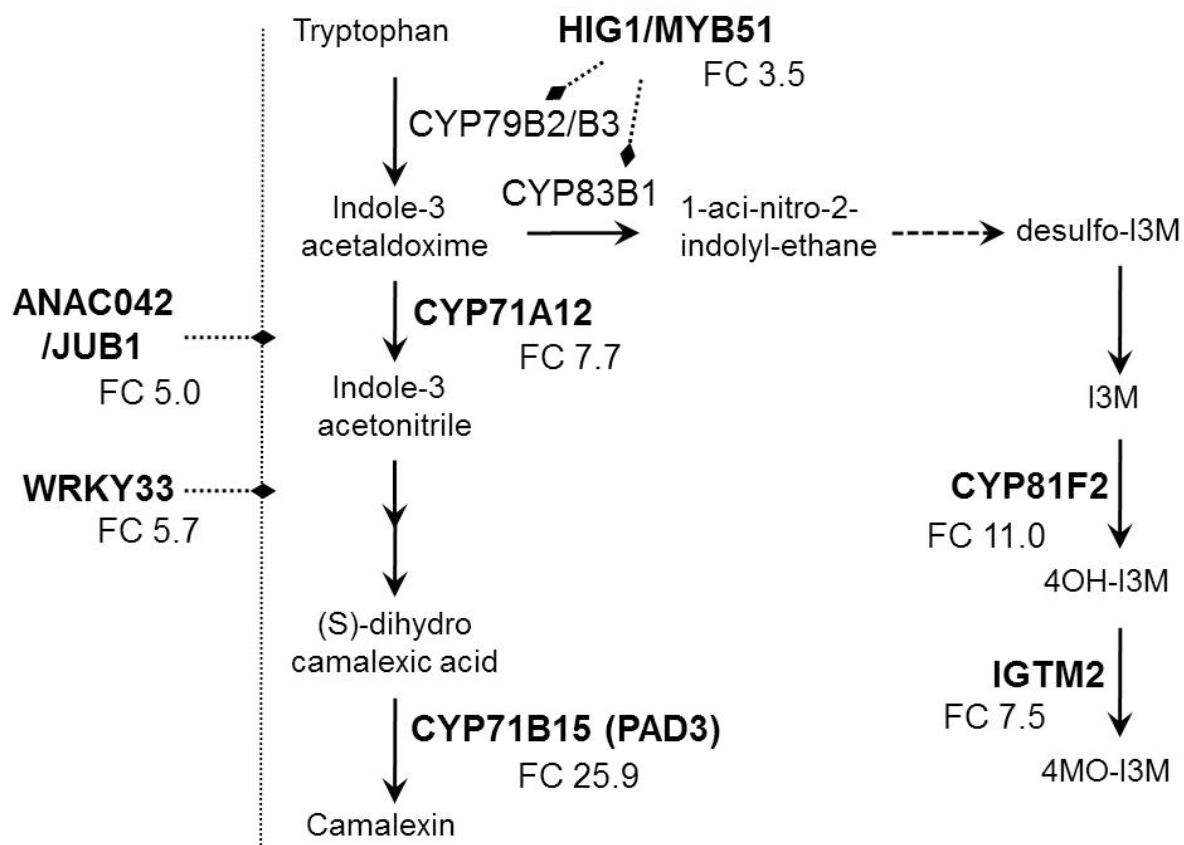


**Figure 5.** Schematic representation of the camalexin and indolic glucosinolate biosynthetic pathways showing the genes upregulated by chloroplastic produced H<sub>2</sub>O<sub>2</sub>. FC indicates the fold change induction of gene expression with respect to the wild type. I3M = indol-3-ylmethyl glucosinolate = Glucobrassicin; 4OH-I3M = 4-hydroxy-indol-3-ylmethyl glucosinolate = 4-hydroxyglucobrassicin; 4MO-I3M = methoxy-indol-3-ylmethyl glucosinolate = 4-methoxyglucobrassicin. Hatched arrow = not all reactions are represent

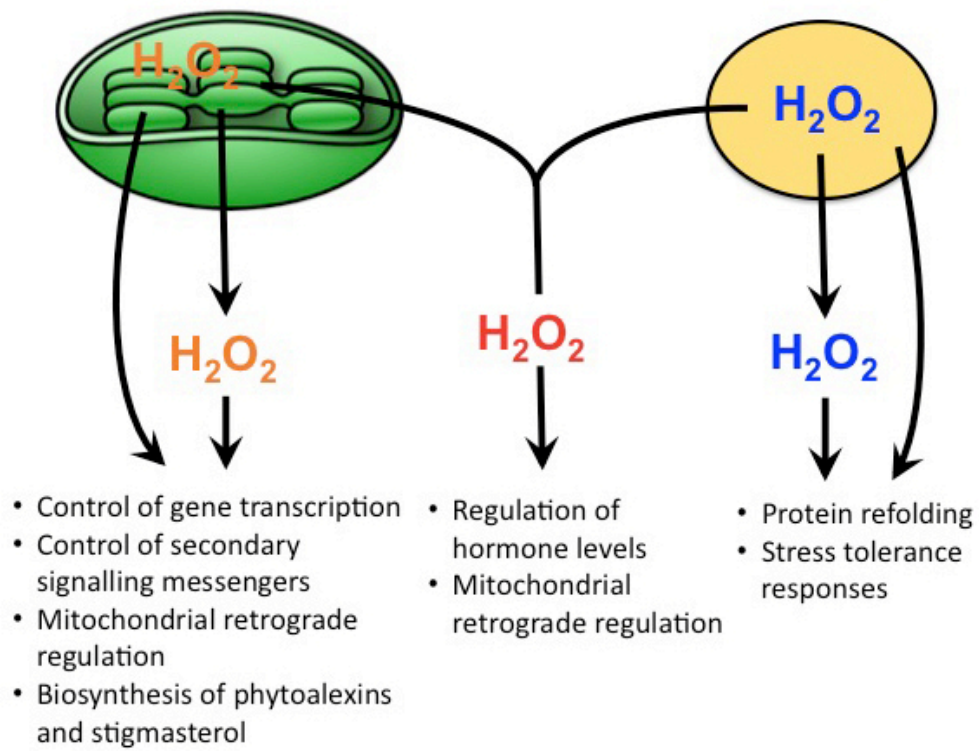
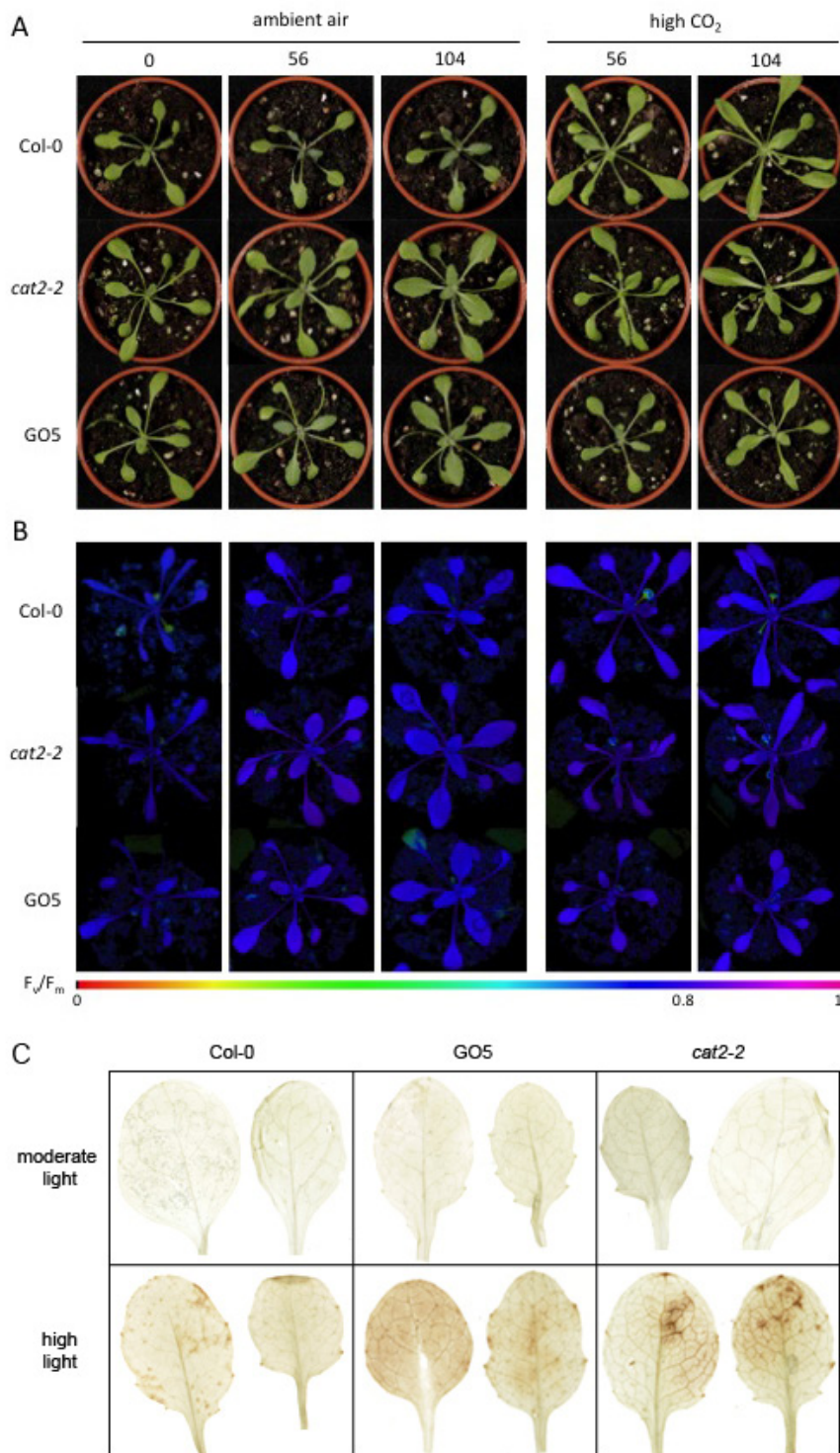


**Figure 6.** Diagram showing spatial H<sub>2</sub>O<sub>2</sub> signalling effects. H<sub>2</sub>O<sub>2</sub> originated in chloroplasts or peroxisomes can induce two different kinds of responses: one, which is dependent of the subcellular production site and other, which integrate H<sub>2</sub>O<sub>2</sub> signals independently from the subcellular site of its production.

**Figure S1.** Photographs (A) and imaging-PAM (pulse amplitude modulation) fluorescence pictures (B) showing  $F_V/F_M$  in false colours of wild-type (Col-0), GO5 and *cat2-2* plants at different time points after transferring high CO<sub>2</sub> grown plants to normal air conditions. (B) DAB staining showing H<sub>2</sub>O<sub>2</sub> production in Col-0, GO5 and *cat2-2* after transfer of high CO<sub>2</sub> grown plants to normal air at normal light (75  $\mu\text{mol quanta m}^{-2} \text{s}^{-1}$ ) and high light (700  $\mu\text{mol quanta m}^{-2} \text{s}^{-1}$ ) intensities for 8 h.



**Supplemental Table 1. Statistical microarray data analysis including the 349 genes, whose expression was modified in the experiment.**

List of genes differentially expressed in GO5 compared to wild type			
<i>array_element_name</i>	<i>locus</i>	<i>logFC</i> ( <i>GO5_8h_avscol_8h_a</i> )	<i>PValue</i> ( <i>GO5_8h_avscol_8h_a</i> )
263231_at	AT1G05680	7,532560573	1,8022E-07
263402_at	AT2G04050	6,953581426	5,56747E-08
266752_at	AT2G47000	6,288458327	7,54779E-07
247435_at	AT5G62480	5,778518271	1,60964E-06
260522_x_at	AT2G41730	5,752438741	2,28244E-06
262518_at	AT1G17170	5,532794836	5,89591E-06
263403_at	AT2G04040	4,988167995	4,04419E-06
263401_at	AT2G04070	4,824044214	1,03652E-05
258277_at	AT3G26830	4,696612234	0,000138369
248434_at	AT5G51440	4,694206228	1,15225E-05
265200_s_at	AT2G36800;AT2G36792;AT2G36790	4,649055159	6,36822E-06
247573_at	AT5G61160	4,529246336	0,000140875
256376_s_at	AT1G66690;AT1G66700	4,443639129	0,000108316
253046_at	AT4G37370	4,375265235	1,24358E-05
260706_at	AT1G32350	4,373660452	0,000116735
264042_at	AT2G03760	4,321369083	7,7711E-05
251176_at	AT3G63380	4,317461584	1,90496E-05
263061_at	AT2G18190	4,251711549	1,20584E-05
265668_at	AT2G32020	4,239460492	2,34508E-05
265428_at	AT2G20720	4,207843864	7,42275E-06
261021_at	AT1G26380	3,973066608	0,00014167
256989_at	AT3G28580	3,961572408	9,77455E-06
252539_at	AT3G45730	3,942592856	2,36828E-05
252131_at	AT3G50930	3,934324547	1,64499E-05
251282_at	AT3G61630	3,916097734	2,28217E-05
252334_at	AT3G48850	3,886838734	4,72102E-05
257840_at	AT3G25250	3,854259046	6,61478E-06
249125_at	AT5G43450	3,802665864	6,32034E-06
255543_at	AT4G01870	3,779493937	2,11828E-05
263096_at	AT2G16060	3,729602802	1,25415E-05
246584_at	AT5G14730	3,715675949	1,81234E-05
265422_at	AT2G20800	3,684066403	3,53964E-05
251772_at	AT3G55920	3,649586444	2,77665E-08
253044_at	AT4G37290	3,627656555	0,000117713
245193_at	AT1G67810	3,561355856	0,000135213
266267_at	AT2G29460	3,556083183	0,000473586
261892_at	AT1G80840	3,490846747	0,00033003



252265_at	AT3G49620	3,461058513	0,000701449
246368_at	AT1G51890	3,461017086	7,86004E-05
247949_at	AT5G57220	3,459915454	0,00032107
263515_at	AT2G21640	3,450596057	1,96221E-05
264832_at	AT1G03660	3,442994663	4,7657E-05
261763_at	AT1G15520	3,422662271	5,88223E-05
266368_at	AT2G41380	3,417908863	2,50176E-05
266995_at	AT2G34500	3,41700649	0,000892523
265197_at	AT2G36750	3,392179517	0,000594312
249377_at	AT5G40690	3,360929194	0,000755216
245082_at	AT2G23270	3,325726053	0,000101416
262517_at	AT1G17180	3,320680779	0,00066512
261394_at	AT1G79680	3,288753555	0,000574155
259439_at	AT1G01480	3,283754408	4,26099E-05
260239_at	AT1G74360	3,266567754	0,000158262
267026_at	AT2G38340	3,26538792	7,66851E-05
258452_at	AT3G22370	3,245786825	1,34634E-05
261192_at	AT1G32870	3,237792388	1,57558E-05
253268_s_at	AT4G34131;AT4G34135	3,230834123	0,000109155
259947_at	AT1G71530	3,186437644	0,000272499
251248_at	AT3G62150	3,182827314	6,7273E-05
255340_at	AT4G04490	3,154685166	4,80141E-05
256442_at	AT3G10930	3,134016443	0,000473133
253796_at	AT4G28460	3,037007131	0,000134477
265501_at	AT2G15490	3,033016989	0,000204207
258100_at	AT3G23550	3,025290041	0,00096888
254215_at	AT4G23700	3,014675337	9,39049E-05
252993_at	AT4G38540	3,002090907	0,000177435
247071_at	AT5G66640	3,001402366	3,40015E-05
265725_at	AT2G32030	2,991640537	0,00023815
265499_at	AT2G15480	2,983746825	0,000215672
259937_s_at	AT3G13080;AT1G71330	2,98316904	3,12084E-06
255430_at	AT4G03320	2,977019767	0,000174476
262213_at	AT1G74870	2,963305861	0,000740135
260933_at	AT1G02470	2,945763781	0,000398238
247704_at	AT5G59510	2,941478639	0,000648663
267565_at	AT2G30750	2,938016529	0,00055372
261450_s_at	AT1G21110;AT1G21120	2,900617507	0,000305168
261449_at	AT1G21120	2,861806906	0,000234591
259979_at	AT1G76600	2,848041344	0,000240477
259033_at	AT3G09410	2,803303327	0,000134666
264868_at	AT1G24090	2,73870809	0,000252068
253890_s_at	AT4G27585;AT5G54100	2,668502186	2,74295E-05
246927_s_at	AT5G25260;AT5G25250	2,662756276	7,13274E-05
254926_at	AT4G11280	2,647551908	0,000270198

249325_at	AT5G40850	2,61737293	1,50362E-05
264460_at	AT1G10170	2,591322753	4,87936E-05
249942_at	AT5G22300	2,588699047	0,00048849
245119_at	AT2G41640	2,585039939	9,59811E-05
253416_at	AT4G33070	2,577853786	5,45997E-05
266071_at	AT2G18680	2,552472908	0,000601003
254408_at	AT4G21390	2,518955165	0,000678371
251884_at	AT3G54150	2,506707	0,000334613
267028_at	AT2G38470	2,499632666	1,88709E-05
248870_at	AT5G46710	2,459828361	1,57428E-05
247707_at	AT5G59450	2,441666115	0,000529364
262118_at	AT1G02850	2,439183379	0,000502269
266618_at	AT2G35480	2,428673701	9,79458E-05
261242_at	AT1G32960	2,425720573	3,77703E-05
249784_at	AT5G24280	2,422024874	4,1255E-05
262381_at	AT1G72900	2,410743904	9,46029E-05
261240_at	AT1G32940	2,357584361	0,000161115
250670_at	AT5G06865;AT5G06860	2,34479079	0,00034933
258349_at	AT3G17609	2,340767335	0,000111358
267230_at	AT2G44080	2,339647118	0,000325185
261063_at	AT1G07520	2,336024089	0,000255119
254241_at	AT4G23190	2,327569955	0,000675591
257694_at	AT3G12860	2,320457457	0,000186033
263184_at	AT1G05560	2,313824873	0,000313789
266290_at	AT2G29490	2,313158875	0,000568441
265260_at	AT2G43000	2,307924962	0,000924594
245221_s_at	AT1G58889;AT1G59265	2,298792342	0,000257153
264859_at	AT1G24280	2,29135867	2,70528E-05
246858_at	AT5G25930	2,261845344	0,000104015
258606_at	AT3G02840	2,26177066	0,000641322
260602_at	AT1G55920	2,251663829	0,00049784
251096_at	AT5G01550	2,251254954	0,000365898
262731_at	AT1G16420	2,224306043	0,000220363
265723_at	AT2G32140	2,223228278	0,00020372
264102_at	AT1G79270	2,212268659	0,000247332
251776_at	AT3G55620	2,207899905	4,0418E-05
250024_at	AT5G18270	2,200451425	0,000300418
260037_at	AT1G68840	2,189183829	0,000581111
261806_at	AT1G30510	2,182785107	8,07675E-05
259297_at	AT3G05360	2,182470808	0,00044909
261648_at	AT1G27730	2,172408171	0,00098177
266606_at	AT2G46310	2,153474468	0,000111657
251745_at	AT3G55980	2,153458932	4,06479E-05
248794_at	AT5G47220	2,145229887	0,000179017
259272_at	AT3G01290	2,144507206	0,000315878

260362_at	AT1G70530	2,130775848	0,000781387
253824_at	AT4G27940	2,073862887	0,000166871
261193_at	AT1G32920	2,057464032	0,000748526
267246_at	AT2G30250	2,051027279	0,000295583
249494_at	AT5G39050	2,049211283	4,53398E-05
267493_at	AT2G30400	2,030551761	0,000491961
267559_at	AT2G45570	2,016385951	0,001049297
254289_at	AT4G22980	2,005188411	0,000550165
264757_at	AT1G61360	2,003822015	0,000272069
267083_at	AT2G41100	1,98608277	0,000181524
249896_at	AT5G22530	1,973765263	0,001023911
249983_at	AT5G18470	1,96998069	0,000190326
256756_at	AT3G25610	1,946730272	0,00010041
255230_at	AT4G05390	1,893692704	0,000458877
253414_at	AT4G33050	1,89267442	6,07433E-05
247772_at	AT5G58610	1,879940761	9,58675E-05
252383_at	AT3G47780	1,879525128	0,00016242
252977_at	AT4G38560	1,856093923	2,01421E-05
261249_at	AT1G05880	1,856057814	0,000212342
246133_at	AT5G20960	1,855457448	0,000227392
254759_at	AT4G13180	1,854719469	0,000666013
262180_at	AT1G78050	1,843479025	0,000258176
261718_at	AT1G18390	1,8365428	6,46637E-05
260243_at	AT1G63720	1,830486419	0,000181155
246821_at	AT5G26920	1,824758848	0,000373469
253453_at	AT4G31860	1,822880587	0,000480582
256852_at	AT3G18610	1,821389219	0,000696062
255753_at	AT1G18570	1,807063367	0,000230917
257216_at	AT3G14990	1,804315996	0,000254498
256833_at	AT3G22910	1,803976251	0,000811977
253013_at	AT4G37910	1,802369877	0,000825242
247351_at	AT5G63790	1,793543263	0,000510551
267451_at	AT2G33710	1,782714727	0,000434545
259428_at	AT1G01560	1,781701445	0,000650431
259875_s_at	AT1G76690;AT1G76680	1,781440659	3,82929E-05
260477_at	AT1G11050	1,774860534	7,11817E-05
263251_at	AT2G31410	1,767547937	0,000347253
258926_s_at	AT3G10490;AT3G10480	1,762272414	1,51652E-05
251769_at	AT3G55950	1,759635643	0,000970985
246831_at	AT5G26340	1,748871317	0,000803169
245977_at	AT5G13110	1,733779591	0,000228105
267623_at	AT2G39650	1,730130423	0,000337774
260405_at	AT1G69930	1,725672249	0,000312597
258679_at	AT3G08590	1,723884246	0,000148531
248101_at	AT5G55200	1,70521088	0,000200013

254343_at	AT4G21990	1,694761283	0,000504101
248487_at	AT5G51070	1,687861274	2,98648E-05
263935_at	AT2G35930	1,667679503	0,000415865
265475_at	AT2G15620	1,658401747	7,88427E-06
249266_at	AT5G41670	1,657935402	8,83369E-05
250094_at	AT5G17380	1,65771888	0,00031637
261023_at	AT1G12200	1,655361197	0,000875645
255893_at	AT1G17960	1,654200783	0,000622515
248394_at	AT5G52070	1,644600714	0,000138298
247989_at	AT5G56350	1,640101835	0,0001729
265817_at	AT2G18050	1,638987121	6,52805E-05
252483_at	AT3G46600	1,636081319	8,44294E-05
250944_at	AT5G03380	1,635117927	0,000390615
246988_at	AT5G67340	1,62898192	6,6012E-05
253841_at	AT4G27830	1,627576767	7,52602E-05
262133_at	AT1G78000	1,61385855	0,000441323
267300_at	AT2G30140	1,612864835	0,000215326
262177_at	AT1G74710	1,605620187	0,000261603
253284_at	AT4G34150	1,598016061	0,000769652
255341_at	AT4G04500	1,58860619	0,000164326
262219_at	AT1G74750	1,568869292	0,000760309
258282_at	AT3G26910	1,561717594	0,00027475
265649_at	AT2G27510	1,557562658	0,000431729
254592_at	AT4G18880	1,510858828	0,000404699
252940_at	AT4G39270	1,51039416	0,000900693
264663_at	AT1G09970	1,5074343	7,22583E-05
258921_at	AT3G10500	1,503439354	9,14165E-05
266835_at	AT2G29990	1,491782427	0,00044055
249264_s_at	AT5G41750;AT5G41740	1,490358264	5,65114E-05
262331_at	AT1G64050	1,463214191	0,000697245
254409_at	AT4G21400	1,462924387	0,000352387
257466_at	AT1G62840;AT1G62850	1,460672956	0,000819628
254707_at	AT4G18010	1,456532931	0,000948646
247176_at	AT5G65110	1,447904903	0,000111404
254593_s_at	AT4G18900;AT4G18905	1,443733219	0,001082704
259403_at	AT1G17745	1,440752088	0,000152988
264514_at	AT1G09500	1,425655953	0,00027044
245277_at	AT4G15550	1,407614936	0,000313301
251288_at	AT3G61620	1,404699587	0,000611709
259043_at	AT3G03440	1,403565669	5,86983E-05
245951_at	AT5G19550	1,389729685	0,00024152
255462_at	AT4G02940	1,389191726	0,000486779
254231_at	AT4G23810	1,388803213	0,000899032
257185_at	AT3G13100	1,380151617	0,000146239
263847_at	AT2G36970	1,368911626	0,000532953

245306_at	AT4G14690	1,355233876	0,000309019
261027_at	AT1G01340	1,348858496	0,000866167
257846_at	AT3G12910	1,347837024	0,001038648
258179_at	AT3G21690	1,34756616	8,31911E-05
264624_at	AT1G08930	1,343153807	0,000276104
254249_at	AT4G23280	1,340312718	9,88849E-05
248448_at	AT5G51190	1,334215389	0,000738875
247137_at	AT5G66210	1,329797265	0,000280577
265999_at	AT2G24100	1,314013619	0,000197902
255502_at	AT4G02410	1,311810485	0,000333533
263379_at	AT2G40140	1,309798752	0,000213991
265199_s_at	AT2G36780;AT2G36770	1,305408789	0,000880419
260398_at	AT1G72320	1,305281958	0,000989323
254459_at	AT4G21200	1,275504533	0,000248999
249237_at	AT5G42050	1,270322701	9,59486E-05
261973_at	AT1G64610	1,264727321	0,000611034
264223_s_at	AT3G16030	1,258912322	0,000421071
254549_at	AT4G19880	1,227757892	0,000725793
257623_at	AT3G26210	1,217871788	0,000687402
253281_at	AT4G34138	1,192046954	6,88388E-05
263348_at	AT2G05710	1,185366795	0,000604194
256366_at	AT1G66880	1,168988342	0,00032471
267624_at	AT2G39660	1,154010894	0,001066385
245768_at	AT1G33590	1,149453285	0,000853974
252592_at	AT3G45640	1,148758791	0,000184221
254247_at	AT4G23260	1,148405638	0,000268843
266288_s_at	AT2G29200;AT2G29140	1,14666539	0,000279429
253596_s_at	AT4G30730;AT4G30750	1,135092684	0,000759045
255319_at	AT4G04220	1,129192295	0,000422768
250028_at	AT5G18130	1,109030316	0,000984943
267138_s_at	AT2G38230;AT2G38210	1,104958667	0,000186093
264951_at	AT1G76970	1,100260301	0,000861764
266514_at	AT2G47890	1,098476968	0,000531687
266231_at	AT2G02220	1,089337592	0,000105326
263783_at	AT2G46400	1,080967478	0,000774897
256300_at	AT1G69490	1,078335367	0,000988983
254204_at	AT4G24160	1,051546854	0,000483264
261526_at	AT1G14370	1,049367094	0,000515085
258259_s_at	AT3G26820;AT3G26840	1,03820368	0,000529751
260847_s_at	AT1G17290;AT1G72330	1,034401483	0,000565541
252303_at	AT3G49210	1,01935974	0,000587328
250829_at	AT5G04720	1,011649259	0,000618419
<b>Repressed genes</b>			
263209_at	AT1G10522	-1,019495025	0,00032933
261790_at	AT1G16000	-1,064308105	0,000254486

258412_at	AT3G17210	-1,06481522	0,000524892
267586_at	AT2G41950	-1,082344547	7,54854E-05
249718_at	AT5G35740	-1,090366417	0,000593641
252442_at	AT3G46940	-1,100227257	0,000473223
258708_at	AT3G09580	-1,110217193	0,000536505
253817_at	AT4G28310	-1,136679572	0,001078873
266889_at	AT2G44640	-1,148713691	3,36848E-05
252105_at	AT3G51470	-1,153525132	0,000221034
253736_at	AT4G28780	-1,15617132	0,000168333
251704_at	AT3G56360	-1,207656168	0,000127324
251730_at	AT3G56330	-1,255874249	3,03776E-05
260125_at	AT1G36390	-1,259635054	6,98442E-05
261203_at	AT1G12845	-1,276864905	0,000449814
245275_at	AT4G15210	-1,608770623	0,000417456
<b>List of genes differentially expressed in <i>cat2-2</i> compared to wild type</b>			
<b>array_element_name</b>	<b>locus</b>	<b>logFC (<i>cat_8h_avscol_8h_a</i>)</b>	<b>PValue</b> logFC ( <i>cat_8h_avscol_8h_a</i> )
262518_at	AT1G17170	5,335172367	8,94599E-07
262517_at	AT1G17180	5,022441491	4,12261E-05
256589_at	AT3G28740	4,446085537	5,0949E-08
263231_at	AT1G05680	4,372013987	4,17404E-08
251772_at	AT3G55920	4,003042554	1,74953E-08
262911_s_at	AT1G59860;AT1G07400	3,99832769	0,000176587
248434_at	AT5G51440	3,869702725	2,36703E-05
256576_at	AT3G28210	3,740231985	9,42097E-05
250296_at	AT5G12020	3,499931511	0,000480679
266294_at	AT2G29500	3,394552732	0,000165611
255543_at	AT4G01870	3,327860386	3,49005E-05
250351_at	AT5G12030	3,302263717	0,001519344
248332_at	AT5G52640	3,164017992	0,000228753
266290_at	AT2G29490	2,967371796	2,26528E-05
256245_at	AT3G12580	2,938576715	0,000217796
253268_s_at	AT4G34131;AT4G34135	2,878038524	0,000681375
252515_at	AT3G46230	2,786792087	0,004198838
260978_at	AT1G53540	2,77965139	0,006348655
251975_at	AT3G53230	2,710656117	8,65357E-05
254839_at	AT4G12400	2,418569485	0,000694526
263184_at	AT1G05560	2,407852492	8,07519E-05
252984_at	AT4G37990	2,374350975	0,03187489
257670_at	AT3G20340	2,349560068	0,010798555
248657_at	AT5G48570	2,275612557	0,004825025
262307_at	AT1G71000	2,274618405	0,031602948
265197_at	AT2G36750	2,226264488	1,19849E-05
265200_s_at	AT2G36800;AT2G36792;AT2G36790	2,207161157	3,6683E-05

246464_at	AT5G16980	2,183116359	2,49339E-05
266752_at	AT2G47000	2,17364748	0,000257712
245306_at	AT4G14690	2,172959748	0,008377771
266368_at	AT2G41380	2,172942175	0,001408206
253416_at	AT4G33070	2,048786743	0,000572243
264514_at	AT1G09500	2,020782096	1,24241E-05
264648_at	AT1G09080	2,018073359	0,004574144
259875_s_at	AT1G76690;AT1G76680	1,998759731	7,86131E-06
263073_at	AT2G17500	1,982664341	0,006195868
263210_at	AT1G10585	1,978248225	0,032368532
247327_at	AT5G64120	1,90237489	0,04655073
250054_at	AT5G17860	1,891872957	0,010059771
252487_at	AT3G46658;AT3G46660	1,889649089	0,035875706
261240_at	AT1G32940	1,860844496	0,000528169
267168_at	AT2G37770	1,849245108	0,0044684
260522_x_at	AT2G41730	1,833715747	0,004111804
259037_at	AT3G09350	1,820042006	0,005309832
256937_at	AT3G22620	1,769531612	0,039162902
248607_at	AT5G49480	1,749577895	0,004861791
249289_at	AT5G41040	1,74767153	0,002846737
255430_at	AT4G03320	1,719078569	0,001560508
253046_at	AT4G37370	1,714616162	0,010679467
267436_at	AT2G19190	1,694240397	0,049415154
256596_at	AT3G28540	1,641919968	0,006954428
245193_at	AT1G67810	1,634187694	0,015782698
262128_at	AT1G52690	1,62866722	0,038017567
254447_at	AT4G20860	1,582197833	0,020657841
246584_at	AT5G14730	1,576380603	0,000385549
249769_at	AT5G24120	1,563059123	0,048178502
264042_at	AT2G03760	1,504084972	0,021026314
257100_at	AT3G25010	1,502530028	0,029717937
254343_at	AT4G21990	1,460896407	0,000521914
254059_at	AT4G25200	1,458354275	0,020379154
251176_at	AT3G63380	1,438754807	0,049736732
246403_at	AT1G57590	1,396477246	0,000497863
260567_at	AT2G43820	1,380156755	0,003220377
256249_at	AT3G11270	1,360611298	0,000311383
251503_at	AT3G59140	1,357175847	0,001775644
260116_at	AT1G33960	1,34421462	0,043941864
267026_at	AT2G38340	1,33442047	0,045819914
260803_at	AT1G78340	1,330940532	0,008795837
259979_at	AT1G76600	1,330756737	0,008778627
253343_at	AT4G33540	1,31378608	0,001620235
260248_at	AT1G74310	1,313722481	0,024826617
247488_at	AT5G61820	1,291304772	0,001100813

261339_at	AT1G35710	1,282348406	0,01880139
267266_at	AT2G23150	1,266280025	0,000123437
267546_at	AT2G32680	1,262268382	0,030755416
248487_at	AT5G51070	1,259762612	0,011316634
266296_at	AT2G29420	1,258623164	0,007438084
267319_at	AT2G34660	1,258463283	0,008019113
261618_at	AT1G33110	1,258365928	0,021300806
256308_s_at	AT1G30420;AT1G30410	1,24912032	0,009292764
245313_at	AT4G15420	1,247042888	0,001528252
265499_at	AT2G15480	1,224258058	0,017375082
254759_at	AT4G13180	1,210536317	0,009377108
260602_at	AT1G55920	1,204864825	0,002658413
249494_at	AT5G39050	1,202059661	0,012127579
246189_at	AT5G20910	1,189426453	0,001644639
255595_at	AT4G01700	1,186179762	0,040671913
254166_at	AT4G24190	1,181928625	0,039818561
264657_at	AT1G09100	1,179537544	0,000267351
246463_at	AT5G16970	1,169851731	0,000425076
264102_at	AT1G79270	1,160708495	0,007177557
266778_at	AT2G29090	1,146939377	8,8695E-05
260362_at	AT1G70530	1,133730233	0,016071761
257708_at	AT3G13330	1,130462532	0,011400929
257466_at	AT1G62840;AT1G62850	1,129927451	0,045968041
256854_at	AT3G15180	1,127009566	0,005407763
249942_at	AT5G22300	1,12352745	0,001641961
258033_at	AT3G21250	1,114899271	0,032555652
250994_at	AT5G02490	1,111437866	0,025052013
267300_at	AT2G30140	1,108450928	0,028185843
256300_at	AT1G69490	1,103296192	0,026182949
265119_at	AT1G62570	1,093994743	0,037581225
258452_at	AT3G22370	1,093846902	0,001045825
265161_at	AT1G30900	1,081012282	0,018648786
249125_at	AT5G43450	1,067170699	0,001590528
262935_at	AT1G79410	1,056046973	0,003140942
263406_at	AT2G04160	1,045047328	0,003090035
257185_at	AT3G13100	1,03933744	0,008620343
259403_at	AT1G17745	1,037522116	0,007163709
250500_at	AT5G09530	1,033891584	0,001732398
263904_at	AT2G36380	1,023481287	0,008316476
245277_at	AT4G15550	1,021730045	0,000537245
263570_at	AT2G27150	1,01947731	0,010020342
253281_at	AT4G34138	1,017342237	0,000243664
260878_at	AT1G21450	1,016411871	0,029728795
249264_s_at	AT5G41750;AT5G41740	1,012402417	0,033444117
<b>Repressed genes</b>			



Supplemental data Sewelam *et al.* (2014) submitted to Molecular Plant

---

253720_at	AT4G29270	-1,094231886	0,000595549
247814_at	AT5G58310	-1,172307654	0,024354611

**Supplemental Table 2.** List of 213 genes specifically up-regulated after 8 h of H<sub>2</sub>O<sub>2</sub> production in chloroplasts. Loc, Localization; C, cytosol; Ch, chloroplast; CW, cell wall; EC, extracellular; ER, endoplasmic reticulum; G, Golgi apparatus; M, mitochondrion; MM, mitochondrial membrane; N, nucleous; PM, plasma membrane; V, Vacuole; VM, vacuolar membrane; Cat, Category; DD, detoxification and defence; M, metabolism; R, repair; S, signalling; TF, transcription factor; PFR, protein folding and repair. -, unknown. FC, fold change.

Locus	Description	Molecular/Biological function	Loc	Cat	FC
At2g04050	DTX3	MATE efflux carrier, putative/ Mitochondrial retrograde regulation of oxidative stress response	PM	DD	124.0
At5g62480	GSTU9	Tau glutathione S-transferase	C	DD	54.9
At2g04040	DTX1	MATE efflux carrier /Detoxification of Cd <sup>2+</sup>	PM	DD	31.7
At2g04070	DTX4	MATE efflux carrier, putative/ Mitochondrial retrograde regulation of oxidative stress response	PM	DD	28.3
At3g26830	PAD3; CYP71B15	Cytochrome P450/Camalexin synthase	ER	DD	25.9
At5g61160	AACT1	Agmatine coumaroyltransferase/ Biosynthesis of hydroxycinnamic acid amides. Defense against pathogens.	C	M	23.1
At1g66690	-	S-adenosyl-L-methionine methyltransferase, putative	C	M	21.8
At1g32350	AOX1D	Alternative oxidase	MM	DD	20.7
At2g18190	-	AAA-type ATPase, putative	Ch	M	19.1
At2g32020	-	Alanine acetyl transferase, putative/ Mitochondrial retrograde regulation of oxidative stress response	C	M	18.9
At2g20720	-	-	-	-	18.5
At1g26380	-	ATP-binding reticuline dehydrogenase, putative	ER	M	15.7

At3g28580	-	AAA-type ATPase, putative	M, ER	M	15.6
At3g45730	-	-	-	-	15.4
At3g50930	-	AAA-type ATPase, putative	M	M	15.3
At3g61630	CRF6	Upregulated by cytokinin; Regulator of senescence	N	TF	15.1
At3g48850	PHT3;2	Phosphate transporter	M	M	14.8
At3g25250	AGC2-1; OXI1	Protein kinase, putative/ Mitochondrial retrograde regulation of oxidative stress response	-	S	14.5
At2g26560	PLP2	Phospholipase; lipid acyl hydrolase/ role in cell death; affects the accumulation of oxylipins; resistance to virus	C	M	14.0
At2g16060	AHB1	Nonsymbiotic hemoglobin/Oxygen sensor or electron transfer	C, PM	M	13.2
At2g20800	NDB4	External alternative NAD(P)H-ubiquinone oxidoreductase/Mitochondrial retrograde regulation of oxidative stress response	M	M	12.9
At4g37290	-	-	-	-	12.4
At2g29460	GSTU4	Tau Glutathione transferase	C	DD	11.8
At1g80840	WRKY40	Pathogen-induced; Mitochondrial retrograde regulation	N	TF	11.2
At1g51890	-	LRR-like receptor protein kinase	PM	S	11.0
At3g49620	DIN11	2-oxoacid-dependent dioxygenase, putative	M	M	11.0
At5g57220	CYP81F2	Cytochrome P450/catalyzes the conversion of indole-3-yl-methyl to 4-hydroxy-indole-3-yl-methyl glucosinolate; Mutants had impaired resistance to fungi and insects	M, ER	M	11.0
At2g21640	-	-	-	-	10.9
At1g03660	-	-	-	-	10.9
At1g15520	PDR12	ABC transporter; ATPase/General defence	PM	DD	10.7

		protein					
At2g34500	CYP710A1	Cytochrome P450; C-22 sterol desaturase/Conversion of $\beta$ -sitosterol to stigmasterol. Sterol desaturation reduce membrane fluidity and permeability	PM	M	10.7		
At5g40690	-	-	-	-	10.3		
At2g23270	-	-	-	-	10.0		
At1g79680	WALK10	Receptor protein kinase, putative/Defense response	PM	S	9.8		
At1g01480	ACS2	1-Amino-cyclopropane-1-carboxylate synthase/Ethylene biosynthesis	C	M	9.7		
At1g74360	-	LRR-like receptor protein kinase	MM	S	9.6		
At1g32870	ANAC013	Mitochondrial retrograde regulation of oxidative stress response	N	TF	9.4		
At1g71530	-	Protein kinase, putative	N	S	9.1		
At3g62150	PGP21	ABC transporter/Control auxin levels	PM	M	9.1		
At4g04490	CRK36	Receptor-like protein kinase	PM	S	8.9		
At3g10930	-	-	-	-	8.8		
At4g28460	-	-	-	-	8.2		
At2g15490	UGT73B4	UDP-glycosyltransferase; Quercetin 3-O-glucosyltransferase/ Induced by pathogen infection and salicylic acid		M	8.1		
At3g23550	DTX18	MATE efflux carrier, putative	PM	DD	8.1		
At4g23700	CHX17	Na <sup>+</sup> /H <sup>+</sup> antiporter, putative	PM	M	8.1		
At4g38540	MO2	Monooxygenase, putative		M	8.0		
At5g66640	DAR3	DA1-related protein	N	M	8.0		
At2g32030	-	Acyl-CoA N-acetyltransferase, putative	C	M	8.0		
At5g66640	-	-	-	-	8.0		
At3g13080	MRP3	ABC transporter/ transport glutathione-conjugates	VM	DD	7.9		

At1g74870	-	-	-	-	7.8
At1g02470	-	Polyketide cyclase/dehydrase and lipid transport, putative	Ch	M	7.7
At5g59510	RTFL5	Monooxygenase, Rotundifolia like	N	M	7.7
At2g30750	CYP71A12	cytochrome P450	PM, ER	M	7.7
At1g21110	-	O-methyltransferase, putative	C, N	M	7.5
At1g21120	IGTM2	Indole glucosinolate O-methyltransferase	C	M	7.3
At3g09410	-	Pectinacetyltransferase, putative		M	7.0
At1g24090	-	Ribonuclease H domain-containing protein, putative	N	M	6.7
At4g27585	-	-	-	-	6.4
At5g25260	FLOT2	Band 7-type protein/ scaffolding protein, regulation of signalling, putative	PM, VM	DD	6.3
At4g11280	ACS6	1-aminocyclopropane-1-carboxylate synthase/Ethylene biosynthesis	C	M	6.3
At5g40850	UPM1	Uroporphyrin methylase/siroheme biosynthetic process; sulfur metabolism	Ch	M	6.1
At1g10170	NFXL1	RING-type zinc finger protein/Mediates protein ubiquitination	N	DD	6.0
At2g41640	-	Glycosyltransferase, putative	-	M	6.0
At2g18680	-	-	-	-	5.9
At4g21390	B120	S-domain-type receptor protein kinase, putative	PM	S	5.7
At3g54150	-	S-adenosyl-L-methionine methyltransferase, putative	C	M	5.7
At2g38470	WRKY33	Regulates camalexin biosynthesis	N	TF	5.7
At5g46710	-	-	N	TF	5.5
At5g59450	SCL11	-	N	TF	5.4
At1g02850	BGLU11	Beta glucosidase	C	M	5.4

At2g35480	-	-	-	-	5.4
At1g32960	SBT3.3	Subtilase, putative	PM, ER	M	5.3
At5g24280	GMI1	Involved in somatic homologous recombination	N	M	5.3
At1g72900	-	disease resistance protein; TIR-NBS class	C	DD	5.3
At5g06865	PGIP1	Potential natural antisense gene, locus overlaps with At5g06860: Polygalacturonase/Inhibits fungal cell wall pectin degrading enzymes	CW, PM	DD	5.1
At3g17609	bZIP64; HYH	Involved in photomorphogenesis	N	TF	5.1
At2g44080	ARL	ARGOS-like/signal transduction; cell and organ growth via brassinosteroids signaling	-	M	5.1
At1g07520	SCL31	-	N	TF	5.1
At4g23190	CRK11; RLK3	Cysteine-rich receptor-like protein kinase/Induced by bacterial infection and oxidative stress	PM	S	5.0
At2g43000	ANAC042; JUB1	Regulates camalexin biosynthesis and longevity	N	TF	5.0
At3g12860	-	Pre RNA processing ribonucleoprotein, putative	N	M	5.0
At1g58889	-	-	-	-	4.9
At1g24280	G6PD3	Glucose-6-phosphate dehydrogenase/ Oxidative pentose-phosphate pathway	C	M	4.9
At5g25930	-	LRR receptor like protein kinase, putative	PM	S	4.8
At3g02840	-	U-box-type E3 ubiquitin ligase, putative	N, C	DD	4.8
At5g01550	LECRK6A4.2	Lectin receptor protein kinase/Negative regulation of ABA response in seed germination	PM	S	4.8
At2g32140	-	Transmembrane receptor, putative	Ch	S	4.7
At1g16420	MC8	Cysteine protease; metacaspase/Promotes programmed cell death	-	DD	4.7

At3g55620	EMB1624	Translation initiation factor/Protein biosynthesis	C, N	M	4.6
At5g18270	ANAC087	-	N	TF	4.6
At1g68840	RAV2/TEM2	Repressor of flowering	N	TF	4.6
At1g30510	RFNR2	Ferredoxin-NADP reductase	C	M	4.5
At3g05360	RLP30	Receptor like protein/Defense response	PM	DD	4.5
At1g27730	STZ/ZAT10	Involved in defence responses	N	TF	4.5
At2g46310	CRF5	Upregulated by cytokinin; Involved in morphogenesis	N	TF	4.5
At3g55980	SZF1	Regulate salt stress responses	N	TF	4.5
At5g47220	ERF2	Regulator of JA-responsive defense genes	N	TF	4.4
At3g01290	HIR2	Band 7-type protein/Hypersensitive response	-	DD	4.4
At4g27940	MTM1	Mitochondrial carrier/Activation of SOD1 by facilitating insertion of Mn <sup>2+</sup>	M	M	4.2
At1g32920	-	-	-	-	4.2
At2g30250	WRKY25	Involved in salt stress responses	N	TF	4.1
At2g30400	OFP2	-	N	TF	4.1
At2g45570	CYP76C2	Cytochrome P450	PM, ER	M	4.1
At4g22980	-	-	-	-	4.0
At1g61360	-	S-domain receptor protein kinase	PM	S	4.0
At2g41100	TCH3	Calmodulin-like protein 4/ Potential Ca <sup>2+</sup> sensor	M	S	4.0
At5g22530	-	-	-	-	3.9
At5g18470	-	Mannose-binding lectin family protein	PM	M	3.9
At3g25610	ALA10	Phospholipid-transporting ATPase; Flippase	PM	M	3.9
At4g05390	RFNR1	Ferredoxin-NADP reductase	C	M	3.7
At4g33050	EDA39	Calmodulin binding protein, putative/Involved in stomatal movement	C, N	S	3.7

At5g58610	-	-	N	TF	3.7
At3g47780	ATH6	ABC transporter; ATPase	PM	M	3.7
At4g38560	-	Phospholipase, putative	N	M	3.6
At1g18390	-	Protein kinase, putative	PM	S	3.6
At1g05880	ARI12	E3 ubiquitin-protein ligase, putative	N	DD	3.6
At5g20960	AAO1	IAA oxidase/ biosynthesis of auxins and ABA	C	M	3.6
At1g78050	PGM	Phosphoglycerate-bisphosphoglycerate mutase/Glycolysis	C	M	3.6
At1g18390	-	Protein kinase, putative	PM	S	3.6
At1g63720	-	-	-	-	3.6
At5g26920	CBP60G	Calmodulin binding protein/ Response to hypoxia, pathogen	N	S	3.5
At4g31860	PP2C60	Protein phosphatase 2C, putative	PM	M	3.5
At3g18610	NUCL2	Involved in pre-rRNA processing and ribosome assembly	N	M	3.5
At1g18570	HIG1/MYB51	Regulation of indole glucosinolate biosynthesis	N	TF	3.5
At3g14990	DJ1A	Interacts with SOD1 and GPX2; Oxidative stress response	C	DD	3.5
At3g22910	ACA13	Ca <sup>2+</sup> -transporting ATPase	PM	S	3.5
At4g37910	MTHSC70-1	Heat shock protein/stabilize proteins against aggregation	M	PFR	3.5
At5g63790	ANAC102	Involved in the response to hypoxia	N	TF	3.5
At2g33710	ERF112	-	N	TF	3.4
At1g01560	MPK11	MAP kinase/Response to ABA	C, N	S	3.4
At1g11050	-	Receptor-like protein kinase, putative	PM	S	3.4
At2g31410	-	-	-	-	3.4
At3g10490	ANAC051/ANAC052	-	N	TF	3.4



At3g55950	CRR3	Receptor like protein kinase, putative	PM	S	3.4
At5g26340	STP13	Carbohydrate transporter	PM, RE	M	3.4
At5g13110	G6PD2	Glucose-6-phosphate dehydrogenase/ oxidative pentose-phosphate pathway	Ch	M	3.3
At2g39650	-	-	-	-	3.3
At1g69930	GSTU11	Tau Glutathione transferase	C	DD	3.3
At3g08590	IPGAM2	Phosphoglycerate mutase/Glycolysis	C	M	3.3
At5g55200	MGE1	Co-chaperone GrpE protein, putative/translocation of proteins/ Mitochondrial retrograde regulation of oxidative stress response	M	M	3.3
At2g35930	PUB23	U-box domain-E3 ubiquitin ligase/Protein turn over; regulator of the immunity triggered by PAMPs	C	DD	3.2
At2g15620	NIR1	Ferredoxin-nitrate reductase/Nitrate assimilation	Ch	M	3.2
At5g41670	-	6-phosphogluconate dehydrogenase, putative/Oxidative pentose-phosphate pathway	Ch	M	3.2
At5g17380	-	2-hydroxyacyl-CoA lyase	C	M	3.2
At1g12200	-	Flavin monooxygenase/glucosinolate S- oxygenase	-	DD	3.2
At1g17960	-	Threonine-tRNA synthetase, putative/Protein translation	C	M	3.2
At5g52070	-	Agenet domain-containing protein/ Chromatin- associated functions		M	3.1
At5g56350	PK	Pyruvate kinase, putative	C	M	3.1
At2g18050	HIS1-3	Linker Histone/Nucleosome assembly	N	M	3.1
At3g46600	SCL30	-	N	TF	3.1
At5g03380	HIPP6	Heavy metal transport-detoxification	PM	DD	3.1

At5g67340	PUB2	U-box-type E3 ubiquitin ligase, putative	-	M	3.1
At4g27830	BGLU10	Beta glucosidase/Anthocyanin formation	V	M	3.1
At1g78000	SULTR1;2	Sulfate transporter	PM	M	3.1
At1g74710	ICS1	Isochorismate synthase/Synthesis of SA	Ch	M	3.0
At4g34150	-	C2 domain-containing protein	C	DD	3.0
At4g04500	CRK37	Receptor-like protein kinase	PM	S	3.0
At1g74750	-	-	-	-	3.0
At3g26910	-	-	-	-	3.0
At2g27510	FD3	Ferredoxin; electron carrier	Ch	M	2.9
At4g39270	-	LRR-like receptor protein kinase	PM	S	2.9
At1g09970	RLK7	Receptor like protein kinase, putative/Control of germination and tolerance to oxidant stress	PM	S	2.8
At3g10500	ANAC053	Induce ROS biosynthetic enzymes during senescence	N	TF	2.8
At2g29990	NDA2	NAD(P)H ubiquinone oxidoreductase	M	M	2.8
At1g64050	-	-	-	-	2.8
At4g21400	CRK37	Receptor-like protein kinase	PM	S	2.8
At4g18010	IP5P2	Inositol-polyphosphate 5-phosphatase/ABA signaling	C	M	2.7
At5g65110	ACX2	Acyl-CoA oxidase/ Long chain fatty acid biosynthesis	P	M	2.7
At4g18900	-	Transducin; WD40 domain-containing protein	N	M	2.7
At3g61620	RRP41	3'-5'-exoribonuclease; RNA processing	C	M	2.7
At3g03440	-	Armadillo/beta-catenin repeat family protein	Ch	M	2.7
At5g19550	ASP2	Aspartate aminotransferase	C	M	2.6
At4g02940	-	2OG-Fe(II) oxygenase; oxidoreductase	-	M	2.6
At4g23810	WRKY53	-	N	TF	2.6
At2g36970	UGT86A1	UDP-glucosyl transferase	-	M	2.6

At1g01340	CNGC10	Cyclic nucleotide and calmodulin binding ion channel	PM	S	2.6
At3g12910	-	NAC TF	N	TF	2.6
At3g21690	DTX40	MATE efflux carrier, putative	VM	DD	2.5
At4g23280	CRK20	Receptor-like protein kinase/Defense responses	PM	S	2.5
At5g51190	ERF105	-	N	TF	2.5
At5g66210	CPK28	Ca <sup>2+</sup> -dependent protein kinase	PM, Ch	S	2.5
At2g24100	-	-	-	-	2.5
At4g02410	LECRK43;LP K1	Lectin-receptor protein kinase	PM	S	2.5
At2g40140	SZF2/CZF1	Regulate salt stress responses	N	TF	2.5
At2g36780	UGT73C3	UDP-glucosyl transferase	-	M	2.5
At1g72320	APUM23	PUF domain Pumilio protein/RNA binding; regulate mRNA stability and translation	-	M	2.5
At4g21200	GA2OX8	Gibberellin 2-dioxygenase	C	M	2.4
At5g42050	-	-	-	-	2.4
At1g64610	-	Transducin; WD40 domain-containing protein	-	M	2.4
At3g16030	CES101; RFO3	S-domain receptor protein kinase/Response to fungus	PM	S	2.4
At4g19880	-	Glutathione S-transferase, putative	C	M	2.3
At3g26210	CYP71B23	cytochrome P450/ Defence	PM, ER	DDR	2.3
At2g05710	ACO3	Aconitase, putative/TCA cycle	M	M	2.3
At1g66880	-	Protein kinase/Defense responses	PM	S	2.3
At2g39660	BIK1	Protein kinase/Activate the resistance responses to necrotrophic pathogens	PM; Ch	S	2.2
At1g33590	-	LRR family protein	PM	DD	2.2

At3g45640	MPK3	MAP kinase	N	S	2.2
At4g23260	CRK18	Receptor-like protein kinase	PM	S	2.2
At2g29200	APUM1	PUF domain Pumilio protein/RNA binding; regulate mRNA stability and translation	C	M	2.2
At4g30730	-	-	-	-	2.2
At4g04220	RLP46	Receptor like protein	PM	DD	2.2
At5g18130	-	-	-	-	2.2
At2g38230	PDX1.1	Pyridoxal biosynthesis protein	C	M	2.2
At1g76970	TOM1C	Intra-Golgi vesicle-mediated transport, putative	G	M	2.1
At2g47890	COL13	-	N	TF	2.1
At2g02220	PSKR1	Guanylate cyclase and protein kinase activity	PM	S	2.1
At2g46400	WRKY46	-	N	TF	2.1
At4g24160	CGI-58	Lysophosphatidic acid acyltransferase- triacylglycerol lipase/Lipid homeostasis	M	M	2.1
At1g14370	APK2A	Receptor-like protein kinase	Ch	S	2.1
At3g26820	ELT3	esterase/lipase/thioesterase family protein	M	M	2.1
At1g17290	ALAAT1	Alanine transaminase	M	M	2.1
At3g49210	WSD6	O-acyltransferase, putative	-	M	2.0
At5g04720	ADR1-L2	Nucleotide-binding leucine-rich repeat immune receptor, putative	-	DD	2.0

**Supplemental Table 3. List of 70 genes specifically up-regulated after 8 h of H<sub>2</sub>O<sub>2</sub> production in peroxisomes.** Loc, Localization; C, cytosol; Ch, chloroplast; CW, cell wall; EC, extracellular; ER, endoplasmic reticulum; G, Golgi apparatus; M, mitochondrion; MM, mitochondrial membrane; N, nucleous; PM, plasma membrane; V, Vacuole; VM, vacuolar membrane; Cat, Category; DD, detoxification and defence; M, metabolism; PFR, Protein folding and repair; S, signalling; TF, transcription factor. -, unknown. FC, fold change.

Locus	Description	Molecular/Biological function	Loc	Cat	FC
At3g28740	CYP81D11	Cytochrome P450 protein/Defense to insects	PM, ER	DD	21.8
At1g59860	HSP17.6A-CI	Heat shock protein. HSP20-like chaperone	C	PFR	16.6
At3g28210	SAP12	Stress response; Unknown function	N	DD	13.4
At5g12020	HSP17.6-CII	Heat shock protein. HSP20-like chaperone	C	PFR	11.3
At2g29500	HSP17.6B-CI	Heat shock protein. HSP20-like chaperone	C	PFR	10.5
At5g12030	HSP17.6A	Heat shock protein. HSP20-like chaperone	C	PFR	9.9
At5g52640	HSP90.1	Heat shock protein	C	PFR	9.0
At3g12580	HSP70	Heat shock protein/Regulation of transcription; Stabilization of proteins	C, N	PFR	7.7
At3g46230	HSP17.4-CI	Heat shock protein	C	PFR	6.9
At1g53540	HSP17.6C-CI	Heat shock protein. HSP20-like chaperone	C	PFR	6.9
At3g53230	CDC48	AAA-typeATPase, putative/Cell division and growth processes; Protein catabolism	N	PFR	6.6
At4g12400	HOP3	Co-chaperone, putative	C	PFR	5.4
At4g37990	CAD8, ELI3-2	Aromatic alcohol:NADP oxidoreductase/Lignin biosynthesis	C	DD	5.2
At3g20340	-	Unknown protein	-	-	5.1
At5g48570	FKBP65, ROF2	Co-chaperone	C, N	PFR	4.8
At1g71000	-	DNAJ heat shock protein /Chaperone, putative	C, N	PFR	4.8

At5g16980	-	Oxidoreductase, putative	C	M	4.5
At1g09080	BiP-3	Heat shock protein. HSP70-like chaperone/ Regulation of transcription; Stabilization of proteins	N, ER	PFR	4.1
At2g17500	PILS5	Auxin efflux carrier, putative	PM, ER	S	4.0
At1g10585	-	bHLH transcription factor. unkonwn	N	TF	4.0
At5g64120	Per71	Peroxidase/Lignification; Removal of H <sub>2</sub> O <sub>2</sub>	CW	DD	3.7
At5g17860	CAX7	Cation exchanger, putative	VM	DD	3.7
At3g46658	-	Potential natural antisense gene, locus overlaps with At3g46660 (UGT76E12) a UDP-glycosyl transferase	-	DD	3.7
At2g37770	AKR4C9	Aldo/keto reductase/Detoxification of aldehydes and ketones produced during stress	C	DD	3.6
At3g09350	FES1A	HSP70 protein binding	C, N	PFR	3.5
At3g22620	-	Protease inhibitor/lipid transfer protein	Ch	DD	3.4
At5g49480	CP1	Ca <sup>2+</sup> - binding protein	C	S	3.4
At5g41040	ASFT	Feruloyl-CoA transferase/Suberin synthesis	C	DD	3.4
At2g19190	FRK1	Receptor-like protein kinase/Early defense signaling	PM	S	3.2
At3g28540	-	AAA-type ATPase, putative	PM	-	3.1
At1g52690	-	Late embryogenesis abundant protein, putative	-	DD	3.1
At4g20860	-	FAD oxidase, berberine bridge like	C	DD	3.0
At5g24120	SIG5	RNA polymerase sigma factor/Regulation of transcription of plastid genes (e.g., psbD)	Ch	TF	3.0
At3g25010	RLP41	Receptor like protein	PM	DD	2.8
At4g25200	HSP23.6	Heat shock protein. HSP20 chaperone	M	PFR	2.8
At1g57590	-	Pectinacylesterase, putative	EC	DD	2.6
At2g43820	GT/UGT74F2	UDP-glucosyltransferase/Tryptophan synthesis pathway	C	DD	2.6

At3g11270	MEE34	Regulatory subunit of the 26S proteasome involved in the degradation of ubiquitinated proteins	N	PFR	2.6
At3g59140	MRP14	ABC transporter/Pump for Glutathione S-conjugates	PM, VM	DD	2.6
At1g33960	AIG1	GTP binding	-	DD	2.5
At1g78340	GSTU22	Tau Glutathione S-transferase	C	DD	2.5
At4g33540	-	Beta-lactamase like	Ch	M	2.5
At1g74310	ATHSP101	Heat shock protein, Clp/Hsp100 type	C	PFR	2.5
At5g61820	-	-	V	-	2.5
At1g35710	-	Leucine-rich receptor like protein kinase	PM	S	2.4
At2g23150	NRAMP3	Metal transporter/Intracellular metal homeostasis	VM	S	2.4
At2g32680	RLP23	Receptor like protein kinase	PM	S	2.4
At2g29420	GSTU7	Tau Glutathione S-transferase	C	DD	2.4
At2g34660	MRP2	ABC-type transporter/Transport of glutathione S-conjugates	V	DD	2.4
At1g33110	DTX21	MATE efflux carrier, putative	PM	DD	2.4
At1g30420	MRP12	ABC-type transporter/Transport of glutathione S-conjugates	PM	DD	2.4
At4g15420	-	PRLI-interacting factor K ubiquitin-dependent protein degradation	N	PFR	2.4
At5g20910	AIP2	E3 ubiquitin-protein ligase/Negatively regulates ABA signalling by targeting ABI3 for post-translational destruction	C, N	PFR	2.3
At4g01700	-	Chitinase, putative	CW	DD	2.3
At4g24190	SHD, HSP90-7	HSP90-like protein/Chaperone; Regulation of meristem growth	ER	PFR	2.3
At1g09100	RPT5B	26S proteasome AAA-type ATPase subunit	C, N	PFR	2.3
At5g16970	AER	2-alkenal reductase/Detoxification of reactive	C,N	DD	2.3

		carbonyls; Antioxidant defense				
At2g29090	CYP707A2	Cytochrome P450;Abscisic acid 8'-hydroxylase/Involved in ABA catabolism	PM, CM	S		2.2
At3g13330	PA200	Proteasome activating protein/Interacts with the 26S proteasome	N	PFR		2.2
At3g15180	-	Putative regulatory subunit of 26S proteasome complex	N	PFR		2.2
At3g21250	MRP6	ABC-type transporter/Transport of glutathione S-conjugates	VM	DD		2.2
At5g02490	HSP70-2	Heat shock protein 70/Protein folding; Component of the Mediator complex, involved in the regulated transcription	C, N	PFR		2.2
At1g62570	FMOGS-OX4	Glucosinolate S-oxygenase, putative	N	DD		2.1
At1g30900	VSR6	Vacuolar sorting receptor, putative/Clathrin-coated vesicles sorting from Golgi apparatus to vacuoles	G	-		2.1
At1g79410	OCT5	Organic cation - carnitine transporter	VM	DD		2.1
At2g04160	AIR3	Subtilisin-like serine protease	CW	PFR		2.1
At5g09530	PRP10	Hydroxyproline-rich glycoprotein	PM, ER	-		2.1
At2g36380	PDR6	ABC-type transporter	PM	DD		2.0
At2g27150	AAO3	Abscisic aldehyde oxidase/Final step in abscisic acid biosynthesis	C	S		2.0
At1g21450	SCL1	Scarecrow-like protein	N	TF		2.0



**Supplemental Table 4. List of 46 genes up-regulated after 8 h of H<sub>2</sub>O<sub>2</sub> production in chloroplasts and peroxisomes.** The genes are listed following the FC in GO5 plants. Loc, Localization; C, cytosol; Ch, chloroplast; CW, cell wall; EC, extracellular; ER, endoplasmic reticulum; G, Golgi apparatus; M, mitochondrion; MM, mitochondrial membrane; N, nucleus; PM, plasma membrane; V, Vacuole; VM, vacuolar membrane; Cat, Category; DD, detoxification and defence; M, metabolism; PFR, protein folding/repair; S, signalling; TF, transcription factor. -, unknown. FC, fold change.

Locus	Description	Molecular/Biological function	Loc	Cat	FC GO5	FC <i>cat2-2</i>
At1g05680	UGT74E2	UDP-glucosyltransferase /Acts on IBA; Responses to abiotic stress by regulating auxin homeostasis; <a href="#">Mitochondrial retrograde regulation of oxidative stress response</a>	C	DD, S	185.2	20.7
At2g47000	PGP4	ABC transporter/Auxin transmembrane transporter	PM	DD	78.2	4.5
At2g41730	-	Unknown; <a href="#">Mitochondrial retrograde regulation of oxidative stress response</a>	N	DD, S	53.9	3.6
At1g17170	GSTU24	Tau Glutathione S-transferase	C	DD	46.3	40.4
At5g51440	HSP23.5-M	Heat shock protein; chaperone/ <a href="#">Mitochondrial retrograde regulation of oxidative stress response</a>	M	PFR, S	25.9	14.6
At2g36800	UGT73C5	UDP-glucosyltransferase/Acts on brassinolides and trans-zeatin	C	DD	25.1	4.6
At4g37370	CYP81D8	Cytochrome P450	PM, ER	-	20.8	3.3
At2g03760	SOT12	Brassinosteroid sulfotransferase/Involved in detoxification	C	DD	20.0	2.8
At3g63380	ACA12	Ca <sup>2+</sup> -transporting ATPase	PM	S	19.9	2.7

At5g43450	-	2OG-Fe(II) oxygenase; Similar to ACC oxidase/ Mitochondrial retrograde regulation of oxidative stress response	C	S	14.0	2.1
At4g01870	-	Contains WD40-like Beta propeller repeat	N	-	13.7	10.0
At5g14730	-	Unknown/ Mitochondrial retrograde regulation of oxidative stress response	-	S	13.1	3.0
At3g55920	CYP21-2	Peptidyl-prolyl isomerase, putative/ Protein folding	C	PFR	12.6	16.0
At1g67810	SUFE2	Activates cysteine desulfurase; involved in iron-sulfur cluster assembly	Ch	PFR	11.8	3.1
At2g41380	-	S-adenosyl-L-methionine-dependent methyltransferase-like	C	M	10.7	4.5
At2g36750	UGT73C1	UDP-glucosyltransferase/Acts on trans-zeatin and dihydrozeatin	C	M	10.5	4.7
At1g17180	GSTU25	Tau Glutathione S-transferase	C	DD	10.0	32.5
At2g38340	DRE2B	AP2 domain-transcription factor, putative		TF	9.6	2.5
At3g22370	AOX1A	Alternative oxidase/Reduction of ROS production; Mitochondrial retrograde regulation of oxidative stress response	MM	DD, S	9.5	2.1
At4g34131	UGT73B3	UDP-glucosyl transferase/Resistance to pathogens	C	DD	9.4	7.4
At2g15480	UGT73B5	UDP-glucosyl transferase/ Resistance to pathogens	C	DD	7.9	2.3
At4g03320	TIC20-IV	Protein translocase	Ch	M	7.9	3.3
At1g76600	SBT3.5	-		-	7.2	2.5
At5g22300	NIT4	Nitrilase/cyanide detoxification	PM	DD	6.0	2.2
At4g33070	PDC1	Pyruvate decarboxylase	C	M	6.0	4.1
At1g32940	SBT3.5	Subtilase; serine endopeptidase	CW	PFR	5.1	3.6
At1g05560	UGT75B1	UDP-glucosyl transferase/Synthesis of	C;	DD	5.0	5.3

		callose; Activity on IAA	Ch				
At2g29490	GSTU1	Tau Glutathione S-transferase	C	DD	5.0	7.8	
At1g55920	Serat2;1	Serine O-acetyltransferase/ Sulfur assimilation and cysteine biosynthesis	Ch	M	4.8	2.3	
At1g79270	ECT8	-	N	-	4.6	2.2	
At1g70530	CRK3	Cysteine-rich receptor-like protein kinase	PM	S	4.4	2.2	
At5g39050	PMAT1	Phenolic glucoside malonyltransferase	C	DD	4.1	2.3	
At4g13180	-	NAD(P)-dehydrogenase	Ch	M	3.6	2.3	
At1g76690	OPR2	12-oxophytodienoate reductase/ Metabolism of oxylipin signaling molecules	C	S	3.4	4.0	
At4g21990	APR3	5'-adenylylsulfate reductase/Cystein biosynthesis	Ch	M	3.2	2.8	
At5g51070	ERD1	Chaperone/Degradation of denatured proteins	Ch	PFR	3.2	2.4	
At2g30140	UGT87A2	UDP-glucosyl transferase/Regulation of flowering	C	M	3.1	2.2	
At5g41750	-	IR-NBS-LRR class disease resistance protein/Unknown function	N	DD	2.8	2.0	
At1g62840	-	-	-	-	2.8	2.2	
At1g17745	PGDH2	3-phosphoglycerate dehydrogenase/L- serine biosynthesis	Ch	M	2.7	2.1	
At1g09500	-	Alcohol dehydrogenase, putative	C	M	2.7	4.1	
At4g15550	UGT75D1	UDP-glycosyltransferase	Ch	DD	2.7	2.0	
At3g13100	MRP7	ABC-type transporter/Transport of glutathione S-conjugates	VM	DD	2.6	2.1	
At4g14690	ELIP2	Early light-induced protein/ Prevents excess accumulation of free chlorophyll; Photoprotection	Ch	DD	2.6	4.5	
At4g34138	UGT73B1	UDP-glycosyltransferase/ abscisic acid	Ch	S	2.3	2.0	

---

		glucosyltransferase				
At1g69490	NAC29; NAP	TF/Senescence; May function in the transition between active cell division and cell expansion	N	TF	2.1	2.2

---

**Supplemental Table 5. List of 30 transcription factor-encoding genes specifically up-regulated after 8 h of H<sub>2</sub>O<sub>2</sub> production in chloroplasts.** -, unknown. FC, fold change.

<b>Locus</b>	<b>Description</b>	<b>Gene Family</b>	<b>Function</b>	<b>FC</b>
At3g61630	CRF6	AP2/EREBP	Upregulated by cytokinin; Regulator of senescence	15.1
At1g80840	WRKY40	WRKY	Pathogen-induced; Mitochondrial retrograde regulation	11.2
At1g32870	ANAC013	NAC	Mitochondrial retrograde regulation of oxidative stress response	9.4
At2g38470	WRKY33	WRKY	Regulates camalexin biosynthesis	5.7
At5g46710	-	PLATZ	-	5.5
At5g59450	SCL11	GRAS	-	5.4
At3g17609	bZIP64; HYH	bZIP	Involved in photomorphogenesis	5.1
At1g07520	SCL31	GRAS	-	5.1
At2g43000	ANAC042; JUB1	NAC	Regulates camalexin biosynthesis and longevity	5.0
At5g18270	ANAC087	NAC	-	4.6
At1g68840	RAV2/TEM2	AP2/EREBP	Repressor of flowering	4.6
At1g27730	STZ/ZAT10	C2H2	Involved in defence responses	4.5
At2g46310	CRF5	AP2/EREBP	Upregulated by cytokinin; Involved in morphogenesis	4.5
At3g55980	SZF1	C3H	Regulate salt stress responses	4.5
At5g47220	ERF2	AP2/EREBP	Regulator of JA-responsive defense genes	4.4
At2g30250	WRKY25	WRKY	Involved in salt stress responses	4.1
At2g30400	OFP2	OFP	-	4.1
At5g58610	-	PHD	-	3.7
At1g18570	HIG1/MYB51	MYB	Regulation of indole glucosinolate	3.5

			biosynthesis	
At5g63790	ANAC102	NAC	Involved in the response to hypoxia	3.5
At2g33710	ERF112	AP2/EREBP	-	3.4
At3g10490	ANAC051/AN AC052	NAC	-	3.4
At3g46600	SCL30	GRAS	-	3.1
At3g10500	ANAC053	NAC	Induce ROS biosynthetic enzymes during senescence	2.8
At4g23810	WRKY53	WRKY	-	2.6
At3g12910	-	NAC	-	2.6
At5g51190	ERF105	AP2/EREBP	-	2.5
At2g40140	SZF2/CZF1	C3H	Regulate salt stress responses	2.5
At2g47890	COL13	C2C2CO-like	-	2.1
At2g46400	WRKY46	WRKY	-	2.1

---

**Supplemental Table 6. List of 35 signalling genes specifically up-regulated after 8 h of H<sub>2</sub>O<sub>2</sub> production in chloroplasts.** Loc, Localization; C, cytosol; Ch, chloroplast; CW, cell wall; EC, extracellular; ER, endoplasmic reticulum; G, Golgi apparatus; M, mitochondrion; MM, mitochondrial membrane; N, nucleous; PM, plasma membrane; V, Vacuole; VM, vacuolar membrane; . -, unknown. FC, fold change.

Locus	Description	Molecular/Biological function	Loc	FC
At3g25250	AGC2-1; OXI1	Protein kinase, putative/ Mitochondrial retrograde regulation of oxidative stress response	-	14.5
At1g51890	-	LRR-like receptor protein kinase	PM	11.0
At1g79680	WALK10	Receptor protein kinase, putative/Defense response	PM	9.8
At1g74360	-	LRR-like receptor protein kinase	MM	9.6
At1g71530	-	Protein kinase, putative	N	9.1
At4g04490	CRK36	Receptor-like protein kinase	PM	8.9
At4g21390	B120	S-domain-type receptor protein kinase, putative	PM	5.7
At4g23190	CRK11; RLK3	Cysteine-rich receptor-like protein kinase/Induced by bacterial infection and oxidative stress	PM	5.0
At5g25930	-	LRR receptor like protein kinase, putative	PM	4.8
At5g01550	LECRK6A4.2	Lectin receptor protein kinase/Negative regulation of ABA response in seed germination	PM	4.8
At2g32140	-	Transmembrane receptor, putative	Ch	4.7
At1g61360	-	S-domain receptor protein kinase	PM	4.0
At2g41100	TCH3	Calmodulin-like protein 4/ Potential Ca <sup>2+</sup> sensor	M	4.0
At4g33050	EDA39	Calmodulin binding protein, putative/Involved in stomatal movement	C, N	3.7
At1g18390	-	Protein kinase, putative	PM	3.6
At5g26920	CBP60G	Calmodulin binding protein/ Response to hypoxia, pathogen	N	3.5
At3g22910	ACA13	Ca <sup>2+</sup> -transporting ATPase	PM	3.5

At1g01560	MPK11	MAP kinase/Response to ABA	C, N	3.4
At1g11050	-	Receptor-like protein kinase, putative	PM	3.4
At3g55950	CRR3	Receptor like protein kinase, putative	PM	3.4
At4g04500	CRK37	Receptor-like protein kinase	PM	3.0
At4g39270	-	LRR-like receptor protein kinase	PM	2.9
At1g09970	RLK7	Receptor like protein kinase, putative/Control of germination and tolerance to oxidant stress	PM	2.8
At4g21400	CRK37	Receptor-like protein kinase	PM	2.8
At1g01340	CNGC10	Cyclic nucleotide and calmodulin binding ion channel	PM	2.6
At4g23280	CRK20	Receptor-like protein kinase/Defense responses	PM	2.5
At5g66210	CPK28	Ca <sup>2+</sup> -dependent protein kinase	PM, Ch	2.5
At4g02410	LECRK43;LP K1	Lectin-receptor protein kinase	PM	2.5
At3g16030	CES101; RFO3	S-domain receptor protein kinase/Response to fungus	PM	2.4
At1g66880	-	Protein kinase/Defense responses	PM	2.3
At2g39660	BIK1	Protein kinase/Activate the resistance responses to necrotrophic pathogens	PM, Ch	2.2
At3g45640	MPK3	MAP kinase	N	2.2
At4g23260	CRK18	Receptor-like protein kinase	PM	2.2
At2g02220	PSKR1	Guanylate cyclase and protein kinase activity	PM	2.1
At1g14370	APK2A	Receptor-like protein kinase	Ch	2.1



**Supplemental Table 7. List of 30 defense and detoxification genes specifically up-regulated after 8 h of H<sub>2</sub>O<sub>2</sub> production in chloroplasts.** Loc, Localization; C, cytosol; Ch, chloroplast; CW, cell wall; EC, extracellular; ER, endoplasmic reticulum; G, Golgi apparatus; M, mitochondrion; MM, mitochondrial membrane; N, nucleus; PM, plasma membrane; V, Vacuole; VM, vacuolar membrane; -, unknown. FC, fold change.

Locus	Description	Molecular/Biological function	Loc	FC
At2g04050	DTX3	MATE efflux carrier, putative/ Mitochondrial retrograde regulation of oxidative stress response	PM	124.0
At5g62480	GSTU9	Tau glutathione S-transferase	C	54.9
At2g04040	DTX1	MATE efflux carrier /Detoxification of Cd <sup>2+</sup>	PM	31.7
At2g04070	DTX4	MATE efflux carrier, putative/ Mitochondrial retrograde regulation of oxidative stress response	PM	28.3
At3g26830	PAD3; CYP71B15	Cytochrome P450/Camalexin synthase	ER	25.9
At1g32350	AOX1D	Alternative oxidase	MM	20.7
At2g29460	GSTU4	Tau Glutathione transferase	C	11.8
At1g15520	PDR12	ABC transporter; ATPase/General defence protein	PM	10.7
At3g23550	DTX18	MATE efflux carrier, putative	PM	8.1
At3g13080	MRP3	ABC transporter/ transport glutathione-conjugates	VM	7.9
At5g25260	FLOT2	Band 7-type protein/ scaffolding protein, regulation of signalling, putative	PM, VM	6.3
At1g10170	NFXL1	RING-type zinc finger protein/Mediates protein ubiquitination	N	6.0
At1g72900	-	disease resistance protein; TIR-NBS class	C	5.3
At5g06865	PGIP1	Potential natural antisense gene, locus overlaps with At5g06860: Polygalacturonase/Inhibits fungal cell wall pectin degrading enzymes	CW, PM	5.1
At3g02840	-	U-box-type E3 ubiquitin ligase, putative	N, C	4.8

---

At1g16420	MC8	Cysteine protease; metacaspase/Promotes programmed cell death	-	4.7
At3g05360	RLP30	Receptor like protein/Defense response	PM	4.5
At3g01290	HIR2	Band 7-type protein/Hypersensitive response	-	4.4
At1g05880	ARI12	E3 ubiquitin-protein ligase, putative	N	3.6
At3g14990	DJ1A	Interacts with SOD1 and GPX2; Oxidative stress response	C	3.5
At1g69930	GSTU11	Tau Glutathione transferase	C	3.3
At2g35930	PUB23	U-box domain-E3 ubiquitin ligase/Protein turn over; regulator of the immunity triggered by PAMPs	C	3.2
At1g12200	-	Flavin monooxygenase/glucosinolate S-oxygenase	-	3.2
At5g03380	HIPP6	Heavy metal transport-detoxification	PM	3.1
At4g34150	-	C2 domain-containing protein	C	3.0
At3g21690	DTX40	MATE efflux carrier, putative	VM	2.5
At3g26210	CYP71B23	cytochrome P450/ Defence	PM, ER	2.3
At1g33590	-	LRR family protein	PM	2.2
At4g04220	RLP46	Receptor like protein	PM	2.2
At5g04720	ADR1-L2	Nucleotide-binding leucine-rich repeat immune receptor, putative	-	2.0

---

**Supplemental Table 8. List of 89 metabolic genes specifically up-regulated after 8 h of H<sub>2</sub>O<sub>2</sub> production from chloroplasts.** Loc, Localization; C, cytosol; Ch, chloroplast; CW, cell wall; EC, extracellular; ER, endoplasmic reticulum; G, Golgi apparatus; M, mitochondrion; MM, mitochondrial membrane; N, nucleus; PM, plasma membrane; V, Vacuole; VM, vacuolar membrane; -, unknown. FC, fold change.

Locus	Description	Molecular/Biological function	Loc	FC
At5g61160	AACT1	Agmatine coumaroyltransferase/Biosynthesis of hydroxycinnamic acid amides. Defense against pathogens.	C	23.1
At1g66690	-	S-adenosyl-L-methionine methyltransferase, putative	C	21.8
At2g18190	-	AAA-type ATPase, putative	Ch	19.1
At2g32020	-	Alanine acetyl transferase, putative/Mitochondrial retrograde regulation of oxidative stress response	C	18.9
At1g26380	-	ATP-binding reticuline dehydrogenase, putative	ER	15.7
At3g28580	-	AAA-type ATPase, putative	M, ER	15.6
At3g50930	-	AAA-type ATPase, putative	M	15.3
At3g48850	PHT3;2	Phosphate transporter	M	14.8
At2g26560	PLP2	Phospholipase; lipid acyl hydrolase/Role in cell death; Affects the accumulation of oxylipins; Resistance to virus	C	14.0
At2g16060	AHB1	Nonsymbiotic hemoglobin/Oxygen sensor or electron transfer	C, PM	13.2
At2g20800	NDB4	External alternative NAD(P)H-ubiquinone oxidoreductase/Mitochondrial retrograde regulation of oxidative stress response	M	12.9
At3g49620	DIN11	2-oxoacid-dependent dioxygenase, putative	M	11.0
At5g57220	CYP81F2	Cytochrome P450/Catalyzes the conversion of	M, ER	11.0

		indole-3-yl-methyl to 4-hydroxy-indole-3-yl-methyl glucosinolate; Mutants had impaired resistance to fungi and insects		
At2g34500	CYP710A1	Cytochrome P450; C-22 sterol desaturase/Conversion of $\beta$ -sitosterol to stigmasterol. Sterol desaturation reduce membrane fluidity and permeability	PM	10.7
At1g01480	ACS2	1-Amino-cyclopropane-1-carboxylate synthase/Ethylene biosynthesis	C	9.7
At3g62150	PGP21	ABC transporter/Control auxin levels	PM	9.1
At2g15490	UGT73B4	UDP-glycosyltransferase;Quercetin 3-O-glucosyltransferase/ Induced by pathogen infection and salicylic acid		8.1
At4g23700	CHX17	Na <sup>+</sup> /H <sup>+</sup> antiporter, putative	PM	8.1
At4g38540	MO2	Monooxygenase, putative		8.0
At5g66640	DAR3	DA1-related protein	N	8.0
At2g32030	-	Acyl-CoA N-acetyltransferase, putative	C	8.0
At1g02470	-	Polyketide cyclase/dehydrase and lipid transport, putative	Ch	7.7
At5g59510	RTFL5	Monooxygenase, Rotundifolia like	N	7.7
At2g30750	CYP71A12	Cytochrome P450; Camalexin biosynthesis	PM, ER	7.7
At1g21110	-	O-methyltransferase, putative	C, N	7.5
At1g21120	IGTM2	Indole glucosinolate O-methyltransferase	C	7.3
At3g09410	-	Pectinacetylerase, putative		7.0
At1g24090	-	Ribonuclease H domain-containing protein, putative	N	6.7
At4g11280	ACS6	1-aminocyclopropane-1-carboxylate synthase/Ethylene biosynthesis	C	6.3
At5g40850	UPM1	Urophorphyrin methylase/Siroheme biosynthetic process; Sulfur metabolism	Ch	6.1
At2g41640	-	Glycosyltransferase, putative	-	6.0

At3g54150	-	S-adenosyl-L-methionine methyltransferase, putative	C	5.7
At1g02850	BGLU11	Beta glucosidase	C	5.4
At1g32960	SBT3.3	Subtilase, putative	PM, ER	5.3
At5g24280	GMI1	Involved in somatic homologous recombination	N	5.3
At2g44080	ARL	ARGOS-like/Signal transduction; Cell and organ growth via brassinosteroids signaling	-	5.1
At3g12860	-	Pre RNA processing ribonucleoprotein, putative	N	5.0
At1g24280	G6PD3	Glucose-6-phosphate dehydrogenase/Oxidative pentose-phosphate pathway	C	4.9
At3g55620	EMB1624	Translation initiation factor/Protein biosynthesis	C, N	4.6
At1g30510	RFNR2	Ferredoxin-NADP reductase	C	4.5
At4g27940	MTM1	Mitochondrial carrier/Activation of SOD1 by facilitating insertion of Mn <sup>2+</sup>	M	4.2
At2g45570	CYP76C2	cytochrome P450	PM, ER	4.1
At5g18470	-	Mannose-binding lectin family protein	PM	3.9
At3g25610	ALA10	Phospholipid-transporting ATPase; Flippase	PM	3.9
At4g05390	RFNR1	Ferredoxin-NADP reductase	C	3.7
At3g47780	ATH6	ABC transporter; ATPase	PM	3.7
At4g38560	-	Phospholipase, putative	N	3.6
At5g20960	AAO1	IAA oxidase/Biosynthesis of auxins and ABA	C	3.6
At1g78050	PGM	Phosphoglycerate-bisphosphoglycerate mutase/Glycolysis	C	3.6
At4g31860	PP2C60	Protein phosphatase 2C, putative	PM	3.5
At3g18610	NUCL2	Involved in pre-rRNA processing and ribosome assembly	N	3.5
At5g26340	STP13	Carbohydrate transporter	PM, RE	3.4

At5g13110	G6PD2	Glucose-6-phosphate dehydrogenase/ Oxidative pentose-phosphate pathway	Ch	3.3
At3g08590	IPGAM2	Phosphoglycerate mutase/Glycolysis	C	3.3
At5g55200	MGE1	Co-chaperone GrpE protein, putative/translocation of proteins/ Mitochondrial retrograde regulation of oxidative stress response	M	3.3
At2g15620	NIR1	Ferredoxin-nitrate reductase/Nitrate assimilation	Ch	3.2
At5g41670	-	6-phosphogluconate dehydrogenase, putative/Oxidative pentose-phosphate pathway	Ch	3.2
At5g17380	-	2-hydroxyacyl-CoA lyase	C	3.2
At1g17960	-	Threonine-tRNA synthetase, putative/Protein translation	C	3.2
At5g56350	PK	Pyruvate kinase, putative	C	3.1
At5g52070	-	Agenet domain-containing protein/Chromatin- associated functions	-	3.1
At2g18050	HIS1-3	Linker Histone/Nucleosome assembly	N	3.1
At5g67340	PUB2	U-box-type E3 ubiquitin ligase, putative	-	3.1
At4g27830	BGLU10	Beta glucosidase/Anthocyanin formation	V	3.1
At1g78000	SULTR1;2	Sulfate transporter	PM	3.1
At1g74710	ICS1	Isochorismate synthase/Synthesis of SA	Ch	3.0
At2g27510	FD3	Ferredoxin; electron carrier	Ch	2.9
At2g29990	NDA2	NAD(P)H ubiquinone oxidoreductase	M	2.8
At4g18010	IP5P2	Inositol-polyphosphate 5-phosphatase/ABA signaling	C	2.7
At5g65110	ACX2	Acyl-CoA oxidase/ Long chain fatty acid biosynthesis	P	2.7
At4g18900	-	Transducin; WD40 domain-containing protein	N	2.7
At3g61620	RRP41	3'-5'-exoribonuclease; RNA processing	C	2.7

---

At3g03440	-	armadillo/beta-catenin repeat family protein	Ch	2.7
At5g19550	ASP2	Aspartate aminotransferase	C	2.6
At4g02940	-	2OG-Fe(II) oxygenase; oxidoreductase	-	2.6
At2g36970	UGT86A1	UDP-glucosyl transferase	-	2.6
At2g36780	UGT73C3	UDP-glucosyl transferase	-	2.5
At1g72320	APUM23	PUF domain Pumilio protein/RNA binding; regulate mRNA stability and translation	-	2.5
At4g21200	GA2OX8	gibberellin 2-dioxygenase	C	2.4
At1g64610	-	Transducin; WD40 domain-containing protein	-	2.4
At4g19880	-	Glutathione S-transferase, putative	C	2.3
At2g05710	ACO3	Aconitase, putative/TCA cycle	M	2.3
At2g29200	APUM1	PUF domain Pumilio protein/RNA binding; regulate mRNA stability and translation	C	2.2
At2g38230	PDX1.1	Pyridoxal biosynthesis protein	C	2.2
At1g76970	TOM1C	Intra-Golgi vesicle-mediated transport, putative	G	2.1
At4g24160	CGI-58	Lysophosphatidic acid acyltransferase- triacylglycerol lipase/Lipid homeostasis	M	2.1
At3g26820	ELT3	esterase/lipase/thioesterase family protein	M	2.1
At1g17290	ALAAT1	Alanine transaminase	M	2.1
At3g49210	WSD6	O-acyltransferase, putative	-	2.0

---

**Supplemental Table 9.** Timecourse analysis of  $\beta$ -sistosterol, campesterol and cholesterol concentrations in leaves of wild type (WT, Col-0), GO5 and *cat2-2* plants under non-photorespiratory and photorespiratory conditions. The samples were harvested at 0, 8, 32 and 56 h after transferring long day-grown plants from high CO<sub>2</sub> to normal air conditions. Concentrations are given in  $\mu\text{g}$  phytosterol/g FW. Values are means  $\pm$  standard error from three samples, each consisting of six leaves. H, High CO<sub>2</sub> concentration (3,000 ppm CO<sub>2</sub>); non-photorespiratory conditions. A, Ambient CO<sub>2</sub> concentration (380 ppm CO<sub>2</sub>); photorespiratory conditions.

	$\beta$ -sistosterol		Campesterol		Cholesterol	
	H	A	H	A	H	A
<b>WT 0</b>	274 $\pm$ 35	-	23.3 $\pm$ 3.8	-	5.3 $\pm$ 1.0	-
8	352 $\pm$ 58	311 $\pm$ 51	30.9 $\pm$ 8.0	27.4 $\pm$ 4.7	5.1 $\pm$ 1.7	5.1 $\pm$ 1.0
32	266 $\pm$ 40	308 $\pm$ 101	23.4 $\pm$ 3.8	24.8 $\pm$ 5.6	4.5 $\pm$ 0.8	3.7 $\pm$ 0.1
56	368 $\pm$ 131	238 $\pm$ 86	32.4 $\pm$ 12.2	25.1 $\pm$ 8.0	6.3 $\pm$ 2.6	4.7 $\pm$ 1.6
<b>GO50</b>	518 $\pm$ 286	-	41.5 $\pm$ 21.7	-	8.1 $\pm$ 4.8	-
8	452 $\pm$ 165	283 $\pm$ 56	39.3 $\pm$ 15.1	22.7 $\pm$ 5.0	6.1 $\pm$ 2.0	4.3 $\pm$ 1.0
32	223 $\pm$ 23	327 $\pm$ 91	17.8 $\pm$ 2.5	19.8 $\pm$ 1.5	3.1 $\pm$ 0.4	4.8 $\pm$ 2.1
56	247 $\pm$ 54	239 $\pm$ 19	22.4 $\pm$ 4.4	27.4 $\pm$ 10.9	3.6 $\pm$ 0.7	3.4 $\pm$ 2.1
<b><i>cat2-20</i></b>	347 $\pm$ 27	-	28.0 $\pm$ 2.8	-	6.8 $\pm$ 1.1	-
8	265 $\pm$ 31	449 $\pm$ 80	25.0 $\pm$ 6.6	38.1 $\pm$ 7.6	4.5 $\pm$ 1.0	6.1 $\pm$ 0.6
32	478 $\pm$ 164	633 $\pm$ 287	39.0 $\pm$ 13.4	61.1 $\pm$ 29.0	6.5 $\pm$ 2.0	11.4 $\pm$ 4.5
56	269 $\pm$ 36	301 $\pm$ 96	23.1 $\pm$ 3.4	34.0 $\pm$ 7.0	4.5 $\pm$ 0.9	7.0 $\pm$ 2.3



**Supplemental Table 10.** Timecourse analyses of glucosinolate concentrations in leaves of wild type (WT, Col-0), GO5 and *cat2-2* plants under non-photorespiratory and photorespiratory conditions. The samples were harvested at 0, 8, 32 and 56 h after transferring long day-grown plants from high CO<sub>2</sub> to normal air conditions. The glucosinolate concentrations are given in  $\mu\text{mol/g}$  dry weight. Camalexin contents are expressed as relative content per g fresh weight. Values are means  $\pm$  standard error from three samples, each consisting of six leaves. H, High CO<sub>2</sub> concentration (3,000 ppm CO<sub>2</sub>); non-photorespiratory conditions. A, Ambient CO<sub>2</sub> concentration (380 ppm CO<sub>2</sub>); photorespiratory conditions. Values statistically different from the wild type at the same time point are highlighted in bold case. 3M-SOP = Glucoiberin, 4M-SOB = Glucoraphain; 5M-SOP = Glucoalysin; 8M-SOO = Glucohirsutin; I3M = Glucobrassicin; 4MO-I3M = 4-Methoxyglucobrassicin; 1MO-I3M = Neoglucobrassicin; Sum GSL = Sum of glucosinolates; Sum AG = Sum of aliphatic glucosinolates; Sum IG = Sum of indolic glucosinolates.

		3MSOP		4MSOB		5MSOP		8MSOO	
		H	A	H	A	H	A	H	A
WT	0	2.3 $\pm$ 0.1		11.1 $\pm$ 0.7		0.5 $\pm$ 0.0		1.2 $\pm$ 0.1	
	8	2.1 $\pm$ 0.1	1.7 $\pm$ 0.2	10.4 $\pm$ 0.6	9.1 $\pm$ 0.9	0.5 $\pm$ 0.1	0.5 $\pm$ 0.0	1.3 $\pm$ 0.1	1.5 $\pm$ 0.1
	56	1.8 $\pm$ 0.1	1.7 $\pm$ 0.3	8.8 $\pm$ 0.8	10.7 $\pm$ 1.9	0.4 $\pm$ 0.0	0.5 $\pm$ 0.0	1.2 $\pm$ 0.2	1.5 $\pm$ 0.0
	128	1.5 $\pm$ 0.0	1.2 $\pm$ 0.1	9.5 $\pm$ 0.1	7.7 $\pm$ 0.6	0.5 $\pm$ 0.0	0.3 $\pm$ 0.0	1.3 $\pm$ 0.0	1.8 $\pm$ 0.1
GO5	0	2.5 $\pm$ 0.2		11.6 $\pm$ 1.1		0.5 $\pm$ 0.0		1.2 $\pm$ 0.1	
	8	<b>1.3 <math>\pm</math> 0.3</b>	2.3 $\pm$ 0.2	<b>6.0 <math>\pm</math> 1.4</b>	10.6 $\pm$ 1.2	<b>0.3 <math>\pm</math> 0.0</b>	<b>0.3 <math>\pm</math> 0.0</b>	1.0 $\pm$ 0.1	1.3 $\pm$ 0.1
	56	<b>2.5 <math>\pm</math> 0.1</b>	1.9 $\pm$ 0.4	<b>11.0 <math>\pm</math> 0.2</b>	8.7 $\pm$ 1.7	0.4 $\pm$ 0.0	0.4 $\pm$ 0.0	1.4 $\pm$ 0.1	1.5 $\pm$ 0.2
	128	1.7 $\pm$ 0.2	1.7 $\pm$ 0.2	8.9 $\pm$ 0.7	7.3 $\pm$ 0.9	<b>0.4 <math>\pm</math> 0.0</b>	<b>0.2 <math>\pm</math> 0.0</b>	1.3 $\pm$ 0.1	1.7 $\pm$ 0.1
<i>cat2-2</i>	0	1.8 $\pm$ 0.4		8.5 $\pm$ 1.7		0.5 $\pm$ 0.1		1.3 $\pm$ 0.2	
	8	1.6 $\pm$ 0.2	1.6 $\pm$ 0.2	9.0 $\pm$ 1.1	8.7 $\pm$ 0.9	0.4 $\pm$ 0.1	0.5 $\pm$ 0.0	1.2 $\pm$ 0.1	1.3 $\pm$ 0.0
	56	1.8 $\pm$ 0.1	1.3 $\pm$ 0.1	9.6 $\pm$ 0.4	8.6 $\pm$ 1.1	0.4 $\pm$ 0.0	0.4 $\pm$ 0.1	1.3 $\pm$ 0.1	1.6 $\pm$ 0.1
	128	1.3 $\pm$ 0.2	1.2 $\pm$ 0.2	8.9 $\pm$ 1.8	8.2 $\pm$ 1.2	0.4 $\pm$ 0.1	0.4 $\pm$ 0.0	1.4 $\pm$ 0.2	1.9 $\pm$ 0.1

		I3M		4MOI3M		1MOI3M		Sum GSL	
		H	A	H	A	H	A	H	A
WT	0	3.0 $\pm$ 0.2		2.1 $\pm$ 0.2		3.9 $\pm$ 0.6		24.4 $\pm$ 1.1	
	8	2.8 $\pm$ 0.2	2.5 $\pm$ 0.3	2.2 $\pm$ 0.2	1.7 $\pm$ 0.1	4.1 $\pm$ 0.4	4.2 $\pm$ 0.7	23.7 $\pm$ 1.3	21.7 $\pm$ 0.8
	56	1.8 $\pm$ 0.1	2.9 $\pm$ 0.2	1.9 $\pm$ 0.2	1.1 $\pm$ 0.1	4.2 $\pm$ 0.5	2.5 $\pm$ 0.1	20.3 $\pm$ 1.3	21.3 $\pm$ 2.2
	128	2.8 $\pm$ 0.1	3.1 $\pm$ 0.1	1.2 $\pm$ 0.1	0.9 $\pm$ 0.1	3.6 $\pm$ 0.5	1.4 $\pm$ 0.2	20.7 $\pm$ 0.5	16.7 $\pm$ 0.8
GO5	0	3.2 $\pm$ 0.3		2.2 $\pm$ 0.1		5.1 $\pm$ 0.8		26.6 $\pm$ 1.4	
	8	<b>2.0 <math>\pm</math> 0.2</b>	2.9 $\pm$ 0.4	<b>1.6 <math>\pm</math> 0.1</b>	<b>2.1 <math>\pm</math> 0.1</b>	3.0 $\pm$ 0.3	3.7 $\pm$ 0.4	<b>15.5 <math>\pm</math> 2.2</b>	23.5 $\pm$ 1.8
	56	<b>2.3 <math>\pm</math> 0.1</b>	2.8 $\pm$ 0.1	2.1 $\pm$ 0.1	<b>1.5 <math>\pm</math> 0.1</b>	<b>5.8 <math>\pm</math> 0.4</b>	2.0 $\pm$ 0.3	<b>25.8 <math>\pm</math> 0.8</b>	19.2 $\pm$ 2.5
	128	2.9 $\pm$ 0.3	3.2 $\pm$ 0.0	1.2 $\pm$ 0.1	0.9 $\pm$ 0.1	3.5 $\pm$ 0.3	1.3 $\pm$ 0.2	20.1 $\pm$ 1.0	16.8 $\pm$ 1.4
<i>cat2-2</i>	0	2.6 $\pm$ 0.4		2.2 $\pm$ 0.3		4.0 $\pm$ 0.3		21.3 $\pm$ 2.9	
	8	<b>2.0 <math>\pm</math> 0.1</b>	3.2 $\pm$ 0.1	<b>1.6 <math>\pm</math> 0.1</b>	1.8 $\pm$ 0.1	4.8 $\pm$ 0.6	3.8 $\pm$ 0.6	20.9 $\pm$ 1.8	21.1 $\pm$ 1.0
	56	2.3 $\pm$ 0.3	2.7 $\pm$ 0.1	2.0 $\pm$ 0.2	<b>1.5 <math>\pm</math> 0.1</b>	3.4 $\pm$ 0.2	3.5 $\pm$ 1.2	21.0 $\pm$ 0.9	20.0 $\pm$ 2.6
	128	<b>3.1 <math>\pm</math> 0.1</b>	3.3 $\pm$ 0.2	<b>1.4 <math>\pm</math> 0.0</b>	1.0 $\pm$ 0.0	4.0 $\pm$ 0.4	1.7 $\pm$ 0.2	20.9 $\pm$ 2.3	17.9 $\pm$ 1.6

		Sum AG		Sum IG		Camalexin	
		H	A	H	A	H	A
<b>WT</b>	0	15.5 ± 0.9		9.0 ± 0.4		73.8 ± 19.5	
	8	14.7 ± 0.8	13.2 ± 1.0	9.0 ± 0.7	8.5 ± 0.8	35.5 ± 16.0	38.9 ± 8.6
	56	12.4 ± 1.2	14.8 ± 2.3	7.9 ± 0.6	6.5 ± 0.3	52.6 ± 30.1	73.8 ± 52.6
	128	13.1 ± 0.1	11.3 ± 0.7	7.6 ± 0.6	5.4 ± 0.3	15.6 ± 5.9	1.2 ± 0.14
<b>G05</b>	0	16.1 ± 1.3		10.5 ± 0.7		80.3 ± 59.2	
	8	<b>8.9 ± 1.8</b>	14.8 ± 1.4	<b>6.7 ± 0.5</b>	8.7 ± 0.5	41.5 ± 19.9	68.8 ± 28.5
	56	<b>15.7 ± 0.4</b>	12.9 ± 2.3	<b>10.1 ± 0.5</b>	6.3 ± 0.4	75.2 ± 22.8	31.4 ± 15.5
	128	12.6 ± 0.9	11.4 ± 1.2	7.6 ± 0.3	5.4 ± 0.2	62.5	5.8 ± 4.9
<b>cat2-2</b>	0	12.4 ± 2.2		8.9 ± 0.8		187.7 ± 110.2	
	8	12.5 ± 1.4	12.3 ± 1.1	8.4 ± 0.6	8.8 ± 0.7	85.0 ± 57.8	66.9
	56	13.3 ± 0.5	12.3 ± 1.5	7.7 ± 0.6	7.7 ± 1.3	52.3 ± 16.8	5.2 ± 1.6
	128	12.3 ± 2.2	12.0 ± 1.5	8.6 ± 0.4	5.9 ± 0.4	<b>92.6 ± 24.3</b>	10.9 ± 6.7

**Supplemental Table 11.** Primers used for the qRT-PCR analysis.

<b>Locus</b>	<b>Description</b>	<b>Forward primer (5'-&gt;3')</b>	<b>Reverse primer (5'-&gt;3')</b>
At1g21120	IGTM2	GATGTGGGAGGTGGAGTTGG	TGCCAAGGCGCAAGTTAGAT
At2g04050	DTX3	TCCTTTATCCTCGACGGTTTCA	GCTACCACGTTGTTCAAAGCTC
At2g38470	WRKY33	GTGGGAGTGAACCTGAAGCA	TGCACTACGATTCTCGGCTC
At3g18780	Actin	AGTGGTCGTACAACCGGTATTGT	GATGGCATGAGGAAGAGAGAAAC
At3g25250	AGC2-1	TTGGTGGTCGTTAGGGGTTG	CACCAGTTAGATTCGGCGGT
At3g28740	CYP81D11	GGCAAAGACCGAAATCGACG	GCCACCGGATAAAGCCGTAA
At5g62480	GSTU9	TAGCCCTTACAAGGCACACG	CTTTGACCACGCTGGTTTCG

**Manuscript 2:** Spatial H<sub>2</sub>O<sub>2</sub> Signalling Specificity: H<sub>2</sub>O<sub>2</sub> from Chloroplasts and Peroxisomes Modulates the Plant Transcriptome Differentially

**Status:** Submitted to Molecular Plant (January 2014)

Nasser Sewelam, Nils Jaspert, Katrien Van Der Kelen, Jessica Schmitz, Henning Frerigmann, Vanesa B. Tognetti, Elia Stahl, Jürgen Zeier, Frank Van Breusegem and Veronica G. Maurino

**Journal:**Molecular Plant

**Impact factor:** 6,126

1. Co-Author

**Own contribution:**50 %

- Plant growth and harvest
- DAB-Staining
- Sample preparation of Camalexin/Glycosinolates/Sterols
- Analysis of measured Camalexin/Glycosinolates/Sterols
- Co-writing Manuscript

## **Manuscript 3**

Substrate specificities of peroxisomal H<sub>2</sub>O<sub>2</sub>-producing (L)-2 hydroxyacid oxidases.

**Substrate specificities of peroxisomal H<sub>2</sub>O<sub>2</sub>-producing (L)-2 hydroxyacid oxidases**

Anke Kuhn<sup>1</sup>, Martin KM Engqvist<sup>1</sup>, Nils Jaspert<sup>2</sup>, Jessica Schmitz<sup>2</sup> and Veronica G Maurino<sup>2</sup>

<sup>1</sup>Botanical Institute, Cologne Biocenter, University of Cologne, 50674 Cologne, Germany

<sup>2</sup>Institut of Developmental and Molecular Biology of Plants, Plant Molecular Physiology and Biotechnology Group, Heinrich-Heine-Universität, Universitätsstraße 1, 40225 Düsseldorf, Germany

To whom correspondence should be addressed. E-mail [veronica.maurino@uni-duesseldorf.de](mailto:veronica.maurino@uni-duesseldorf.de), tel. 49-211-8112368

## Abstract

Expression of GO1, -2 and -3 in *E. coli* and analysis of their kinetic parameters show, that GO1 and GO2 are highly selective towards glycolate while GO3 oxidizes both glycolate and L-lactate with comparable efficiencies. To assess the *in vivo* substrate of GO3, homozygous loss-of-function mutants (*go3*) were isolated and GO3 overexpressing lines were generated. Root development on medium supplemented with glycolate was impaired in all genotypes analysed. In contrast, root development on medium supplemented with L-lactate was impaired in *go3* lines with respect to the wild-type while GO3 overexpressing lines showed longer roots than wild-type. Next a complementation assay with yeast was carried out. A yeast strain deficient in the protein CYB2 is not able to grow on L-lactate as sole carbon source. Overexpression of GO3 from *A. thaliana* complemented this phenotype, strongly suggesting that L-lactate is the *in vivo* substrate of GO3.

## Introduction

In all photosynthetic organisms RubisCO performs a dual function, it carboxylates and oxygenates ribulose-1,5-bisphosphate (RuBP). During CO<sub>2</sub> fixation two molecules of 3-phosphoglycerate (3-PGA) are produced, while during O<sub>2</sub> fixation, one molecule of 3-PGA and one molecule of 2-phosphoglycolate (2-PGA) are formed (Ogren and Bowes, 1971). 3-PGA is used for biosynthetic reactions and the recycling of the acceptor molecule RuBP, while 2-PGA cannot be used by plants for biosynthetic reactions and it is a potent inhibitor of chloroplastic function (Anderson, 1971). The photorespiratory cycle serves as a carbon recovery system converting 2-PGA to 3-PGA (Maurino and Peterhansel, 2010). In C<sub>3</sub> plants, while there is not a single photorespiratory phenotype (Timm *et al.*, 2012), null-mutations in many of the enzymatic steps of the photorespiratory cycle result in plants that can survive in high CO<sub>2</sub> but are unviable in normal air, the so called conditional lethal high-CO<sub>2</sub> requiring phenotype (Somerville, 2001). Recently, it was shown that all organisms performing oxygenic photosynthesis (cyanobacteria, C<sub>3</sub> and C<sub>4</sub> plants) require photorespiration to survive, because a complete interruption of 2-PGA metabolism is lethal under normal growth conditions independent of the amounts of 2-PGA formed (Eisenhut *et al.*, 2008; Zelitch *et al.*, 2009).

During photorespiration dephosphorylation of 2-PGA in the chloroplasts yields glycolate, which is transported to the peroxisomes. Glycolate oxidase (GO) catalyses the oxidation of

glycolate into equimolar amounts of glyoxylate and H<sub>2</sub>O<sub>2</sub> (Maurino and Peterhansel, 2010). GO-suppressed maize, containing an activator insertion in the GO1 locus, showed the typical conditional lethal high-CO<sub>2</sub> requiring phenotype suggesting that in this C<sub>4</sub> plant the majority of the GO activity is associated with GO1 (Zelitch *et al.*, 2009). On the other hand, an inducible antisense suppression of GO in rice resulting in very low expression of OsGO1 and reduced expression of OsGO4 and OsGO5, resulted in plants that were severely stunted under normal air conditions (Xu *et al.*, 2009). Mutants lacking GO were never recovered by reverse genetic screens looking for plants that could survive in high CO<sub>2</sub> but were unviable in normal air. This failure was explained by the presence of multiple GO gene members.

GO belong to the gene family of (L)-2-hydroxyacid-oxidases ((L)-2-HAOX; Esser *et al.*, 2014). The biological role of plantae (L)-2-HAOX in photorespiration evolved by co-opting an existing eukaryotic GO (Esser *et al.*, 2014). In addition to GO, plants possess (L)-2-HAOX proteins with different specificities for medium- and long-chain hydroxyacids (IHAOX). The duplication and diversification of a common (L)-2-HAOX ancestor in plants giving rise to GO and IHAOX proteins occurred at the base of vascular plants (Esser *et al.*, 2014).

The Arabidopsis genomes contain a (L)-2-HAOX family composed of five paralogues predicted to encode peroxisomal proteins as they contain conserved peroxisomal targeting sequences (PTS1) and most of them were found in proteome analyses of peroxisomes (Reumann *et al.*, 2007; Reumann *et al.*, 2009). Two close related genes At3g14420 (GO1) and At3g14415 (GO2) would support photorespiration, as they are highly expressed in photosynthetic tissues (Reumann *et al.*, 2004). A third paralogue, At4g18360 (GO3) showed lower expression in autotrophic tissues (Kamada *et al.*, 2003) and it is predominantly expressed in roots and senescence leaves (eFP Browser; <http://www.bar.utoronto.ca/>). These three (L)-2-HAOX are predicted to use glycolate as main substrate (Esser *et al.*, 2014). The two more distant paralogues, At3g14130 (IHAOX1) and At3g14150 (IHAOX2) possess different specificities for medium- and long-chain hydroxyacids and are likely involved in fatty acid and protein catabolism (Esser *et al.*, 2014). IHAOX1 and IHAOX2 are mainly expressed in seeds at different developing stages (eFP Browser; <http://www.bar.utoronto.ca/>).

While there exist supporting evidence for the role of GO1 and GO2 in photorespiration, the biological significance for the other three glycolate oxidase paralogues remains to be further understood in plants. In this work, the Arabidopsis GOs paralogues GO1, GO2 and GO3 were expressed as recombinant proteins, the substrate specificities and kinetic constants were



determined and the cofactor identity was established. To assess the substrate of GO3 *in vivo*, knock-out mutants and overexpression lines were produced and analysed and complementation assays were performed. Our results indicated that GO3 is not involved in photorespiration and that it may be involved in the metabolism of L-lactate.

## Results

### Biochemical characterization of heterologously expressed GO1-3

To analyse the biochemical properties of *A. thaliana* GO paralogues, GO1, GO2 and GO3 were heterologously expressed in *E. coli* and purified to homogeneity (Figure 1). The isolated recombinant proteins have expected molecular masses of approximately 45 kDa (GO1: 43 kDa plus an approximately 3 kDa fragment encoded by the expression vector; GO2 and GO3: 42 kDa plus an approximately 3 kDa fragment encoded by the expression vector) (Figure 1).

To biochemically characterize GO1-3 the enzymatic activities using glycolate were determined using a number of different electron acceptors. None of the enzymes displayed activity using cytochrome c, NAD or NADP as electron acceptor. In contrast, when measuring the activity with molecular oxygen (O<sub>2</sub>) as an acceptor or the artificial electron acceptor DCIP high activities could be determined with all isozymes (Table 1). GO1 showed the highest activity using DCIP as electron acceptor, and displayed 74% activity using O<sub>2</sub>. The behaviour of GO2 was opposite, it showed the highest activity using O<sub>2</sub> as electron acceptor, and displayed 75% activity with DCIP. GO3 had similar activities using either O<sub>2</sub> (100%) or DCIP (99%). These results show that all isolated GO isozymes can act as oxidases and dehydrogenases *in vitro*. The fact that GO1-3 did not show activity with cytochrome c, NAD or NADP as electron acceptor suggests that if the enzymes would act as dehydrogenases they may transfer the electrons to other protein/s *in vivo*.

Although all GO isozymes can similarly function *in vitro* as oxidases and dehydrogenases, it is universally accepted that the photorespiratory isozymes act *in vivo* as oxidases producing H<sub>2</sub>O<sub>2</sub>, which is further dismutated by catalase (Foyer *et al.*, 2009). Thus, the kinetic constants of GO1 and GO3 for molecular oxygen were determined, assuming that large differences in the affinity for O<sub>2</sub> or the respective catalytic efficiency could give an indication, whether or not GO3 is a dehydrogenase rather than an oxidase. The kinetic constants for O<sub>2</sub> were determined for three different glycolate (5, 7.5 and 10 mM) and two different enzyme concentrations by

using an O<sub>2</sub> electrode. A sigmoidal kinetic was observed for both GO1 and GO3. The S<sub>0.5</sub> value for molecular oxygen, which represents the molecular oxygen concentration at which half of an enzyme is saturated when the reaction follows a sigmoidal, was approximately 190 and 200 μM for GO1 and GO3, respectively (Table 2). Both GO1 and GO3 had a Hill coefficient >1, indicating a positive cooperativity for the binding of molecular oxygen. Moreover, the respective catalytic rates of GO1 and GO3 were in the same order (Table 2). Taken all together, GO3 may function as an oxidase rather than a dehydrogenase *in vivo*, as is the case of the photorespiratory homologues.

### **Substrate screening**

A substrate screen performed with the recombinant GO1-3 indicated that all isozymes have narrow substrate specificities (Table 3). GO1-3 had the highest activities using glycolate as substrate, followed by L-lactate. The relative activities with L-lactate were 46%, 48% and 76% in the case of GO1, GO2 and GO3, respectively. These results indicate that GO3 can use L-lactate more effectively than the photorespiratory isozymes. On the other hand, GO1-3 could use other long- and medium-chain 2-hydroxyacids although with much lower activities (Table 3). None of the isozymes used the D-lactate as substrate nor catalysed the reverse reaction using glyoxylate with either NADH or NADPH.

### **Determination of kinetic constants**

A kinetic characterization of GO1-3 was performed using the best substrates. All GO isozymes showed similar catalytic efficiencies ( $k_{cat}/K_m$ ) when using glycolate. The higher catalytic efficiencies were observed when the isozymes act on glycolate. Differences in the kinetic properties of the GO isozymes were found when L-lactate was used as substrate. GO1 and GO2 displayed very low catalytic efficiencies using L-lactate (22- and 31-fold lower catalytic efficiencies as with glycolate, respectively). These low catalytic efficiencies result from low affinities towards L-lactate (Table 4). The higher catalytic efficiencies of GO3 towards L-lactate result from much higher affinities towards L-lactate in comparison to GO1 and GO2 (Table 4). This suggests that GO3 is able to use L-lactate with a similar efficiency as it uses glycolate; in contrast GO1 and GO2, would use glycolate with much higher efficiencies.

The kinetic parameters determined indicated that both glycolate and L-lactate are putative substrates of GO3 *in vivo*. To evaluate if the use of L-lactate as substrate influence the preference for an electron acceptor, the kinetic constants of GO3 for molecular oxygen were also determined using L-lactate. As shown in Table 2, GO3 presented a similar behaviour towards O<sub>2</sub> when using L-lactate as substrate as those presented by GO1 and GO3 using glycolate as substrate. Again, the Hill coefficient was >1, indicating a positive cooperativity towards molecular oxygen. These results indicate that, as in the case of the photorespiratory counterparts, GO3 acts on glycolate and L-lactate as an oxidase *in vivo*.

Taken together, GO1 and GO2 exhibited very similar kinetic constants and prefer glycolate as substrate, while GO3 possessed different catalytic properties being less substrate-specific than the photorespiratory isozymes.

### **Subcellular localization of GO3**

GO1 and GO2 are well known to support photorespiration by oxidising glycolate into glyoxylate with the production of H<sub>2</sub>O<sub>2</sub> in the peroxisomes. GO3 was also predicted to localize to peroxisomes (Reumann *et al.*, 2004). To experimentally verify this, the full coding sequence of GO3 was fused in frame to the N-terminal YFP. This construct was expressed together with the peroxisomal control CFP-PTS1 (Linka *et al.*, 2008) in *N. benthamiana* leaves. Protoplasts of transformed *N. benthamiana* leaves showed CFP fluorescence of the peroxisomal control with the typical punctuate pattern for peroxisomes (Figure 2). The same pattern was observed for YFP-GO3 and the overlay showed that both patterns of fluorescence merged, confirming the peroxisomal localization of GO3 (Figure 2).

### **Conditional phenotype of *go3* plants and its complementation**

We isolated two independent T-DNA insertion lines in *GO3*; *go3-1* (GK\_523D09) and *go3-2* (SALK\_020909), with insertions in exon 10 and intron 10, respectively (Figure 3A). All lines were confirmed as knock-out mutants since no transcript could be detected in either case (Figure 3B).

The *in vitro* activity assays with purified recombinant GO3 revealed high enzymatic activity with both glycolate and L-lactate (Table 4). To further analyse which of these 2-hydroxyacids

is the most probable physiological substrate, wild-type and *go3* knock-out plants (*go3-1* and *go3-2*) were grown on sterile medium supplemented with either glycolate or L-lactate. Both genotypes developed roots of similar length on plates supplemented with glycolate (Figure 4). In contrast, root growth on medium supplemented with L-lactate was impaired in all *go3* insertional mutants (Figure 4). This difference in root growth was consistently seen in a dose-dependent manner over the concentration range of 0.5 mM to 10 mM L-lactate (not shown).

To confirm that the lack of GO3 was responsible for the enhanced toxicity towards L-lactate, a construct with the full length GO3 cDNA driven by its own promoter was used to produce overexpressing lines in the Col-0 wild-type background (GO3-OX2 line). Moreover, to assure high expression levels of GO3, lines overexpressing GO3 constitutively, using the 35S CaMV promoter, were also produced (GO3-OX1). In the several independent lines obtained the presence of the overexpression construct was confirmed by PCR analysis (not shown). The transgenic plants were allowed to self-pollinate until non-segregating T3 lines were obtained and the expression of GO3 was analysed by RT-PCR. The overexpressing lines showed no phenotypically differences when compared to the wild-type in normal conditions of growth. The growth of overexpressing lines was analysed on sterile medium supplemented with either glycolate or L-lactate (Figure 4). All these plants showed similar development to other genotypes assayed when grown in the presence of glycolate. In the presence of L-lactate, the overexpressing lines presented longer roots than the wild-type (Figure 4 B). These results suggested that GO3 is able to metabolize L-lactate *in vivo*.

### **Complementation of yeast deficient in L-lactate cytochrome c reductase with GO3**

In yeast L-lactate is produced during anoxia and upon re-oxygenation the L-lactate cytochrome c oxidoreductase (CYB2) is induced and metabolizes L-lactate to pyruvate. The catalytic domains of GO3 and CYB2 of *S. cerevisiae* showed high homology (40% identity, 57% similarity) (Figure 5A). The comparison of GO3 and CYB2 shows a lack of a cytochrome c binding domain in GO3 (Figure 5A). A loss-of-function mutant of CYB2 (*Δyml054c*) cannot grow on L-lactate as sole carbon source, but didn't show differences in growth to yeast with intact CYB2 (*yml054c*) on glucose (Figure 5B). To test if GO3 can complement the mutant phenotype, GO3 was overexpressed in *Δyml054c*. A semiquantitative PCR showed that neither in *Δyml054c* mutant nor in *yml054c* transcripts of GO3 were found

(Figure 5C). A droptest of all lines confirmed that GO3 can complement the *Δyml054c* growth phenotype on L-lactate as sole carbon source, indicating that GO3 can metabolize L-lactate to pyruvate *in vivo* (Fig 5B). Also a native PAGE assayed for activity indicated that the complemented line with GO3 used L-lactate as substrate (Figure 5D). These results also support the hypothesis, that GO3 might use L-lactate as substrate *in vivo*.

## Discussion

In contrast to the idea that the existence of two photorespiratory GO (GO1 and GO2) may represent the existence of isoforms with different catalytic properties, we found that both isoforms share extremely similar enzymatic properties. Although GO1-3 can function *in vitro* as oxidases and dehydrogenases, it is accepted that the photorespiratory isozymes act *in vivo* as oxidases.

The measurements of the enzyme kinetics show that GO1 and GO2 are typical photorespirational enzymes, which show the highest catalytic efficiency with glycolate as substrate. In contrast to that GO3 has similar catalytic efficiencies for L-lactate than for glycolate (Table 3). The comparison of the catalytic efficiencies of GO1 and GO3 with O<sub>2</sub> as electron acceptor and the fact, that GO3 cannot use NAD, NADP or cytochrome c as acceptor show that GO3 is an oxidase rather than a dehydrogenase. We also showed that GO3, like all other members of the (L)-2-HAOX family, is localized in the peroxisomes (Figure 2).

L-lactate is oxidized by L-lactate:NAD oxidoreductase (L-LDHn, EC 1.1.1.27), which catalyses the reaction  $\text{L-lactate} + \text{NAD} \rightarrow \text{pyruvate} + \text{NADH}$ , and by L-lactate cyt c oxidoreductase (L-LDHc, EC 1.1.2.3), which catalyses the reaction  $\text{L-lactate} + 2 \text{ cyt c (oxidized)} \rightarrow \text{pyruvate} + 2 \text{ cyt c (reduced)}$ . All known plant sequences belong to the EC 1.1.1.27 group, which *in vivo* catalyse only the reverse reaction:  $\text{pyruvate} + \text{NADH} \rightarrow \text{L-lactate} + \text{NAD}$  (L-LDH, At4g17260). Thus, plants lack such an activity to convert L-lactate into pyruvate (Cristescu *et al.*, 2008). Our hypothesis is that GO3 can resume this function in plants.

To find out the most probable substrate of GO3 *in vivo* we blasted GO3 and found a high similarity to an enzyme in *S. cerevisiae* (Figure 5A). CYB2 is a soluble protein from the mitochondrial intermembrane space, which catalyses the oxidation of L-lactate into pyruvate

and the transfer of electrons to cytochrome c (Ramil *et al.*, 2000; Hartl *et al.*, 1987). As showed in Guiard, (1985) a *S. cerevisiae* strain deficient in CYB2 cannot grow on L-lactate as sole carbon source. Here, we could show that *A. thaliana* GO3 can rescue this phenotype (Figure 5B). On L-lactate as sole carbon source the complemented yeast strains grow like the wild-type strain, although GO3 was not expressed in mitochondrial intermembrane space but in the cytosol. Most probable, the pyruvate produced by GO3 in the cytosol of the cells is transported to the mitochondria to be further metabolized. This result suggests that GO3 would be involved in plant L-lactate metabolism.

Plants produce L-lactate under anoxia/hypoxia through the L-lactate dehydrogenase (L-LDH, At4g17260) (Dolferus *et al.*, 2008) and have the ability to transport L-lactate out of the cell through NIP2-1, a major intrinsic protein transporter (At2g34390) (Choi and Roberts, 2007). Interestingly, the catalytic domain of GO3 and CYB2 are homologous (40% identity, 57% similarity) and in accordance to the putative activity of GO3 as oxidase in root peroxisomes it lacks the cyt c binding domain. In roots GO3 may fulfil a similar function as CYB2 in yeast: GO3 might be involved in the conversion of L-lactate back to pyruvate after the recovery from anoxia/hypoxia, and thus would ensure to maintain low, non-toxic levels of L-lactate after its formation during anoxia/hypoxia.

The loss-of-function mutants of GO3 cannot maintain low levels of L-lactate in the cells. Because L-lactate is toxic in higher amounts these mutants show retarded root growth on medium containing L-lactate (Figure 4). In contrast the overexpression lines of GO3, both GO3-OX1 and GO3-OX2, show a better root development. All mutant lines and Col-0 show no differences on plates containing glycolate, supporting that GO3 is not directly involved in the metabolization of this substrate.

The present results show that L-lactate is the most probable substrate of GO3 *in vivo*. But taking into account the affinity of GO3 to glycolate (Table 1) we cannot exclude a parallel metabolization of glycolate, yet. To answer this question feeding experiments with <sup>13</sup>C labeled L-lactate and glycolate should be performed in future. Nevertheless, independent of the substrate of GO3, this enzyme produces H<sub>2</sub>O<sub>2</sub> in the peroxisomes. We hypothesize that the produced H<sub>2</sub>O<sub>2</sub> could be involved in cellular signalling under specific physiological conditions.



## Methods

### Cloning of GO1-3 cDNAs in an expression vector

Full-length coding sequences of *A. thaliana* GO1 and GO3 were obtained through PCR amplification with *Pfu* Turbo DNA polymerase (Stratagene) using as template RNA extracted from leaf in the cases of GO1 and from roots in the case of GO3. The oligonucleotide primers used, designed to introduce XhoI sites at both ends of *GO1* and BamHI sites at both ends of *GO3*, were as follow: GO1-F (5'-TACTCGAGATGGAGATCACTAACGTTACCGA-3') and GO1-R (5'-ATCTCGAGGCTCAGCCTATAACCTGGCTGAAGGACGT-3), and GO3-F (5'-GGATCCGATGGAGATAACAAACGTGATGGA-3') and GO3-R (5'-GGATCCCTACAGCTTGGCCGAGAGG-3). PCR amplification conditions were as follows: initial denaturation at 95°C for 1.5 min followed by 37 cycles of denaturation at 95°C for 30 s, annealing at 64°C for 40 s, elongation at 72°C for 2 min, and a final elongation step at 72°C for 10 min. The amplified products were cloned into PCR-BluntII-TOPO (Invitrogen) and the generated plasmids were sequenced using the PRISM fluorescent dye-terminator system (Applied Biosystems). The inserts were cut out using the introduced restriction sites and ligated into the pET16b vector (Novagen) linearized with the same restriction enzyme. The resulting expression vectors, pET-16b-GO1 and pET-16b-GO3 were transformed into the BLR DE3 pLysS *E. coli* strain (Novagen). The vector pET-28a-GO2, kindly provided by Prof. Dr. Martin Hagemann (University of Rostock) was used for the heterologous expression of GO2 in Rosetta cells.

### Expression and purification of recombinant GO1-3

The vectors pET16b-GO1, pET-28a-GO2 and pET16b-GO3 generate fusion proteins with an N-terminal His-Tag facilitating the purification of the recombinant proteins. The cells transformed with the vectors were grown overnight in LB medium at 37°C and agitation at 220 rpm in the presence of 50 µg/ml carbencillin, 50 µg/ml chloramphenicol and in the case of BLR cells additional 5 µg/ml tetracycline. These pre-cultures were used to inoculate fresh LB medium in a relationship of 1:50. The cultures were grown at 37 °C in an orbital shaker at 220 rpm until the culture reached an OD<sub>600</sub> of 0.6. GO1 expression was induced by addition of 0.1 mM isopropyl-beta-D-thiogalactopyranoside (IPTG) and the culture was transferred to room temperature and grown for 20 h before being harvested. GO2 and GO3 expression was



induced by addition of 1 mM IPTG and the culture was grown at 37 °C for 4 h before being harvested. Cells were harvested by centrifugation at 4,000 x g for 10 min, resuspended in 35 ml 20 mM Tris-HCl (pH 8.0) containing 0.5 mg/ml phenylmethylsulfonyl fluoride (PMSF), sonicated and centrifuged at 10,000 x g for 15 min at 4 °C to remove debris. The supernatant was used for protein purification using immobilised metal ion chromatography on Ni<sup>2+</sup>-nitriloacetic acid agarose (Ni<sup>2+</sup>-NTA, Quiagen). The column was equilibrated and washed with 100 mM Na<sub>2</sub>PO<sub>4</sub> buffer (pH 8.0) containing 300 mM NaCl and 10 mM imidazole. The protein was eluted using 3 ml 100 mM Na<sub>2</sub>PO<sub>4</sub> (pH 7.2) and 250 mM imidazole. To remove imidazole and to concentrate the protein samples were spun on Centricon YM-30 spin columns (Amicon) and re-suspended in 20 mM Tris-HCl pH 8.0. The purified enzymes were used immediately for the kinetic measurements.

### **Enzymatic activities**

All enzyme assays were conducted at 25°C using a Tecan Infinite 200 plate reader (Tecan Deutschland GmbH, Crailsheim) in combination with the Magellan data analysis software (Tecan Austria GmbH, Grödig, Austria). The oxidase activity assays were conducted according to a modified protocol of (Feierabend and Beevers, 1972). The standard reaction mixture contained 100 mM Tris-HCl pH 7.5, 5mM substrate, 0.5 mM EDTA, 0.01 mM FMN, 5 mM MgCl<sub>2</sub>, and 4 mM phenylhydrazine in a final volume of 0.2 ml. As oxidases the enzymes use molecular oxygen as electron acceptor. The product of the reaction, the oxoacid of the substrate, reacts with the phenylhydrazine to the phenylhydrazone product, detected at 324 nm. The extinction coefficients ( $\epsilon$ ) for the glyoxylate-phenylhydrazone is 17 cm<sup>-1</sup> mM<sup>-1</sup> and for the pyruvatephenylhydrazone 10.4 cm<sup>-1</sup> mM<sup>-1</sup>. Activities of the enzymes as dehydrogenases were assayed in a reaction mixture containing 100 mM Tris-HCl pH 7.5, 5mM substrate, 0.5 mM EDTA, 0.01 mM FMN, 5 mM MgCl<sub>2</sub>, 200  $\mu$ M 2,6 dichlorophenol-indophenol (DCIP) and 3 mM phenazine methosulfate (PMS) in a final volume of 0.2 ml. The activities were measured by following the reduction of DCIP at 600 nm ( $\epsilon$ , 22 cm<sup>-1</sup> mM<sup>-1</sup>). A base line was determined by monitoring for 4 min before the reactions were started by the addition of purified enzyme (1-5  $\mu$ g).

### **Electron acceptor analysis**

The electron acceptors of the enzymes were evaluated using the standard reaction mixes and varying the type of electron acceptor and detection wavelength. The different electron acceptors used were molecular oxygen (detected at 324 nm, extinction coefficient  $\epsilon = 17 \text{ cm}^{-1} \text{ mM}^{-1}$ ) or 200  $\mu\text{M}$  Cytochrome c (detected at 550 nm, extinction coefficient  $\epsilon = 18.6 \text{ cm}^{-1} \text{ mM}^{-1}$ ) or 200  $\mu\text{M}$  DCIP used together with 3 mM PMS) or 1 mM NAD or NADP (detected at 340 nm, extinction coefficient  $\epsilon = 6.22 \text{ cm}^{-1} \text{ mM}^{-1}$ ).

### **Substrate screening**

The substrate specificities of the enzymes were assayed using standard reaction mixtures at pH 7.5 and either 5 mM of short- and medium-chain 2-hydroxyacids dissolved in water (glycolate, L-lactate, D-lactate, leucic acid, valic acid or isoleucic acid) other 0.5 mM long-chain 2-hydroxy fatty acids (2-hydroxyhexanoic acid, 2-hydroxyoctanoic acid, 2-hydroxydodecanoic acid or 2-hydroxyhexadecanoic acid) dissolved in ethanol.

### **Determination of kinetic constants**

The catalytic constants  $K_m$ ,  $V_{max}$  and  $k_{cat}$  for the substrates glycolate and L-lactate were determined in the standard reaction mixture at pH 7.5 using molecular oxygen (oxidase reaction) or PMS and DCIP (dehydrogenase reaction) as electron acceptors. The concentration of the substrates was varied from 0 mM to 37.9 mM while the concentrations of the other components were kept constant. The kinetic constants were calculated with at least two different enzyme batches each containing at least triplicate determinations and adjusted to non-linear regression to the Michaelis Menten equation  $f(x) = a \cdot x / (b + x)$  (Sigma plot software). One unit of enzyme activity is defined as the amount that oxidizes 1  $\mu\text{mol}$  of substrate/min.

The determination of the catalytic constants  $K_m$ ,  $V_{max}$  and  $k_{cat}$  for molecular oxygen of GO1 and GO3 was conducted with a Clark electrode in combination with the Logger Pro (measurements) and Logger Lite (evaluation) software (Vernier Software and Technology, Beaverton, OR, USA). The standard reaction mix was pipetted onto the calibrated oxygen electrode without the substrate. The basal oxygen consumption was measured for approximately 2 min, then glycolate or L-lactate were added and the oxygen consumption was recorded until the slope reached that of the basal oxygen consumption. Measurements were

conducted with three substrate concentrations 5, 7.5 and 10 mM and using two different enzyme concentrations. The rates of oxygen consumption and the respective oxygen concentrations were determined every 30 s beginning with the highest rate of oxygen consumption. As the kinetics showed a sigmoidal course the constant describing the substrate concentration at which half of the enzyme is saturated ( $S_{0.5}$ ) was determined using the nonlinear regression fit to the sigmoidal Hill equation  $f(x) = a \cdot x^b / c^b + x^b$  (Sigma Plot software).

### **Localization studies of GO3**

The above amplified GO3 full-length coding sequence was cloned into pENTR4 by restriction digestion with NcoI and NotI and subsequently sequenced. This entry vector was further used in a LR recombination reaction (Invitrogen) with the vector pENSGYFP to generate an N-terminal YFP translational fusion (pENSG-YFP-GO3). This construct and the peroxisomal control CFP-PTS1 (Linka *et al.*, 2008) were transformed into the *A. tumefaciens* strains GV3101 pMP90 RK and GV3101 pMP90, respectively, using standard protocols. Transformation of *Nicotiana benthamiana* was performed by injecting recombinant agrobacteria into the apoplast of whole leaves as previously described (Wydro *et al.*, 2006). Three days after infiltration protoplasts were prepared following a modified protocol from (Sheen, 1991). Briefly, 10 leaf discs of 0.75 mm diameter were digested in enzyme solution, protoplasts pelleted by gravitation, resuspended and analysed by confocal laser-scanning microscopy using a LSM700 microscope in combination with the ZEN software (Zeiss, Göttingen).

### **Polyacrylamide gel electrophoresis and protein determination**

Denaturing sodium dodecyl sulfate (SDS)-PAGE was performed using 12.5% (w/v) polyacrylamide gels according to (Laemmli, 1970). Native PAGE was performed employing an 8% (w/v) polyacrylamide gel. Electrophoresis was run at 100 V and 4°C. Proteins were visualized with Coomassie Blue. Gels were also assayed for activity by incubation in the dark at 30°C with 50 mM  $K_2PO_4$  pH 8.75, 5 mM substrate, 0.05% (w/v) nitro blue tetrazolium (NBT) and 150  $\mu$ M PMS in a final volume of 5 ml. Protein concentration was determined according to the method of (Bradford, 1976).

### Screening for T-DNA insertion lines and genotyping

Seeds of the T-DNA insertion lines GABI\_523D09 (*go3-1*) and SALK\_020909 (*go3-2*) were obtained from the Nottingham Arabidopsis Stock Center (NASC, <http://www.Arabidopsis.info/>). Plants homozygous for the insertion were isolated and confirmed by two sets of PCR reactions using genomic DNA as a template. The first PCR was performed using primers GO3F1 (TGGTGGATAATTGCAGACGA) and GO3R1 (AACAGGGGAAATGACAAGAGC), GO3F1 and GO3R2 (CAGCTTGGCCGAGAGGTA) and GO3F2 (CTGTTACTTTTCTCGTCGATGC) and GO3R3 (CCGTTGTGCTCACATCAATC), which are specific for the wild-type gene in *go3-1* and *go3-2*, respectively. The second PCR was carried out with the T-DNA left border primer GABI-KAT-LB (5'-ATAATAACGCTGCGGACATCTACATTTT-3') in combination with *go3F1* and the T-DNA left border primer SALK-LB (5'-GTCCGCAATGTGTTATTAAGTTGTC-3') in combination with GO3F1, in the case of *go3-1* and *go3-2*, respectively.

### RNA isolation and cDNA transcription

Total RNA was isolated from 100 mg roots of 4-week-old plants or alternatively from siliques using the TRIzol reagent (Gibco-BRL). One microgram of total RNA was reverse transcribed into first strand cDNA using the SuperScriptII Reverse Transcriptase (Invitrogen) and used for PCR amplification.

### Construction of a binary vector to express GO3, plant transformation and selection of transformants

In order to complement *go3* loss-of-function mutants and produce overexpressing lines the promoter (1.786 kb) and full-length cDNA (1.107 kb) encoding *GO3* were amplified from root DNA and cDNA, respectively. The pair of primers used was the following, GO3Prom-F (TAGCGGCCGCACCGAGAACAACAGGATTTA) and GO3Prom-R (TAGGTACCTTTTATTTACTCAAACTCAAAAA) and GO3cDNA-F (AAGGTACCATGGAGATAACAAACGTGATGGA) and GO3cDNA-R (TTTCTAGACTACAGCTTGGCCGAGAGGT). The fragments obtained were cloned into

the Topo Vector (Invitrogen). The promoter fragment was further cloned into a modified version of the binary vector pGreen II (*35S-pGreenII-nosBAR*; Fahnenstich *et al.*, 2007) by substitution of the CaMV35S promoter (*GO3Promoter-pGreenII-nosBAR*). The GO3 cDNA was then cloned into pGreenII-GO3Promoter-nosBAR using the restriction sites KpnI and XbaI. The resulting plasmid containing the promoter and full-length GO3 cDNA (*GO3-pGreenII*) was introduced into *A. thaliana* (Col-0) and the knock-out mutants *go3-1* and *go3-2* by *Agrobacterium tumefaciens* (GV3101) mediated transformation using the vacuum infiltration method (Bechtold *et al.*, 1993). Transformants were selected by resistance to BASTA. DNA was extracted from leaf material collected from selected plants and used for PCR analyses. Plants containing the transgene were allowed to self-pollinate. Seeds from the primary (T1) generation were sown, and resultant T2 plants were subjected to another round of BASTA selection and characterization by means of PCR and activity assay. The process was repeated to obtain nonsegregating T3 transgenic lines. All further analyses were performed with homozygous T3 transgene plants.

### **Plant growth conditions**

*A. thaliana* wild-type (Columbia-0) and transgenic lines were grown in pots containing three parts of soil (Gebr. Patzer KG, Sinntal-Jossa) and one part of vermiculite (Basalt Feuerfest, Linz) in a growth cabinet in a 16/8h light/dark cycle at 22°C day/18°C night temperatures and at a photosynthetically active photon flux density of 100  $\mu\text{mol quanta m}^{-2} \text{s}^{-1}$ . Alternatively, plants were grown in liquid medium containing 4.6 g/L Murashige and Skoog (MS) and 3% sucrose at pH 5.6 in the dark at 28°C and constant agitation. Growth of plants in the presence of different concentrations of L-lactate and glycolate was conducted on 1/2 MS-agar plates without sucrose in a growth cabinet as described above. To measure the root length the plates were arranged vertical.

### **Yeast complementation analysis**

In order to complement the CYB2 loss-of function mutant (*Δyml054c*, Euroscarf) from *S. cerevisiae*, full-length cDNA encoding GO3 from *A. thaliana* were amplified from root cDNA (GO3-cDNA-F: AAGGTACCATGGAGATAACAAACGTGATGGAA, GO3-cDNA-R: AAGAATTCCTACAGCTTGGCCGAGAGGTAAT). The PCR fragment was digested with

*KpnI* and *EcoRI* and ligated into the pYes2 vector (life technologies). The resulting vector contains a galactose induced promoter, the full-length cDNA encoding GO3 and a uracil cassette for selection of positive transformants. The plasmid was transformed in *Δyml054c* using Lithium Acetate Method (Gietz *et al.*, 1992). Additionally as a control the empty vector pYes2 was transformed into *Δyml054c* and the yml054c strain, which contains an intact CYB2. Transformants were selected on Drop-out-medium (DO-medium) without Uracil, but containing glucose. The transformants were tested via PCR using the primer mentioned above.

To test the complementation, the two strains *Δyml054c* and yml054c were grown in liquid DO-medium containing 2% (w/v) galactose overnight. The yeast-strains were centrifuged and the pellet was washed three times with sterile water. The yeast cells were resuspended in sterile water diluted to OD<sub>600</sub> 0.05, dropped on DO-medium agar plates containing 0.5% (w/v) L-lactate or 0.5% (w/v) glucose as control and incubated at 30°C for two days.

### **Proteinextraction from yeast**

The yeast strains were grown in DO-medium containing 2% (w/v) glucose overnight. They were centrifuged and washed three times with sterile water. They were resuspended in DO-medium containing 2% galactose or L-lactate to induce the production of GO3 or the wild-type protein Cyb2, diluted to OD<sub>600</sub> 0.5 and were incubated for 4 h at 30°C. Then the yeast cells were centrifuged and resuspend in 500 µl yeast breaking buffer (50 mM Sodium phosphate pH 7.4, 1 mM EDTA, 5% (w/v) glycerol) containing 1 mM phenylmethylsulfonylfluorid. An equal volume of acid-washed glass beads was added and grinded in a cell mill for 2x2 min with 30 Hz frequency. The supernatant was used for activity gel.

### **Statistical analysis**

Significance was determined according to the Student's *t*-test using Excel software (Microsoft Corporation, Unterschleißheim, Germany) and the term "significant" is used only in the case that the change observed has a  $p < 0.05$ .

## Acknowledgements

This work was supported by Deutsche Forschungsgemeinschaft as part of the German Photorespiration Research Network Promics (FOR 1186).

## References

- Anderson, L.E.** (1971) Chloroplast and cytoplasmic enzymes. II. Pea leaf triose phosphate isomerases. *Biochim. Biophys. Acta*, **235**, 237–244.
- Apel, K. and Hirt, H.** (2004) REACTIVE OXYGEN SPECIES: metabolism, oxidative stress, and signal transduction. *Annu. Rev. Plant Biol.*, **55**, 373–99.
- Balazadeh, S., Jaspert, N., Arif, M., Mueller-Roeber, B. and Maurino, V.G.** (2012) Expression of ROS-responsive genes and transcription factors after metabolic formation of H<sub>2</sub>O<sub>2</sub> in chloroplasts. *Front. Plant Sci.*, **3**, 234.
- Barber, J.** (1998) Photosystem two. *Biochim. Biophys. Acta*, **1365**, 269–277.
- Bechtold, N., Ellis, J. and Pelletier, G.** (1993) In planta Agrobacterium-mediated gene transfer by infiltration of adult *Arabidopsis thaliana* plants. *Comptes Rendus L Acad. Des Sci. Ser. Iii-Sciences La Vie-Life Sci.*, **316**, 1194–1199.
- Beezley, B.B., Gruber, P.J. and Frederick, S.E.** (1976) Cytochemical localization of glycolate dehydrogenase in mitochondria of chlamydomonas. *Plant Physiol.*, **58**, 315–319.
- Bhattacharjee, S.** (2005) Reactive oxygen species and oxidative burst: Roles in stress, senescence and signal transduction in plants. *Curr. Sci.*, **89**, 1113–1121.
- Bienert, G.P. and Chaumont, F.** (2013) Aquaporin-facilitated transmembrane diffusion of hydrogen peroxide. *Biochim. Biophys. Acta - Gen. Subj.*
- Bienert, G.P., Schjoerring, J.K. and Jahn, T.P.** (2006) Membrane transport of hydrogen peroxide. *Biochim. Biophys. Acta*, **1758**, 994–1003.
- Boldt, R., Edner, C., Kolukisaoglu, U., Hagemann, M., Weckwerth, W., Wienkoop, S., Morgenthal, K. and Bauwe, H.** (2005) D-GLYCERATE 3-KINASE, the last unknown enzyme in the photorespiratory cycle in *Arabidopsis*, belongs to a novel kinase family. *Plant Cell*, **17**, 2413–2420.
- Bradford, M.M.** (1976) A rapid and sensitive method for the quantitation of microgram quantities of protein utilizing the principle of protein-dye binding. *Anal. Biochem.*, **72**, 248–254.

- Chaouch, S., Queval, G. and Noctor, G.** (2012) AtRbohF is a crucial modulator of defence-associated metabolism and a key actor in the interplay between intracellular oxidative stress and pathogenesis responses in Arabidopsis. *Plant J.*, **69**, 613–627.
- Choi, W.-G. and Roberts, D.M.** (2007) Arabidopsis NIP2;1, a major intrinsic protein transporter of lactic acid induced by anoxic stress. *J. Biol. Chem.*, **282**, 24209–18.
- Costa, A., Drago, I., Behera, S., Zottini, M., Pizzo, P., Schroeder, J.I., Pozzan, T. and Schiavo, F. Lo** (2010) H<sub>2</sub>O<sub>2</sub> in plant peroxisomes: an in vivo analysis uncovers a Ca(2+)-dependent scavenging system. *Plant J.*, **62**, 760–72.
- Cristescu, M.E., Innes, D.J., Stillman, J.H. and Crease, T.J.** (2008) D- and L-lactate dehydrogenases during invertebrate evolution. *BMC Evol. Biol.*, **8**, 268.
- Dean, R.T., Fu, S., Stocker, R. and Davies, M.J.** (1997) Biochemistry and pathology of radical-mediated protein oxidation. *Biochem. J.*, **324** ( Pt 1), 1–18.
- Debska, K., Krasuska, U., Budnicka, K., Bogatek, R. and Gniazdowska, A.** (2013) Dormancy removal of apple seeds by cold stratification is associated with fluctuation in H<sub>2</sub>O<sub>2</sub>, NO production and protein carbonylation level. *J. Plant Physiol.*, **170**, 480–488.
- Dolferus, R., Wolansky, M., Carroll, R., Miyashita, Y., Ismond, K. and Good, A.** (2008) Functional analysis of lactate dehydrogenase during hypoxic stress in Arabidopsis. *Funct. Plant Biol.*, **35**, 131.
- Eisenhut, M., Ruth, W., Haimovich, M., Bauwe, H., Kaplan, A. and Hagemann, M.** (2008) The photorespiratory glycolate metabolism is essential for cyanobacteria and might have been conveyed endosymbiotically to plants. *Proc. Natl. Acad. Sci. U. S. A.*, **105**, 17199–204.
- Engel, N., Daele, K. van den, Kolukisaoglu, U., Morgenthal, K., Weckwerth, W., Pärnik, T., Keerberg, O. and Bauwe, H.** (2007) Deletion of glycine decarboxylase in Arabidopsis is lethal under nonphotorespiratory conditions. *Plant Physiol.*, **144**, 1328–1335.
- Engqvist, M.** (2010) *Characterization of three 2-hydroxy-acid dehydrogenases in the context of a biotechnological approach to short-circuit photorespiration.* Universität zu Köln.
- Esser, C., Kuhn, A., Groth, G., Lercher, M.J. and Maurino, V.G.** (2014) Plant and animal glycolate oxidases have a common eukaryotic ancestor and convergently duplicated to evolve long-chain 2-hydroxy acid oxidases. *Mol. Biol. Evol.*, 1–13.
- Fahnenstich, H., Saigo, M., Niessen, M., Zanon, M.I., Andreo, C.S., Fernie, A.R., Drincovich, M.F., Flügge, U.-I. and Maurino, V.G.** (2007) Alteration of organic acid metabolism in Arabidopsis overexpressing the maize C<sub>4</sub> NADP-malic enzyme causes accelerated senescence during extended darkness. *Plant Physiol.*, **145**, 640–52.
- Fahnenstich, H., Scarpeci, T.E., Valle, E.M., Flügge, U.-I. and Maurino, V.G.** (2008) Generation of hydrogen peroxide in chloroplasts of Arabidopsis overexpressing glycolate oxidase as an inducible system to study oxidative stress. *Plant Physiol.*, **148**, 719–29.



- Feierabend, J. and Beevers, H.** (1972) Developmental studies on microbodies in wheat leaves : I. Conditions influencing enzyme development. *Plant Physiol.*, **49**, 28–32.
- Foreman, J., Demidchik, V., Bothwell, J.H.F., et al.** (2003) Reactive oxygen species produced by NADPH oxidase regulate plant cell growth. *Nature*, **422**, 442–6.
- Foyer, C.H., Bloom, A.J., Queval, G. and Noctor, G.** (2009) Photorespiratory metabolism: genes, mutants, energetics, and redox signaling. *Annu. Rev. Plant Biol.*, **60**, 455–84.
- Fridovich, I.** (1997) Superoxide anion radical, superoxide dismutases, and related matters. *J. Biol. Chem.*, **272**, 18515–18517.
- Frugoli, J.A., Zhong, H.H., Nuccio, M.L., McCourt, P., McPeck, M.A., Thomas, T.L. and McClung, C.R.** (1996) Catalase is encoded by a multigene family in *Arabidopsis thaliana* (L.) Heynh. *Plant Physiol.*, **112**, 327–336.
- Gietz, D., St Jean, A., Woods, R.A. and Schiestl, R.H.** (1992) Improved method for high efficiency transformation of intact yeast cells. *Nucl Acid Res*, **20**, 1425.
- Griebel, T. and Zeier, J.** (2010) A role for beta-sitosterol to stigmasterol conversion in plant-pathogen interactions. *Plant J.*, **63**, 254–68.
- Guiard, B.** (1985) Structure, expression and regulation of a nuclear gene encoding a mitochondrial protein: the yeast L(+)-lactate cytochrome c oxidoreductase (cytochrome b2). *EMBO J.*, **4**, 3265–72.
- Hartl, F.U., Ostermann, J., Guiard, B. and Neupert, W.** (1987) Successive translocation into and out of the mitochondrial matrix: targeting of proteins to the intermembrane space by a bipartite signal peptide. *Cell*, **51**, 1027–1037.
- Hideg, É., Kálai, T., Hideg, K. and Vass, I.** (1998) Photoinhibition of Photosynthesis in Vivo Results in Singlet Oxygen Production Detection via Nitroxide-Induced Fluorescence Quenching in Broad Bean Leaves†. *Biochemistry*, **37**, 11405–11411.
- Hooijmaijers, C., Rhee, J.Y., Kwak, K.J., Chung, G.C., Horie, T., Katsuhara, M. and Kang, H.** (2012) Hydrogen peroxide permeability of plasma membrane aquaporins of *Arabidopsis thaliana*. *J. Plant Res.*, **125**, 147–153.
- Hu, J., Baker, A., Bartel, B., Linka, N., Mullen, R.T., Reumann, S. and Zolman, B.K.** (2012) Plant peroxisomes: biogenesis and function. *Plant Cell*, **24**, 2279–303.
- Igarashi, D., Miwa, T., Seki, M., Kobayashi, M., Kato, T., Tabata, S., Shinozaki, K. and Ohsumi, C.** (2003) Identification of photorespiratory glutamate:glyoxylate aminotransferase (GGAT) gene in *Arabidopsis*. *Plant J.*, **33**, 975–987.
- Jain, V., Kaiser, W. and Huber, S.C.** (2008) Cytokinin inhibits the proteasome-mediated degradation of carbonylated proteins in *Arabidopsis* leaves. *Plant Cell Physiol.*, **49**, 843–852.

- Jamai, A., Salomé, P.A., Schilling, S.H., Weber, A.P.M. and McClung, C.R.** (2009) Arabidopsis photorespiratory serine hydroxymethyltransferase activity requires the mitochondrial accumulation of ferredoxin-dependent glutamate synthase. *Plant Cell*, **21**, 595–606.
- Jang, J.Y., Rhee, J.Y., Chung, G.C. and Kang, H.** (2012) Aquaporin as a membrane transporter of hydrogen peroxide in plant response to stresses. *Plant Signal. Behav.*, **7**, 1180–1181.
- Kamada, T., Nito, K., Hayashi, H., Mano, S., Hayashi, M. and Nishimura, M.** (2003) Functional Differentiation of Peroxisomes Revealed by Expression Profiles of Peroxisomal Genes in *Arabidopsis thaliana*. *Plant Cell Physiol.*, **44**, 1275–1289.
- Kelly, G.J. and Lutzko, E.** (1976) Inhibition of spinach-leaf phosphofructokinase by 2-phosphoglycollate. *FEBS Lett.*, **68**, 55–58.
- Keys, A.J.** (2006) The re-assimilation of ammonia produced by photorespiration and the nitrogen economy of C3 higher plants. *Photosynth. Res.*, **87**, 165–175.
- Kirkman, H.N. and Gaetani, G.F.** (2007) Mammalian catalase: a venerable enzyme with new mysteries. *Trends Biochem. Sci.*, **32**, 44–50.
- Kobayashi, M., Ohura, I., Kawakita, K., Yokota, N., Fujiwara, M., Shimamoto, K., Doke, N. and Yoshioka, H.** (2007) Calcium-dependent protein kinases regulate the production of reactive oxygen species by potato NADPH oxidase. *Plant Cell*, **19**, 1065–80.
- Kovtun, Y., Chiu, W.L., Tena, G. and Sheen, J.** (2000) Functional analysis of oxidative stress-activated mitogen-activated protein kinase cascade in plants. *Proc. Natl. Acad. Sci. U. S. A.*, **97**, 2940–2945.
- Kuhn, A.** (2012) *Functional characterization of 2-hydroxy acid oxidases / dehydrogenases in Arabidopsis thaliana*. Universität zu Köln.
- Kwak, J.M., Mori, I.C., Pei, Z.-M., et al.** (2003) NADPH oxidase AtrbohD and AtrbohF genes function in ROS-dependent ABA signaling in *Arabidopsis*. *EMBO J.*, **22**, 2623–33.
- Laemmli, U.K.** (1970) Cleavage of structural proteins during the assembly of the head of bacteriophage T4. *Nature*, **227**, 680–685.
- Lamb, C. and Dixon, R. a.** (1997) the Oxidative Burst in Plant Disease Resistance. *Annu. Rev. Plant Physiol. Plant Mol. Biol.*, **48**, 251–275.
- Lázaro, J.J., Jiménez, A., Camejo, D., Iglesias-Baena, I., Martí, M.D.C., Lázaro-Payo, A., Barranco-Medina, S. and Sevilla, F.** (2013) Dissecting the integrative antioxidant and redox systems in plant mitochondria. Effect of stress and S-nitrosylation. *Front. Plant Sci.*, **4**, 460.

- Lecourieux, D., Mazars, C., Pauly, N., Ranjeva, R. and Pugin, A.** (2002) Analysis and Effects of Cytosolic Free Calcium Increases in Response to Elicitors in *Nicotiana glauca* Cells. *Plant Cell Online*, **14**, 2627–2641.
- Liepman, A.H. and Olsen, L.J.** (2001) Peroxisomal alanine : glyoxylate aminotransferase (AGT1) is a photorespiratory enzyme with multiple substrates in *Arabidopsis thaliana*. *Plant J.*, **25**, 487–498.
- Linka, N., Theodoulou, F.L., Haslam, R.P., Linka, M., Napier, J.A., Neuhaus, H.E. and Weber, A.P.M.** (2008) Peroxisomal ATP import is essential for seedling development in *Arabidopsis thaliana*. *Plant Cell*, **20**, 3241–3257.
- Maurino, V.G. and Flügge, U.-I.** (2008) Experimental systems to assess the effects of reactive oxygen species in plant tissues. *Plant Signal. Behav.*, **3**, 923–928.
- Maurino, V.G. and Peterhansel, C.** (2010) Photorespiration: current status and approaches for metabolic engineering. *Curr. Opin. Plant Biol.*, **13**, 249–56.
- MEHLER, A.H.** (1951) Studies on reactions of illuminated chloroplasts. II. Stimulation and inhibition of the reaction with molecular oxygen. *Arch. Biochem. Biophys.*, **34**, 339–351.
- Mhamdi, A., Noctor, G. and Baker, A.** (2012) Plant catalases: Peroxisomal redox guardians. *Arch. Biochem. Biophys.*, **525**, 181–194.
- Mhamdi, A., Queval, G., Chaouch, S., Vanderauwera, S., Breusegem, F. Van and Noctor, G.** (2010) Catalase function in plants: a focus on *Arabidopsis* mutants as stress-mimic models. *J. Exp. Bot.*, **61**, 4197–220.
- Miller, G. and Mittler, R.** (2006) Could heat shock transcription factors function as hydrogen peroxide sensors in plants? *Ann. Bot.*, **98**, 279–88.
- Mittler, R., Vanderauwera, S., Suzuki, N., Miller, G., Tognetti, V.B., Vandepoele, K., Gollery, M., Shulaev, V. and Breusegem, F. Van** (2011) ROS signaling: The new wave? *Trends Plant Sci.*, **16**, 300–309.
- Møller, I.M., Jensen, P.E. and Hansson, A.** (2007) Oxidative modifications to cellular components in plants. *Annu. Rev. Plant Biol.*, **58**, 459–481.
- Møller, I.M. and Sweetlove, L.J.** (2010) ROS signalling--specificity is required. *Trends Plant Sci.*, **15**, 370–4.
- Nelson, E.B. and Tolbert, N.E.** (1970) Glycolate dehydrogenase in green algae. *Arch. Biochem. Biophys.*, **141**, 102–110.
- Nürnbergger, T. and Scheel, D.** (2001) Signal transmission in the plant immune response. *Trends Plant Sci.*, **6**, 372–9.
- Ogasawara, Y., Kaya, H., Hiraoka, G., et al.** (2008) Synergistic activation of the *Arabidopsis* NADPH oxidase AtrbohD by Ca<sup>2+</sup> and phosphorylation. *J. Biol. Chem.*, **283**, 8885–8892.

- Ogren, W.L. and Bowes, G.** (1971) Ribulose diphosphate carboxylase regulates soybean photorespiration. *Nat. New Biol.*, **230**, 159–160.
- Pei, Z.M., Murata, Y., Benning, G., Thomine, S., Klüsener, B., Allen, G.J., Grill, E. and Schroeder, J.I.** (2000) Calcium channels activated by hydrogen peroxide mediate abscisic acid signalling in guard cells. *Nature*, **406**, 731–734.
- Petrov, V.D. and Breusegem, F. Van** (2012) Hydrogen peroxide-a central hub for information flow in plant cells. *AoB Plants*, **2012**, pls014.
- Pfalz, M., Vogel, H. and Kroymann, J.** (2009) The gene controlling the indole glucosinolate modifier1 quantitative trait locus alters indole glucosinolate structures and aphid resistance in Arabidopsis. *Plant Cell*, **21**, 985–99.
- Pick, T.R., Bräutigam, A., Schulz, M. a, Obata, T., Fernie, A.R. and Weber, A.P.M.** (2013) PLGG1, a plastidic glycolate glycerate transporter, is required for photorespiration and defines a unique class of metabolite transporters. *Proc. Natl. Acad. Sci. U. S. A.*, **110**, 3185–90.
- Pnueli, L., Liang, H., Rozenberg, M. and Mittler, R.** (2003) Growth suppression, altered stomatal responses, and augmented induction of heat shock proteins in cytosolic ascorbate peroxidase (Apx1)-deficient Arabidopsis plants. *Plant J.*, **34**, 187–203.
- Queval, G., Issakidis-Bourguet, E., Hoerberichts, F. a, Vandorpe, M., Gakière, B., Vanacker, H., Miginiac-Maslow, M., Breusegem, F. Van and Noctor, G.** (2007) Conditional oxidative stress responses in the Arabidopsis photorespiratory mutant cat2 demonstrate that redox state is a key modulator of daylength-dependent gene expression, and define photoperiod as a crucial factor in the regulation of H<sub>2</sub>O<sub>2</sub>-induced cel. *Plant J.*, **52**, 640–57.
- Ramil, E., Agrimonti, C., Shechter, E., Gervais, M. and Guiard, B.** (2000) Regulation of the CYB2 gene expression: transcriptional co-ordination by the Hap1p, Hap2/3/4/5p and Adr1p transcription factors. *Mol. Microbiol.*, **37**, 1116–1132.
- Reumann, S., Babujee, L., Ma, C., et al.**(2007) Proteome analysis of Arabidopsis leaf peroxisomes reveals novel targeting peptides, metabolic pathways, and defense mechanisms. *Plant Cell*, **19**, 3170–93.
- Reumann, S., Ma, C., Lemke, S. and Babujee, L.** (2004) AraPeroX. A Database of Putative Arabidopsis Proteins from Plant Peroxisomes. *Plant Physiol.*, **136**, 2587–2608.
- Reumann, S., Quan, S., Aung, K., et al.** (2009) In-depth proteome analysis of Arabidopsis leaf peroxisomes combined with in vivo subcellular targeting verification indicates novel metabolic and regulatory functions of peroxisomes. *Plant Physiol.*, **150**, 125–43.
- Rio, L.A. del, Sandalio, L.M., Corpas, F.J., Palma, J.M. and Barroso, J.B.** (2006) Reactive Oxygen Species and Reactive Nitrogen Species in Peroxisomes . Production , Scavenging , and Role in Cell Signaling. *Plant Physiol.*, **141**, 330–335.

- Rizhsky, L., Liang, H. and Mittler, R.** (2003) The water-water cycle is essential for chloroplast protection in the absence of stress. *J. Biol. Chem.*, **278**, 38921–5.
- Sagi, M. and Fluhr, R.** (2006) Production of Reactive Oxygen Species by Plant NADPH Oxidases. *Plant Physiol.*, **141**, 336–340.
- Sagi, M. and Fluhr, R.** (2001) Superoxide production by plant homologues of the gp91(phox) NADPH oxidase. Modulation of activity by calcium and by tobacco mosaic virus infection. *Plant Physiol.*, **126**, 1281–90.
- Sheen, J.** (1991) Molecular mechanisms underlying the differential expression of maize pyruvate, orthophosphate dikinase genes. *Plant Cell*, **3**, 225–245.
- Somerville, C.R.** (2001) An early Arabidopsis demonstration. Resolving a few issues concerning photorespiration. *Plant Physiol.*, **125**, 20–4.
- Somerville, C.R. and Ogren, W.L.** (1981) Photorespiration-deficient Mutants of Arabidopsis thaliana Lacking Mitochondrial Serine Transhydroxymethylase Activity. *Plant Physiol.*, **67**, 666–671.
- Stabenau, H. and Winkler, U.** (2005) Glycolate metabolism in green algae. *Physiol. Plant.*, **123**, 235–245.
- SUN, J., WANG, M.-J., DING, M.-Q., et al.** (2010) H<sub>2</sub>O<sub>2</sub> and cytosolic Ca<sup>2+</sup> signals triggered by the PM H<sup>+</sup>-coupled transport system mediate K<sup>+</sup>/Na<sup>+</sup> homeostasis in NaCl-stressed Populus euphratica cells. *Plant. Cell Environ.*, **33**, 943–958.
- Timm, S., Mielewczik, M., Florian, A., Frankenbach, S., Dreissen, A., Hocken, N., Fernie, A.R., Walter, A. and Bauwe, H.** (2012) High-to-low CO<sub>2</sub> acclimation reveals plasticity of the photorespiratory pathway and indicates regulatory links to cellular metabolism of Arabidopsis. *PLoS One*, **7**, e42809.
- Timm, S., Nunes-Nesi, A., Pärnik, T., et al.** (2008) A cytosolic pathway for the conversion of hydroxypyruvate to glycerate during photorespiration in Arabidopsis. *Plant Cell*, **20**, 2848–59.
- Tolbert, N.E.** (1997) the C<sub>2</sub> Oxidative Photosynthetic Carbon Cycle. *Annu. Rev. Plant Physiol. Plant Mol. Biol.*, **48**, 1–25.
- Torres, M.A., Dangl, J.L. and Jones, J.D.G.** (2002) Arabidopsis gp91phox homologues AtrbohD and AtrbohF are required for accumulation of reactive oxygen intermediates in the plant defense response. *Proc. Natl. Acad. Sci. U. S. A.*, **99**, 517–522.
- Triantaphylidès, C., Krischke, M., Hoerberichts, F.A., Ksas, B., Gresser, G., Havaux, M., Breusegem, F. Van and Mueller, M.J.** (2008) Singlet oxygen is the major reactive oxygen species involved in photooxidative damage to plants. *Plant Physiol.*, **148**, 960–968.
- Tripathy, B.C. and Oelmüller, R.** (2012) Reactive oxygen species generation and signaling in plants. *Plant Signal. Behav.*, **7**, 1621–33.

- Vandenabeele, S., Vanderauwera, S., Vuylsteke, M., et al.** (2004) Catalase deficiency drastically affects gene expression induced by high light in *Arabidopsis thaliana*. *Plant J.*, **39**, 45–58.
- Vanlerberghe, G.C.** (2013) Alternative Oxidase: A Mitochondrial Respiratory Pathway to Maintain Metabolic and Signaling Homeostasis during Abiotic and Biotic Stress in Plants. *Int. J. Mol. Sci.*, **14**, 6805–47.
- Wagner, A.M.** (1995) A role for active oxygen species as second messengers in the induction of alternative oxidase gene expression in *Petunia hybrida* cells. *{FEBS} Lett.*, **368**, 339–342.
- Weber, A., Menzlaff, E., Arbinger, B., Gutensohn, M., Eckerskorn, C. and Flügge, U.I.** (1995) The 2-oxoglutarate/malate translocator of chloroplast envelope membranes: molecular cloning of a transporter containing a 12-helix motif and expression of the functional protein in yeast cells. *Biochemistry*, **34**, 2621–2627.
- Winter, D., Vinegar, B., Nahal, H., Ammar, R., Wilson, G. V and Provart, N.J.** (2007) An “Electronic Fluorescent Pictograph” browser for exploring and analyzing large-scale biological data sets. *PLoS One*, **2**, e718.
- Wydro, M., Kozubek, E. and Lehmann, P.** (2006) Optimization of transient *Agrobacterium*-mediated gene expression system in leaves of *Nicotiana benthamiana*. *Acta Biochim. Pol.*, **53**, 289–298.
- Xing, Y., Jia, W. and Zhang, J.** (2008) AtMKK1 mediates ABA-induced CAT1 expression and H<sub>2</sub>O<sub>2</sub> production via AtMPK6-coupled signaling in *Arabidopsis*. *Plant J.*, **54**, 440–51.
- Xu, H., Zhang, J., Zeng, J., Jiang, L., Liu, E., Peng, C., He, Z. and Peng, X.** (2009) Inducible antisense suppression of glycolate oxidase reveals its strong regulation over photosynthesis in rice. *J. Exp. Bot.*, **60**, 1799–809.
- Zelitch, I., Schultes, N.P., Peterson, R.B., Brown, P. and Brutnell, T.P.** (2009) High glycolate oxidase activity is required for survival of maize in normal air. *Plant Physiol.*, **149**, 195–204.
- Zhang, A., Jiang, M., Zhang, J., Tan, M. and Hu, X.** (2006) Mitogen-activated protein kinase is involved in abscisic acid-induced antioxidant defense and acts downstream of reactive oxygen species production in leaves of maize plants. *Plant Physiol.*, **141**, 475–487.

**Figures**

**Figure 1:** Isolation of recombinant *A. thaliana* GO1-3. Coomassie-stained SDS-PAGE of GO1-3. Lane 1 20  $\mu$ g of *E. coli* crude extract before induction of expression; Lane 2, 20  $\mu$ g of *E. coli* crude extract expressing GO1-3 after IPTG induction; lanes 3, 3  $\mu$ g of purified recombinant GO1-3.

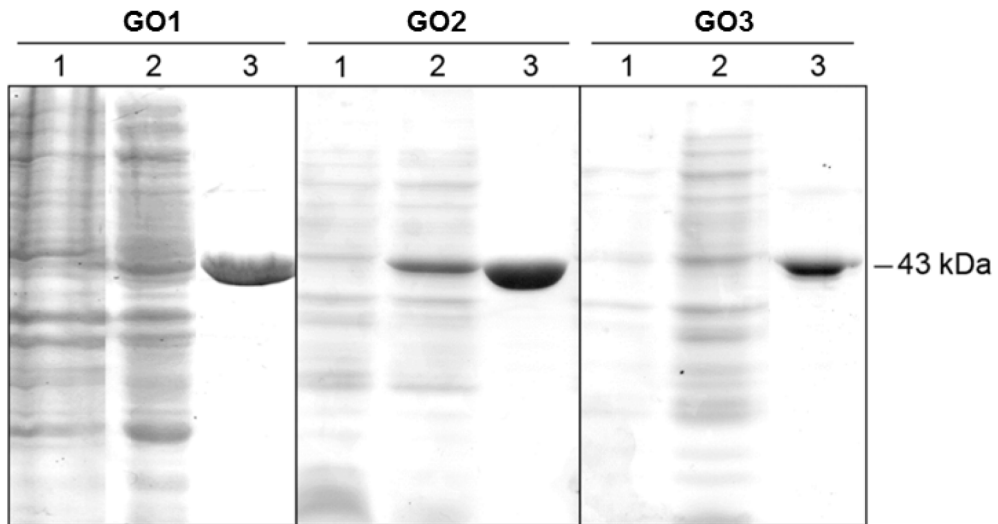


**Figure 2:**Subcellular localization of GO3 in tobacco cells. A: peroxisomes transformed with CFP-PTS1; B: autofluorescence C: Protoplasts transformed with a construct of GO3 with N-terminal YFP translational fusion; D: merge of A, B and C

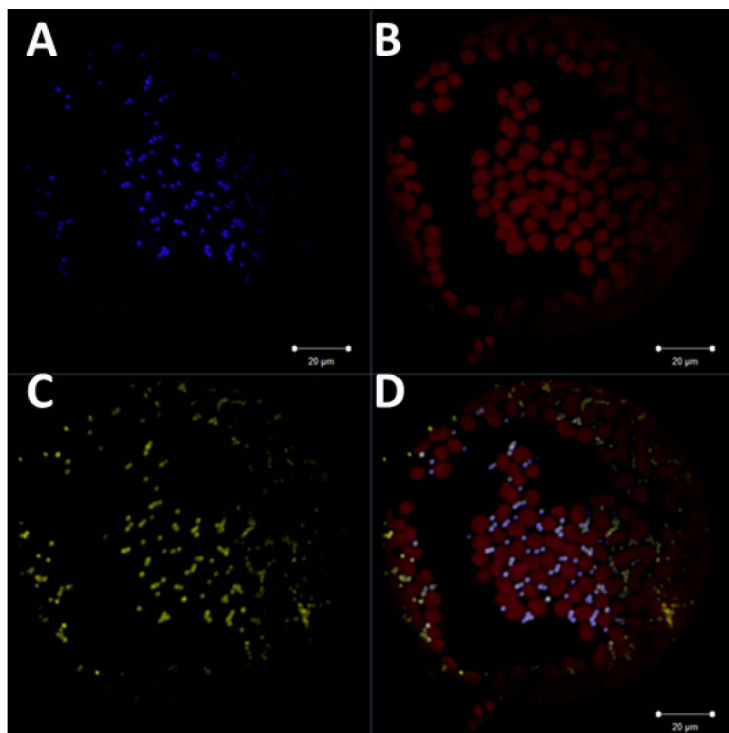




**Figure 3:**A: Schematic representation of At4g18360 encoding GO3. B: genotyping PCR. Exons are shown as blocks and introns as lines, the sites of the T-DNA insertions are indicated but not drawn on scale. Genomic DNA was isolated from wild-type, *go3-1* and *go3-2* respectively and used as template for PCR with GO3 gene-specific and T-DNA-insertion-specific primers.

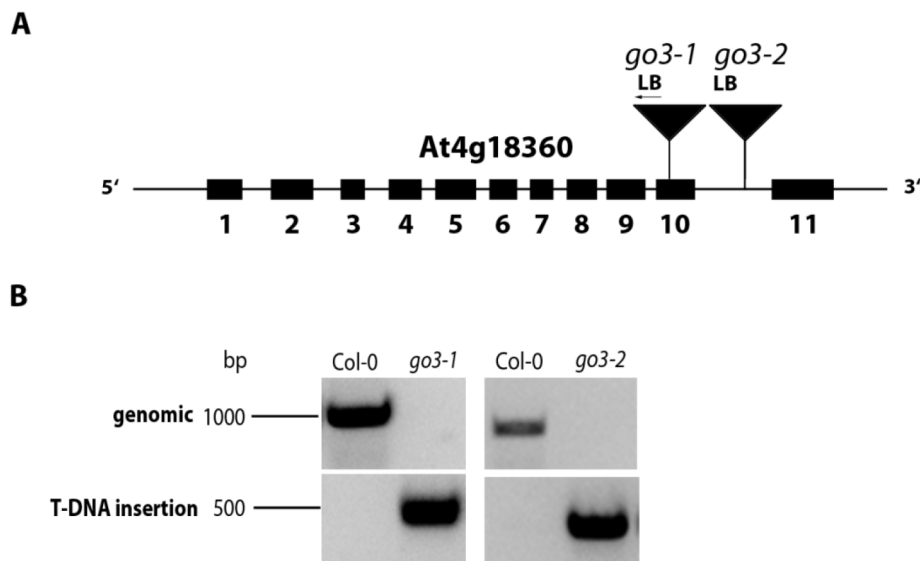


**Figure 4:** Root complementation analysis of GO3. GO3 can use L-lactate and glycolate as substrate. Example of plants grown on  $\frac{1}{2}$  MS plates containing A: 0.5 mM glycolate and B: 1 mM L-lactate. C, D: diagram of root length of plants on C: 0.5 glycolate and D: 1 mM L-lactate. GO3-OX1: Overexpressing of GO3 with 35S CaMV Promoter in Col-0. GO3-OX2: Overexpression of GO3 with GO3 Promoter in Col-0; *go3-1* and *go3-2*: loss-of-function mutants of Gox3. The values presented in C and D are means  $\pm$  SE from at least 15 plants per line. The asterisk (\*) indicates statistically significant difference (\*:  $P < 0.05$ , \*\*:  $P < 0.005$ ) to Col-0.

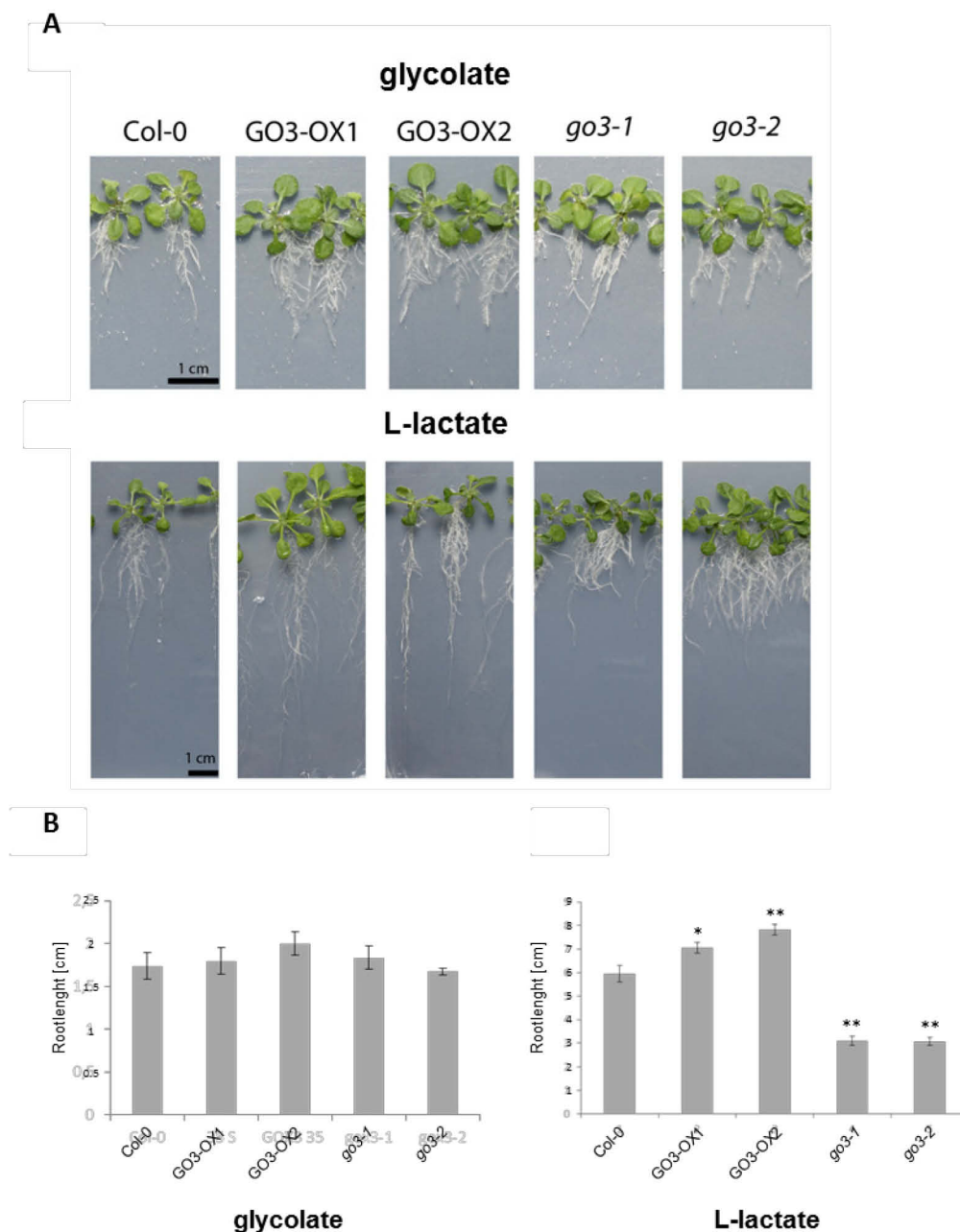




**Table 1:** Analysis of GO1-3 electron acceptor. The preferred co-factors of AtGO1 and AtGO2 were tested by measuring the enzyme activities using the heterologously expressed and purified enzymes. Standard assays contained 10mM glycolate as substrate and either of 200M cytochrome c, 200M DCIP with 3mM PMS or 1mM NAD(P)<sup>+</sup>. Product accumulation using phenylhydrazine (O<sub>2</sub> as electron acceptor) or reduction of the acceptors was monitored photometrically. The listed activities are relative to the best acceptor. Shown are mean values of at least two independent experiments.

	Activity (%)		
	<b>GO1</b>	<b>GO2</b>	<b>GO3</b>
O <sub>2</sub>	74	100	100
CYTc	-	-	-
DCIP	100	75	99
NAD(P) <sup>+</sup>	-	-	-

**Table 2:** Kinetic constants of GO1 and GO3. Kinetic constants were determined using the standard reaction mix and varying the substrate concentration from 5 to 10 mM, and monitoring the decreasing oxygen concentration, 4 to 10 g purified enzyme were used.  $S_{0.5}$  and  $V_{max}$  values were determined using the nonlinear regression fit to the sigmoidal Hill equation  $f(x) = \frac{a x^{bc}}{bc + x^b}$  (Sigma Plot software), shown are mean values SE of three independent experiments.

		$S_{0.5}$ ( $\mu\text{M}$ )	$k_{cat}$ ( $\text{min}^{-1}$ )	$k_{cat}/K_m$ ( $\text{min}^{-1}\text{mM}^{-1}$ )	Hill coefficient
<b>GO1</b>	Glycolate	187 $\pm$ 18	831 $\pm$ 67	4446	1.72 $\pm$ 0.08
<b>GO3</b>	Glycolate	202 $\pm$ 14	538 $\pm$ 35	2656	1.94 $\pm$ 0.07
	L-lactate	153 $\pm$ 6	851 $\pm$ 29	5554	1.93 $\pm$ 0.06

**Table 3:** Substrate specificities of GO1-3. Enzyme activities were determined using heterologously expressed and purified enzymes and standard assay conditions. The used concentration was 5mM for glycolate, L-lactate, Leucic acid, Valic acid and Isoleucic acid and 0.5mM for 2-hydroxyhexanoic acid to 2-hydroxyhexadecanoic acid. Product accumulation (using phenylhydrazine and O<sub>2</sub> as electron acceptor) was monitored photometrically. Shown are mean values of the activities relative to the best substrate of at least two independent experiments.

	Relative oxidase activity (%)		
	<b>GO1</b>	<b>GO2</b>	<b>GO3</b>
Glycolate	100	100	100
L-lactate	45	48	76
2-hydroxyhexanoic acid	0.2	-	9.4
2-hydroxyoctanoic acid	2.4	-	14.3
2-hydroxydodecanoic acid	1.8	-	8.8
2-hydroxyhexadecanoic acid	-	-	0.4
Leucic acid	1	-	6.1
Valic acid	-	-	0.1
Isoleucic acid	0.1	-	-

**Table 4:** Kinetic constants of GO1-3. Kinetic constants were determined using the standard reaction mix varying the substrate concentration from 0 mM to 37.9 mM. 1 to 5  $\mu$ g purified enzyme were used.  $K_m$  and  $V_{max}$  values were determined using the nonlinear regression fit to the Michaelis Menten equation  $f(x) = \frac{axb}{a+x}$  (Sigma Plot software). Shown are mean values  $\pm$  SE of three independent experiments.

	$K_m$ ( $\mu$ M)	$K_{cat}$ ( $\text{min}^{-1}$ )	$K_{cat}/K_m$ ( $\text{min}^{-1} \text{mM}^{-1}$ )
<b>GO1</b>			
Glycolate	278 $\pm$ 13	254 $\pm$ 2	911
L-lactate	2753 $\pm$ 165	114 $\pm$ 2	41
<b>GO2</b>			
Glycolate	327 $\pm$ 21	224 $\pm$ 4	744
L-lactate	4905 $\pm$ 241	116 $\pm$ 2	24
<b>GO3</b>			
Glycolate	144 $\pm$ 10	104 $\pm$ 1	725
L-lactate	420 $\pm$ 4	80 $\pm$ 2	190

**Manuscript 3:** Substrate specificities of peroxisomal H<sub>2</sub>O<sub>2</sub>-producing (L)-2 hydroxyacid oxidases

**Status:** Manuscript

Anke Kuhn, Martin KM Engqvist, Nils Jaspert, Jessica Schmitz and Veronica G Maurino

**Own contribution:** 50 %

- Test of T-DNA insertion
- Alignment of GO3 and CYB2
- Root complementation assays
- Yeast Complementation assays
- Activity gel of GO3 out of yeast
- Semiquantitative PCR of GO3 in yeast
- Data analysis of root length
- Co-writing the manuscript



## **Danksagung**

Am Ende dieser Arbeit möchte ich gerne noch einigen Leuten danken, die zum Gelingen dieser Arbeit beigetragen haben.

Besonderen Dank gilt Frau PD Dr. Verónica G. Maurino für die Möglichkeit in Ihrer Arbeitsgruppe zu promovieren. Außerdem danke ich Ihr für die hervorragende Betreuung während der gesamten Zeit in Köln und Düsseldorf sowie für die zahlreichen Möglichkeiten an Kongressen teilzunehmen und für ihr Vertrauen in meine Arbeit.

Herrn Prof. Dr. Jürgen Zeier danke ich für die freundliche Übernahme des Zweitgutachtens und die Zusammenarbeit für die Sterolmessungen.

Herrn Prof. Dr. Andreas P.M. Weber möchte ich für die Integration unserer Arbeitsgruppe in sein Labor danken.

Bei Herrn Prof. Dr. U.-I. Flügge möchte ich mich für die freundliche Unterstützung zu Beginn meiner Arbeit in Köln danken.

Außerdem möchte ich unseren Kooperationspartner danken. Dr. Frank van Breusegem und Dr. Katrien van der Kelen danke ich für die Zusammenarbeit bei den Microarrays. Prof. Dr. Bernd Müller-Röber und Dr. Salma Balazadeh danke ich für die Zusammenarbeit für das GOX3 Projekt.

Da ich für diese Arbeit in Köln und Düsseldorf gearbeitet habe, möchte ich einer Menge Kollegen für die sehr gute Zusammenarbeit und das freundliche Arbeitsklima während der letzten Jahre danken. Vor allem danke ich meinen aktuellen und ehemaligen Kollegen in der AG Maurino für viele wissenschaftliche und nicht-wissenschaftliche Gespräche: Dr. Alexandra Maier, Dr. Alexander Maier, Dr. Jessica Schmitz, Dr. Martin Engqvist, Dr. Anke Kuhn, Dr. Martina Zell, Judith Wienstroer, Dorien Engeländer, Claudia Nothelle und Ulrike Hebbeker.

Aus Köln danke ich der ehemaligen Kicker Crew Dr. Simon von Berlepsch, Dr. Henning Frerigmann und Dr. Pia Staehr für viele lustige Abende auch außerhalb der Uni.

Dr. Frank Ludewig, Dr. Katja Ludewig, Dr. Markus Gierth, Dr. Henning Kunz und Dr. Annemarie Reichel danke ich ebenfalls für die anregenden Diskussionen bei einem Feierabendbierchen.

## Danksagung

---

Außerdem danke ich allen anderen aktuellen und ehemaligen Kollegen aus Köln: Dr. Stefan Krüger, Elke Hilgers, Veronika Ungewickell, Chillililli Marbaise, Kirsten Bell, Raphael Wemhöner, Natallia Ashykhmina, Nicole Wöstefeld, Dr. Holger Fahnenstich, Dr. Rainer Häusler, Dr. Dereje Mekonnen, Shirin Zamani-Nour, Claudia Schwanitz, Sonja Lott, Diana Vogelmann, Dr. Tamara Gigolashvili, Ruben M. Benstein, Laura Strubl und Sabine Wulfert.

Auch den sehr freundlichen Menschen aus der Gärtnerei und der Werkstatt möchte ich für die Hilfe und Anzucht meiner Pflanzen danken.

Natürlich möchte ich auch allen aktuellen und ehemaligen Kollegen aus Düsseldorf danken, die unsere gesamte Arbeitsgruppe sehr freundlich aufgenommen haben und stets hilfsbereit bei allen Fragen in wissenschaftlichen und nicht-wissenschaftlichen Bereichen waren: Dr. Nicole Linka, Dr. Andrea Bräutigam, Dr. Marion Eisenhut, Dr. Fabio Facchinelli, Dr. Thea Pick, Dr. Peter Lundquist, Dr. Tabea Mettler, Dr. Urte Schlüter, Katja Paas, Christian Bordych, Christian Rosar, Jan Wiese, Simon Schliesky, Canan Kūlahoglu, Manuel Sommer, Alisandra Denton, Martin Schroers, Nadine Hocken, Dominik Brillhaus, Thomas Wrobel, Fabian Brandenburg, Björn Hielscher, Kirsten Abel, Maria Graf, Elisabeth Klemp, Samantha Kurz und Katrin Weber.

Zu guter Letzt möchte ich noch meiner Freundin Nadja Münster, meinen Eltern Jutta und Erich Jaspert sowie meinem Bruder Timm Jaspert und meine Schwägerin Jacqueline Jaspert danken. Ein besonderer Dank geht auch an meine Schwester Dr. Nina Jaspert, die mir während meines gesamten Biologie Studiums stets mit Biobüchern, Antworten und lustigen Geschichten aus ihrem Labor zur Seite stand.

## **CURRICULUM VITAE**

### **PERSONAL DETAILS**

Name	Nils Jaspert
Address	Ägidiusstr. 74 50937 Köln Germany
e-Mail	nils.jaspert@hhu.de
Date of Birth	04.07.1982

### **EDUCATION AND QUALIFICATIONS**

07/1993– 07/2003	Käthe-Kollwitz-Gymnasium, Dortmund, A-Level
10/2004 – 07/2009	Student of Biology, Ruhr-University Bochum, Department for Plant Biochemistry Oral diploma exams: Plant Biochemistry, Grade Biotechnology, Grade Botany, Grade Physiological Chemistry Certificate: Diploma
09/2009 – present	PhD student, Heinrich Heine Universität Düsseldorf, Plant Molecular Physiology and Biotechnology group Supervisor: PD Dr. Veronica Maurino